13 Composite Design and Analysis Details

The purpose of this section is to provide information and guidance for analyzing laminated composite region where (i) the stress distribution through the thickness is complex, (ii) there is significant out-of-plane loading and/or (iii) the failure modes are complex and has an out-of-plane component. These conditions violate the classical lamination theory assumptions and hence the full three dimensional stress state and out-of-plane failure modes such as interlaminar tension (ILT) and interlaminar shear (ILS) have to be considered in the analysis.

These unique parts also may require development of point design allowables that account for disparate loading conditions such as static and fatigue. Examples of complex regions include chevrons, cutouts, joggled features, seal grooves, stiffener runouts, edges and pi-preforms. The section introduces the parts and discusses (i) preliminary design analysis to initially screen and identify critical parts and (ii) a rigorous detailed analysis method for writing the final margins.

13 Composite Design and Analysis Details 13-1
13.1 References 13-2
13.2 Design Guidelines and Structural Development Testing 13-6
13.2.1 Characteristic Dimensions 13-7
13.3 Chevrons 13-8
13.3.1 IDAT/PACT Analysis for Chevron Notches 13-10
13.3.2 Example Problem Using IDAT/PACT 13-12
13.3.3 Fine Grid Finite Element Detailed Analysis for Chevron Notches 13-15
13.4 Cutouts or Holes in Webs or Panels 13-16
13.4.1 Web Buckling with Hole 13-17
13.4.2 Panel Hole Reinforcement 13-19
13.4.3 Strength in Panels with Holes 13-20
13.4.4 Durability and Damage Tolerance Considerations 13-21
13.4.5 Analysis Approaches for Panels with Holes 13-21
13.5 Joggles 13-23
13.5.1 Analysis of Panels with Joggles 13-25
13.6 Seal Grooves 13-27
13.7 Stiffener Run-out 13-31
13.8 Honeycomb Panel Ramps 13-36
13.9 Free Edges 13-39
13.10 3-D Woven Pi-Preform Joint Analysis 13-40
13.10.1 Design Philosophy 13-41
13.10.2 Manufacturing Methods 13-42
13.10.3 Pi-Joint Nomenclature and Coordinate Systems 13-44
13.10.4 Pi-preform Naming Convention 13-45
13.10.5 Pi-Joint Failure Modes 13-46
13.10.6 Design Guidelines 13-48
13.10.7 Summary of LM Documents with Pi-Preform Properties, Allowables and Pi-Joint Allowables .. 13-49
13.10.8 Joint Element Configurations 13-52
13.10.9 IM7/977-3 & FM-300-08K Adhesive, 350ºF Autoclave Cure Material System 13-57
13.10.9.1 Failure Modes Observed 13-57
13.10.9.2 Stress Method and Pull-off Allowables 13-59
13.10.9.3 Stress Method and Joint Shear Allowables 13-64
13.10.9.4 Stress Method and Lateral Bend Allowables 13-65
13.10.9.5 Combined Pull-off and Joint Shear Interaction 13-67
13.10.9.6 Combined Pull-off and Lateral Bend Interaction 13-67

Copyright 2015 Lockheed Martin Corporation.
Note: The current version is always the version on the Lockheed Martin network.

13.10.9.7 Combined Joint Shear and Lateral Bend Interaction 13-68
13.10.9.8 Combined Pull-off, Lateral Bend, and Joint Shear Interaction 13-69
13.10.9.9 Effect of Defects and Repair 13-69
13.10.10 Example Problem 13-70
13.10.11 IM7/977-3 & AF191 Adhesive, 350ºF Autoclave Cure Material System 13-74
13.10.11.1 Stress Method and Pull-off Allowables 13-75
13.10.11.2 Stress Method and Joint Shear Allowables 13-75
13.10.11.3 Stress Method and Lateral Bend Allowables 13-76
13.10.11.4 Combined Pull-off and Joint Shear Interaction 13-76
13.10.11.5 Combined Pull-off and Lateral Bend Interaction 13-76
13.10.11.6 Combined Joint Shear and Lateral Bend Interaction 13-76
13.10.11.7 Combined Pull-off, Lateral Bend, and Joint Shear Interaction 13-76
13.10.12 IM7/MTM45-1 & FM309-1M Adhesive, Out of Autoclave (OoA) Cure Material System 13-76
13.10.13 Durability and Damage Tolerance 13-76
13.10.14 Pi-preform Splicing/Darting Methods 13-79
13.10.15 IBOND Analysis Method 13-80
13.10.16 Other Analysis Methods 13-80
13.10.17 Additional Checks 13-80
13.10.18 Effects of Defects 13-80
13.10.19 Repairs 13-84
13.10.20 FEA Modeling Conventions and Considerations 13-84

13.1 References

13-1. Flansburg, L.K., *Lockheed Martin Aeronautics Procedures Manual 4057 Metallic Structural Analysis Manual*, Lockheed Martin Aeronautics, Fort Worth, TX, 2008
13-2. Staff, *LMTAS Policy and Methods for Stress Analysis*, ST-94-08, 1997.
13-3. SAMDC
13-4. Staff, *LTV Composite Structures Analysis Manual*, LTV Aircraft Products Group, Grand Prairie, TX, August, 1984.
13-5. Kassapoglou, C., *Design and Analysis of Composite Structures with Applications to Aerospace Structures*, John Wiley & Sons, Ltd., 2010.
13-6. Reddy, J.N., *Mechanics of Laminated Composite Plates – Theory and Analysis*, CRC Press, 1997.
13-7. Jones, R.M., *Mechanics of Composite Materials*, 2nd Edition, Brunner-Routledge, 1999.
13-8. EL-49 testing for data supporting analysis methods and allowables for composite hat stiffeners
13-9. EL-65 testing for data supporting analysis method and allowables for analyzing seal grooves in composite strap
13-10. Finite Element Analysis Procedures Manual, PM 4061 (in preparation).
13-11. Martin, J.M., *Cobond/Cocure/Paste Bond of Lockheed Martin 3-D Pi-Preform Structures Design Guidelines*, FZM-9025.
13-12. anon, "*Element and Component Test Results and Evaluation Composite Shear Web Beams*," 5PC00840-07, Lockheed Ft. Worth, July 1995
13-13. anon., "Composite Chevron Notches," 5PC00840-12 Volume 12, Lockheed Aeronautical Systems Company, Ft Worth, TX, (1995)
13-14. anon, "Structural Analysis Methods and Design Criteria (SAMDC)," 2ZSB000001, Rev E, Lockheed Martin Aeronautics, Ft. Worth, TX (2006)
13-15. Jackson, T.L, "Wing Composite Strap Seal Groove Strength Validation," 2WSA00482-0002 (XG-ST-E-65), Lockheed Martin Aeronautics, Ft Worth, TX (2007)
13-16. Klein, M., et. al., "Engineering Final Report for Element Test Series XG-ST-EL-30.2 Core Termination," Lockheed Martin Aeronautics, Ft. Worth, TX (2006)

Copyright 2015 Lockheed Martin Corporation.
Note: The current version is always the version on the Lockheed Martin network.

13-17. Berusch, L., and Taylor, R., *Engineering Final Assessment Report for Element Test Series XG-ST-EL-09*, 3D Woven Pi-Preform Element Test, 2CSA00005-000.
13-18. Finite Element Analysis Procedures Manual, PM 4061 (in preparation).
13-19. Martin, J.M., *Cobond/Cocure/Paste Bond of Lockheed Martin 3D Pi-Preform Structures Design Guidelines*, FZM-9025.
13-20. Reis, C., *Preform Risk Reduction, XG-MT-SB-24*, 2CSA09002-0001, November 2004.
13-21. Final Engineering Assessment Report for 3D Textile Preform Characterizations Tests, XG-ST-CO-13, Fracisco Ramirez, 2ZSA00006-002, August 2004.
13-22. 3D Textile Weave Microdarting Effects Coupon Tests, XG-ST-CO-14, G.S. Abad and C.H. Shah, December 2004.
13-23. Engineering Final Assessment Report for Element Test Series XG-ST-EL-22, Ryan Shea, 2003.
13-24. MB003 drawing.
13-25. Three-dimensional Woven Preforms, for Primary Aircraft Structure, LMA-MB003C, July 2013.
13-26. McClain, M. and Goering, J., *Rapid Assembly of Fiber Preforms Using 3D Woven Components*, SAMPE 2012.
13-27. Composite Crew Module Materials and Processes, NASA Engineering and Safety Center Technical Assessment Report, NESC-RP- 06-019.
13-28. Kelly, K.L., *Advanced Composite Cargo Aircraft (ACCA) Flight Demonstrator Program*, Phase III, Delivery Order 013, AVIATAR, AFRL-RQ-WP-TR_2013-0094
13-29. FZM-10160 M7/MTM45-1 Pi Weave Allowables (In preparation)
13-30. Favela, J., Pi-preform Joint Allowables, Standard Weight IM7/MTM45-1 and FM309-1M, FZM 10161, 2015 (In-preparation)
13-31. FZM-10162, IM7/MTM45-1 Pi Preform Joint Allowables - Light Weight (In preparation)
13-32. Martin, J.M., Lockheed Martin 3D Pi-Preform Bonded Joint Repair Concepts, FZM 9091, 2005.
13-33. Cook, L.M., *Aircraft Primary Structure Adhesive Bonding Development Program*, NJC, June 2003.
13-34. Inspection, Acceptance Criteria, For Composite Parts and Assemblies, LMA-PC005B, Nov. 2006.
13-35. Department of Defense Joint Services Specification Guide 2006, Aircraft Structures. JSSG-2006, Department of Defense, Washington DC, (2006)
13-36. Favela, J., Pi-preform Joint Allowables, Standard Weight IM7/MTM45-1 and FM309-1M, 2015 (In-preparation)
13-37. Shea, R., "Impact Survey", XG-ST-EL-29, July 2005.
13-38. Schmidt, R., "3-D Woven Preform Joint Data Source Summary", 4-30-09.

Table 13.1-1 Symbols and Nomenclature

Symbol	Description	Units
α	undercut angle	^{o}
a	moment arm, defined in Figure 13.8-2	in
A_{cutout}	cross-sectional area of the the cutout	in^2
$A_{doubler}$	cross-sectional area of the the doubler	in^2
AVFEM	Air Vehicle Finite Element Model	
b	Web width of the beam (fastener line or stiffener centroid if bonded)	in
c_i	chord length at the ith step	in
C_t	intercept	lb/in
CTD	Cold Temperature Dry, typically -65 degrees F	^{o}F
D	diameter of the cutout	in
DADT	Durability and Damage Tolerance	

Copyright 2015 Lockheed Martin Corporation.
Note: The current version is always the version on the Lockheed Martin network.

DLL	Design Limit Load	lb
e	distance between centroids from the full-depth core to the edgeband	in
ETW	Elevated Temperature Wet, typically 180, 220 or 275 degrees F, as determined by program based on Aircraft usage.	^oF
f_{13}	interlaminar shear stress in the 1-3 plane of the facesheet	psi
f_{23}	interlaminar shear stress in the 2-3 plane of the facesheet	psi
f_{33}	interlaminar normal stresses in the facesheet	psi
FGFEM	Fine Grid Finite Element Model	
h	web height of the beam (web height to centroid of caps)	in
h_i	distance from the radius center to the ith step of the seal groove	in
ILS	Interlaminar Shear	psi
ILT	Interlaminar Tension	psi
K_{js}	joint shear factor	
$K_{js\text{-}EOD}$	Joint shear Effect of Defect factor	
$K_{js\text{-}ovewrap}$	Joint shear overwrap factor	
$K_{js\text{-}secbond}$	Joint shear secondary bond factor	
$K_{js\text{-}splice}$	Joint shear splice factor	
K_{lb}	lateral bend factor	
$K_{ply\%}$	0° ply percent factor (quasi, soft, hard)	
K_{po}	pull-off factor	
$K_{po\text{-}EOD}$	Pull-off effects of defects	
$K_{po\text{-}ovewrap}$	Pull-off overwrap factor	
$K_{po\text{-}secbond}$	Pull-off secondary bond factor	
$K_{po\text{-}splice}$	Pull-off splice factor	
K_{radius}	empirical correction factor	
K_{span}	Span length factor	
$K_{undercut}$	reduction factor for undercut	
$K_{web\text{-}angle}$	Web angle factor	
L	length of the panel	in
L_1	length of the one side of the chevron notch	in
L_2	length of the notch edge perpendicular to L_1	in
LASER	Light Amplification by Simulated Emission of Radition	
L_i	is the length of the taper for the ith step for steps 2-n; $L_1=c_1/2$	in
M_{lb}	applied lateral bend moment	in-lb/in
$M_{lb\text{-}a}$	lateral bend moment allowable	in-lb/in
MS_{crit}	Critical margin of safety	
MS_{js}	joint shear margin of safety	
$MS_{js\text{-}lb}$	combined joint shear and lateral bend margin of safety	
MSL	maximum spectrum load	lb
MS_{lb}	lateral bend margin of safety	

Copyright 2015 Lockheed Martin Corporation.
Note: The current version is always the version on the Lockheed Martin network.

MS_{po}	pull-off margin of safety	
$MS_{po\text{-}js}$	combined pull-off and joint shear margin of safety	
$MS_{po\text{-}js\text{-}lb}$	combined joint pull-off, shear, and lateral bend margin of safety.	
$MS_{po\text{-}lb}$	combined pull-off and lateral bend margin of safety	
$MS_{straight\ cut}$	margin of safety at the characteristic dimension for a straight cut edge	
m_t	slope	psi
N	running load	lb/in
N_{crit}	critical axial buckling running load	lb/in
NDE	Non-destructive Examination	
NDI	Non-destructive Inspection	
NF	Notched flexure	in-lb/in
N_{max}	maximum in-plane running load for panel at the full-depth centroid perpendicular to the edgeband at the analysis location	lb/in
$N_{xx\text{-}avg}$	average axial running load in x direction	lb/in
$N_{xy\text{-}avg}$	average shear running load in xy plane	lb/in
$N_{yy\text{-}avg}$	average axial running load in y direction	lb/in
OML	outer mold line	
p	pressure	psi
P_{js}	applied joint shear load	lb/in
$P_{js\text{-}a}$	joint shear allowable	lb/in
P_{po}	applied pull-off load	lb/in
$P_{po\text{-}a}$	pull-off allowable	lb/in
$P_{po\text{-}a}$	pull-off allowable	lb/in
PT	Fastener pull-thru	psi
P_{xx}	Residual strength load	lbs
q	web angle	
Q	transverse shear load	lb/in
QA	Quality Assurance	
R	chevron notch root radius, radius of seal groove	in
R_c	characteristic dimension	in
R_{js}	joint shear load ratio	
$R_{js\text{-}lb}$	joint shear, lateral bend load ratio	
R_{lb}	lateral bend load ratio	
R_{po}	pull-off load ratio	
$R_{po\text{-}js}$	pull-off, joint shear load ratio	
$R_{po\text{-}js\text{-}lb}$	pull-off, joint shear, lateral bend load ratio	
$R_{po\text{-}lb}$	pull-off, lateral bend load ratio	
RTA	Room Temperature, typically 75 degrees F, relative humidity no greater than 85%	^oF
S	span length (e.g. spar spacing)	in
SIG33	B-Basis interlaminar tension stress allowable from IDAT/metdb	psi

Copyright 2015 Lockheed Martin Corporation.
Note: The current version is always the version on the Lockheed Martin network.

TAU13	B-Basis interlaminar shear stress allowable in the 1-3 plane from IDAT/ metdb	psi
TAU23	B-Basis interlaminar shear stress allowable in the 2-3 plane	psi
t_{dblr}	thickness of the doubler	in
t_i	is the thickness of the tapered plies as measured from the deepest part of the seal groove	in
t_{skin}	skin thickness	in
UT	Ultra-Sonic	
W	width of the panel or width of reinforcement ring	in
w_{base}	width of the upstanding leg	in
$\varepsilon_{tangential}$	average element strain in the tangential plies at the characteristic distance from the edge of the hole	in/in
$\varepsilon_{unnotched}$	unnotched tension or compression strain allowable	in/in
σ_{zz}	is the interlaminar tension stress	psi
τ_{xz}	is the interlaminar shear stress in the xz-plane	psi
τ_{yz}	is the interlaminar shear stress in the yz-plane	psi

Table 13.1-2 Definition of Terms

Term	Description
Peel Strength (pounds per linear inch)	Bond strength that measures the amount of adhesion between bonded surfaces; It is a measure of the stress required to separate a layer of material from the base to which it is bonded.
Preform	An assembly of dry fabric prepared for one of several different wet resin injection processes.
Prepreg	Ready to mold or cure material in sheet form which may be tow, tape, cloth, or mat impregnated with resin.

13.2 Design Guidelines and Structural Development Testing

General design guidelines for each of the details included in this section will be covered in the appropriate subsection which focuses on the design considerations and structural analysis of that detail. Most of the recommended methods have been correlated with test of the specific detail geometry and staying within the recommended guidelines will mitigate the weight impact and help to minimize structural risk. It is recommended that any new, different or modified design features also undergo testing.

The guidelines and analysis methodology are based on empirical data for specific fiber/resin combinations and results may vary for other materials. Thus, a carefully planned structural development test program must be executed for most of these details as implemented on a particular platform to ensure structural integrity of the airframe. Different materials/resins, geometry and design implementations can affect the strength. The tests should be used to determine the critical failure modes and the strength allowables for cutouts, joggles and bonded stiffeners, *etc*. under worst case environmental conditions in the presence of defects that cannot be detected using typical inspection and NDI techniques employed during manufacturing. The test should also demonstrate that these defects do not grow at a load level specified by the program or if none is specified below the Design Ultimate Load (DUL)

Copyright 2015 Lockheed Martin Corporation.
Note: The current version is always the version on the Lockheed Martin network.

13.2.1 Characteristic Dimensions

A characteristic dimension, R_c, is defined as the distance from the edge of a stress concentration to a point at which the unnotched fiber strain failure value can be applied. This is also sometimes referred to as the characteristic distance. It is based on a correlation between predicted test failures and actual test failures in parts which have stress concentrations due to cutouts. Reference 13-13 uses data from tests of composite panels of 4 different ply layups and two different materials which have radiused rectangular holes to develop characteristic dimensions to be used for analysis. This effort included correlation to 0.25 in diameter open hole test results. The characteristic dimensions for different materials are given in Table 13.2-1.

Table 13.2-1 Characteristic Dimension, R_c, For Different Materials and Loading

Material	Product Form	Loading	$R_{c\text{-}min}$	Cutoff Percent[1]	R_c Equation Below Cutoff Percent
IM7/5250-4	Tape	Tension	0.050	30	$R_c=-0.000739(P_{TF}-7)+0.067$
IM7/5250-4	Tape	Compression	0.018	30	$R_c=-0.001957(P_{TF}-7)+0.063$
IM7/5250-4	Fabric	Tension	0.030	27	$R_c=-0.003172(P_{TF}-12.5)+0.076$
IM7/5250-4	Fabric	Compression	0.017	29	$R_c=-0.003879(P_{TF}-12.5)+0.081$
IM7/977-3	Tape	Tension	0.046	30	$R_c=-0.001348(P_{TF}-7)+0.077$
IM7/977-3	Tape	Compression	0.019	30	$R_c=-0.001826(P_{TF}-7)+0.061$
IM7/977-3	Fabric	Tension	0.033	32	$R_c=-0.002769(P_{TF}-7)+0.087$
IM7/977-3	Fabric	Compression	0.021	29	$R_c=-0.005273(P_{TF}-7)+0.108$
MTM45-1	Tape	Tension	0.0251	25	$R_c=-0.001128P_{TF}+0.053$
MTM45-1	Tape	Compression	0.0136	27	$R_c=-0.0027748P_{TF}+0.090$

1. **Cutoff Percent** is the percent of tangential fibers, P_{TF}, above which R_c is assumed to be constant

For a typical analysis the stress or strain at the characteristic dimension from the edge of the stress concentration is compared to the unnotched allowable for the material and layup and a margin of safety can be calculated. This will be illustrated in Sections 13.3 and 13.4. These characteristic dimensions accurately predicted margins of safety for chevrons and other stress concentrations with variable geometry, material, layup and loads by using IDAT/PACT to predict the strain field and comparing the strain at a distance R_c away from the edge to the unnotched material allowables. This is illustrated in Figure 13.2-1. The value for R_c is based on the percent of tangential fibers at the area of peak stress at the edge of the hole or cutout.

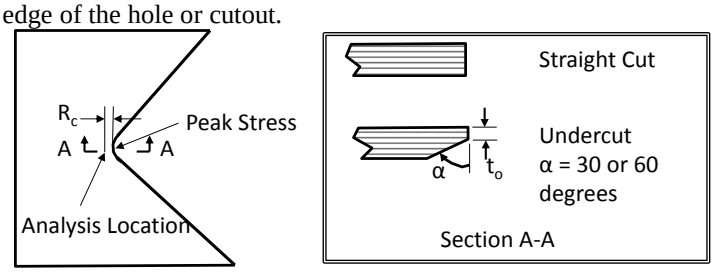

Figure 13.2-1 Illustration of Characteristic Dimension and Edge Geometry

There is an additional reduction, $K_{undercut}$, required if the material is undercut or chamfered as shown Section A-A of Figure 13.2-1. These factors are shown in Table 13.2-2. Do not use radii smaller than 0.06. For radii between 0.06 and 0.25, interpolation is allowed for initial design; however, element testing is recommended prior to final analysis.

Table 13.2-2 Reduction Factors for Undercut at Edge, $K_{undercut}$

Undercut Angle from Vertical	Applicable Radius	
(α, Degrees)	0.25 inch	0.06 inch
0	1.00	1.00
30	1.00	0.73
60	0.90	0.73

Copyright 2015 Lockheed Martin Corporation.
Note: The current version is always the version on the Lockheed Martin network.

The margin of safety at the characteristic dimension for a straight cut edge, $MS_{straight\ cut}$ is determined by the use of IDAT/PACT or through the use of a fine grid finite element model and analysis. If the edge is not undercut, then this is the final margin of safety, *i.e.*, $MS=MS_{straight\ cut}$. If the part is undercut, the final margin of safety is determined from

$$MS = [K_{undercut} \cdot (MS_{straight\ cut} + 1)]-1 \qquad \textbf{Equation 13.2-1}$$

where
$MS_{straight\ cut}$ is the margin of safety at the characteristic dimension for a straight cut edge
$K_{undercut}$ is the correction for chamfer and radius, if required

13.3 Chevrons

Chevrons are common features on the external skins of modern aircraft where fixed skin panels are split or where a fixed skin is adjacent to a removable panel. The discussion in this section concerns chevrons without joggles. For chevrons with joggles see Section 13.5 as some additional failure modes and critical locations must be considered. Figure 13.3-1 shows some areas with skins having chevrons.

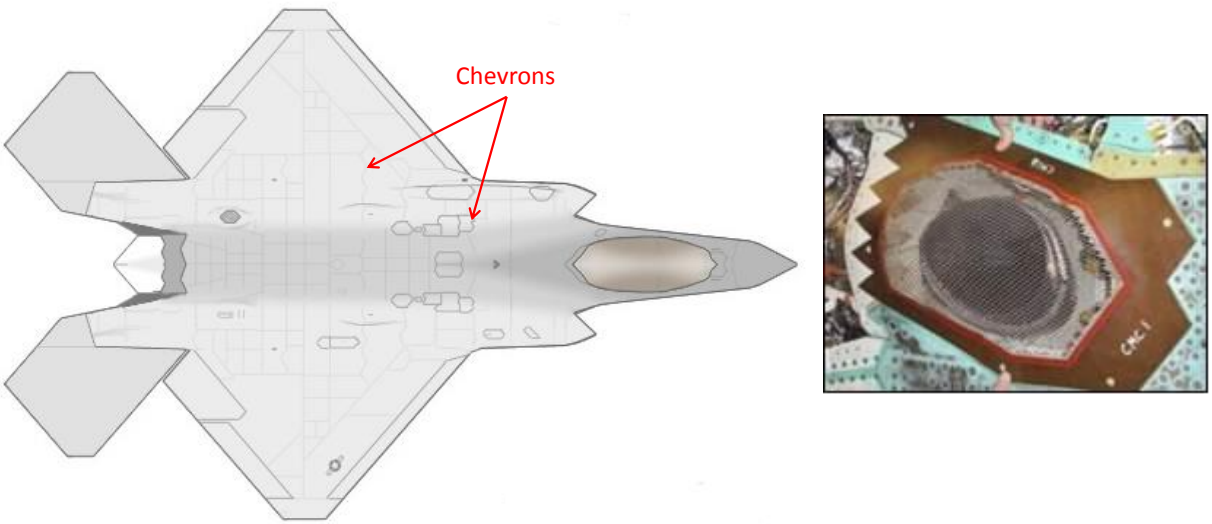

Figure 13.3-1 Examples of Chevrons on Aircraft External Skins

The chevron is a series of peaks and notches at the edge of a panel as shown in Figure 13.3-2. Note that the edge of the chevron can be straight cut or undercut as shown in Detail A-A. Undercutting the edge reduces the allowable strength. The legs of the chevron may be the same length or they may be of different lengths. The presence of chevrons can have an adverse impact on the weight of the skin panel and substructure, so it is crucial that the analyst work with design to minimize the impact to the degree possible.

Testing has been performed on a legacy aircraft program for notch radii of 0.25 and 0.06. The failure mode is a combined stress at the notch radius driven by net section tension. If the chevron is long and the peak overhangs the substructure by a significant amount, the stress at the notch is increased by stress due to bending resulting from aerodynamic pressures. Support of the chevron peak is important to minimize the impact that the chevron design has on the weight. This can be done by strategically placing the chevron peak over substructure such as a frame or rib cap with integral stiffeners or an intersecting longeron.

Copyright 2015 Lockheed Martin Corporation.
Note: The current version is always the version on the Lockheed Martin network.

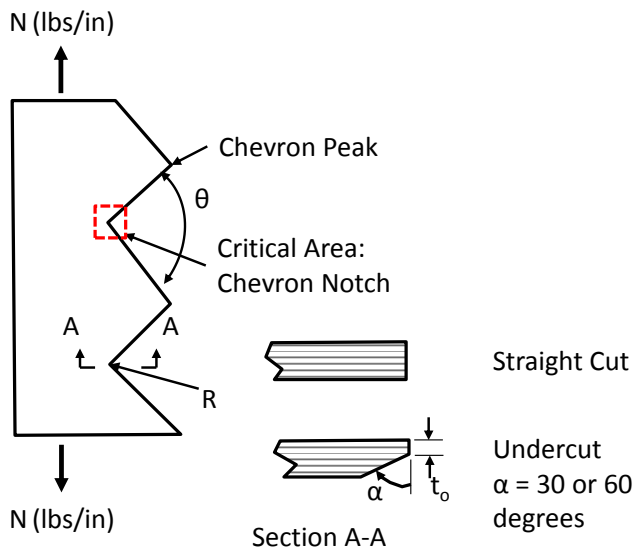

Figure 13.3-2 Laminated Panel with a Chevron Notch

The chevron analysis presented here has been correlated to the testing discussed above, Reference 13-13. The limits for applicability of the method are presented in Table 13.3-1. While the method may be used for preliminary sizing for geometries outside of these parameters, development testing is required for final analysis and verification.

Table 13.3-1 Limitations on Chevron Analysis Methodology

Parameter	Limitation	Discussion
Radius	$0.06 \leq R$	Use as big a radius as possible to minimize weight impact
Included Angle	$75° \leq \theta \leq 105°$	Test Geometry ±15°
Undercut Angle	$\alpha \leq 60°$	Test Limits
Remaining Thickness at Undercut	$t_o \leq t/2$	t is the total laminate thickness t_o is the remaining laminate thickness after undercut
	$t_o > t/2$	No undercut analysis required

The selection of some of the key parameters for the chevron geometry, such as notch radius or undercut angle, will be driven by considerations other than structural integrity; however, these selections can have a profound effect on the panel sizing, *i.e.*, thickness and weight. Figure 13.3-3 examines, parametrically, the effect of the chevron notch radius on remaining strength of the panel for tension and compression loads with all other geometry held constant. Note that a panel with the minimum radius 0.06 is predicted to be about half as strong as a panel with radius of 1.5 inches. While radii of 1.5 inches may not meet other design goals, emphasis should be placed on using the largest radius which satisfies all of the design objectives including strength and weight.

Copyright 2015 Lockheed Martin Corporation.
Note: The current version is always the version on the Lockheed Martin network.

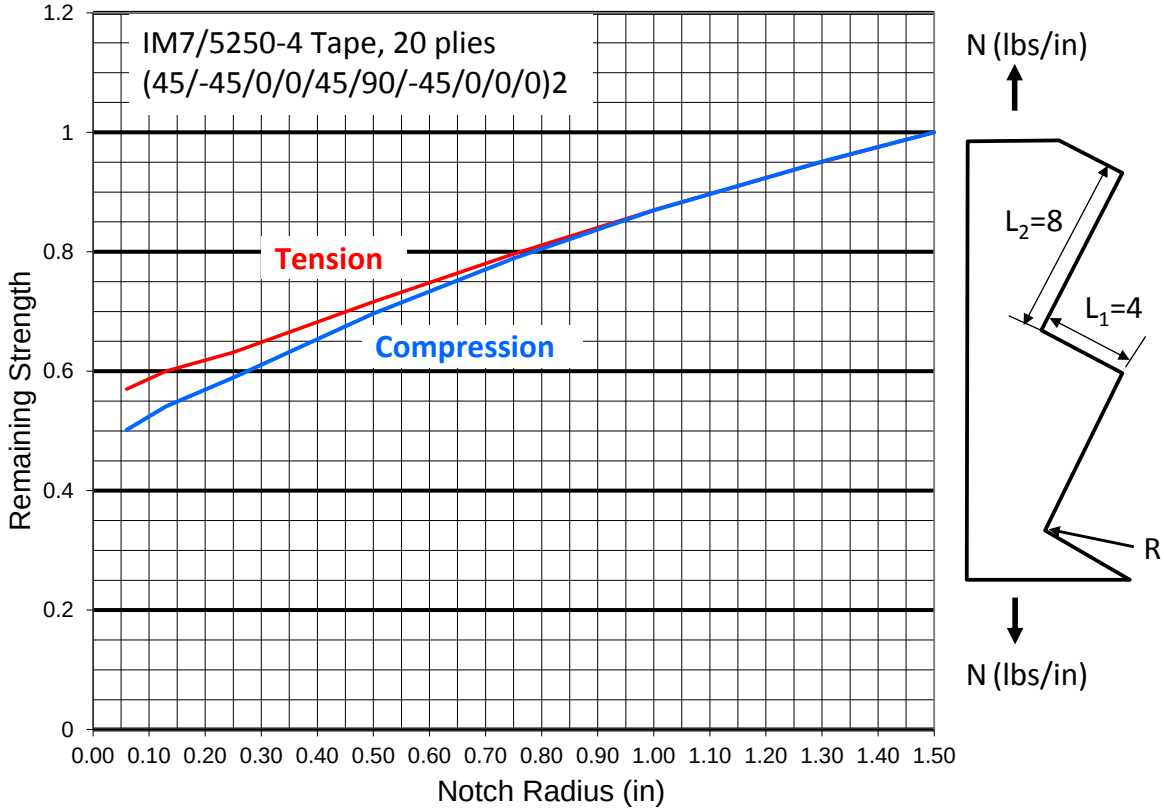

Figure 13.3-3 Effect of Chevron Root Radius on Panel Strength

For panels without pressure loading or for panels where the chevron peaks are adequately supported such that any pressure loading does not increase the stresses, chevron panels can be analyzed using IDAT/PACT. The steps will be discussed in Section 13.3.1. For panels where pressure loads are applied and cause bending stresses at the notch, a fine grid finite element analysis approach is recommended.

13.3.1 IDAT/PACT Analysis for Chevron Notches

The analysis using PACT starts with idealizing the panel with chevrons as a panel with a rotated rectangular hole. The length and width of the hole are the lengths of the adjacent legs in the chevron and the radius at the notch is used as the radius of the rectangular cutout. The hole is rotated to match the orientation of the chevron to ply direction and loading. Figure 13.3-4 shows the geometry of a typical chevron and Figure 13.3-5 shows how that geometry is idealized for input into IDAT/PACT.

The load that is applied to the IDAT/PACT model is dependent on the substructure arrangement and the adjacent fasteners. Figure 13.3-4 shows a possible fastening configuration but a free body diagram of the specific panel should be constructed with the fasteners reacting loads as appropriate. In addition there may be moments due to pressures which also must be included in any final analysis. IDAT/PACT can only accommodate in-plane applied loads and a finite element analysis will be required if the actual panel sees significant bending due to pressure. Note that typically the IDAT/PACT model will be loaded with panel y-direction loading, as defined in Figure 13.3-4 or in a direction that opens the notch created by the chevron. The x direction running load and the running shear are reacted by the fasteners and the centerline of the idealized panel represents the free edge of the actual part.

Copyright 2015 Lockheed Martin Corporation.
Note: The current version is always the version on the Lockheed Martin network.

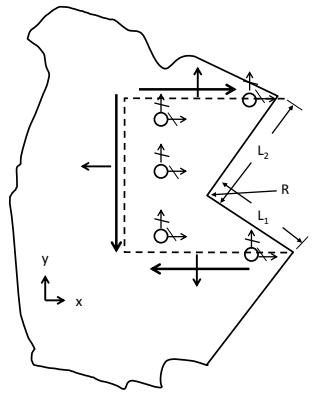

Figure 13.3-4 Panel Chevron Geometry and Possible Loading

The idealized panel used in the analysis has a width and length a minimum of 3 times the notch depth. Figure 13.3-5 shows how to translate the notch dimensions into the appropriate panel dimensions as well as how to rotate the rounded rectangular opening to the appropriate orientation.

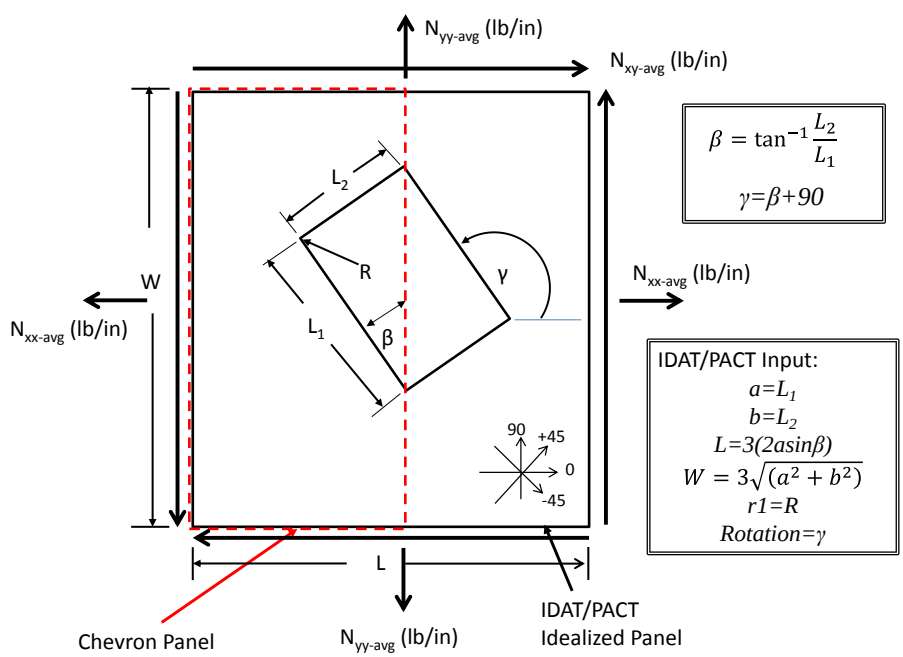

Figure 13.3-5 Idealized Panel Geometry for Input to IDAT/PACT

Chevron analysis also uses a characteristic dimension from the edge of the notch radius for the determination of stresses and the calculation of margins of safety. The development of the characteristic dimension is given in Section 13.2.1. Because the characteristic dimension will change as the ply percentages change, it must be calculated at each analysis location. IDAT/PACT calculates margins of safety for each of eight locations around the rectangular hole and, for materials which have developed equations for the calculations of R_c, will automatically calculate the correct and appropriate value then use it for the determination of margin of safety if the "Calculate Char. Distance" box is checked. For materials not included in Table 13.2-1, element testing may be required to develop the appropriate values for use. The user can also calculate and input the characteristic distance.

One other parameter is of importance and that is the refinement option. Always choose the highest number available. There can be a small time penalty as the refinement goes up.

Copyright 2015 Lockheed Martin Corporation.
Note: The current version is always the version on the Lockheed Martin network.

Because only the chevron notch is of importance in the IDAT/PACT model, if the chevron is idealized as shown in Figure 13.3-5, only the margin of safety at Location 2 will be used because it is the location where the fibers are tangential to the edge.

13.3.2 Example Problem Using IDAT/PACT

Given a chevron panel with the dimensions and loading shown. All remaining loads are reacted by fasteners. Analyze the chevron notch using IDAT/PACT.

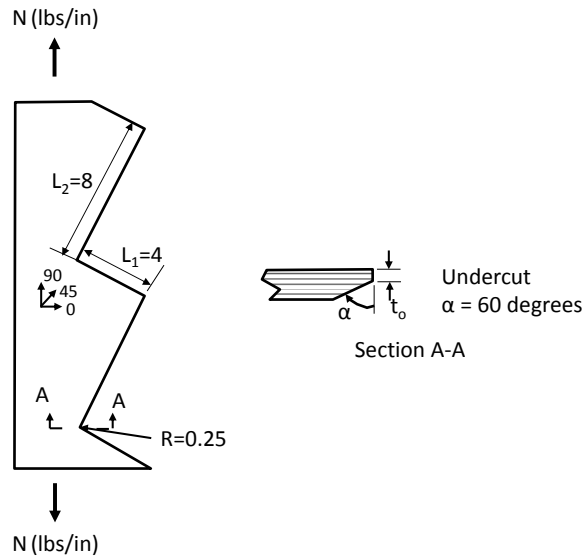

Material and Layup: IM7/5250 Tape at 75 degrees F. 20 ply laminate: (45/-45/0/0/45/90/-45/0/0/0)s

Loading N: 1000 lb/in=N_y in IDAT/PACT

From Figure in Problem Statement:
L_1 = 4 in.
L_2 = 8 in.

From Figure 13.3-4:
$\beta=\tan^{-1}(L_2/L_1) = \tan^{-1}(8/4) = 63.45$ degrees
$\gamma=\beta+90 = 63.45 + 90 = 153.45$ degrees
a=L1=4 in
b=L2=8 in
L= 3[2asin(β)]=3(2)(4 in)sin(63.45 degrees) = 21.46 in. Use 22 in
$W = 3\sqrt{a^2+b^2} = 3\sqrt{4^2+8^2} = 26.82$ Use 27 in.
r1=R=0.25
Rotation = γ = 153.45 degrees

Copyright 2015 Lockheed Martin Corporation.
Note: The current version is always the version on the Lockheed Martin network.

IDAT/PACT Input:

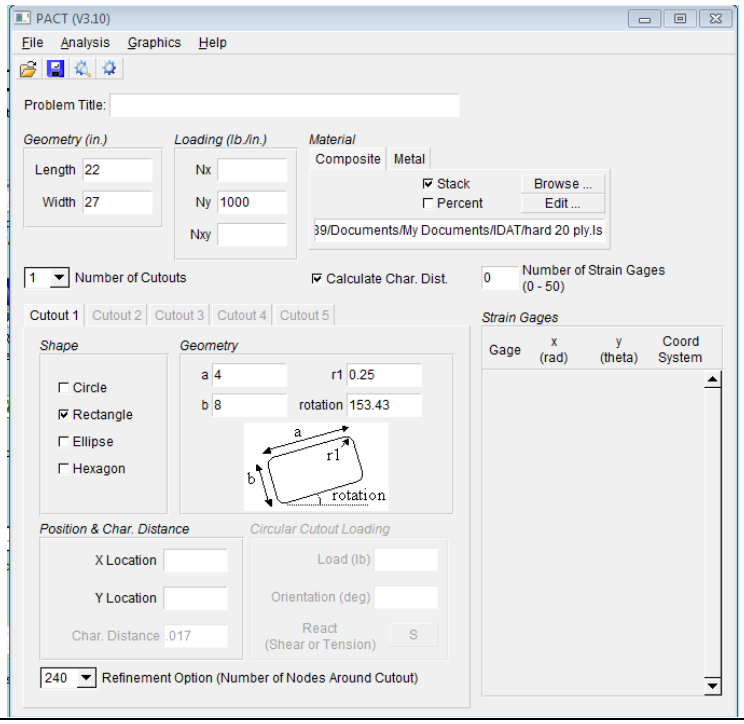

IDAT/PACT Depiction of Problem:

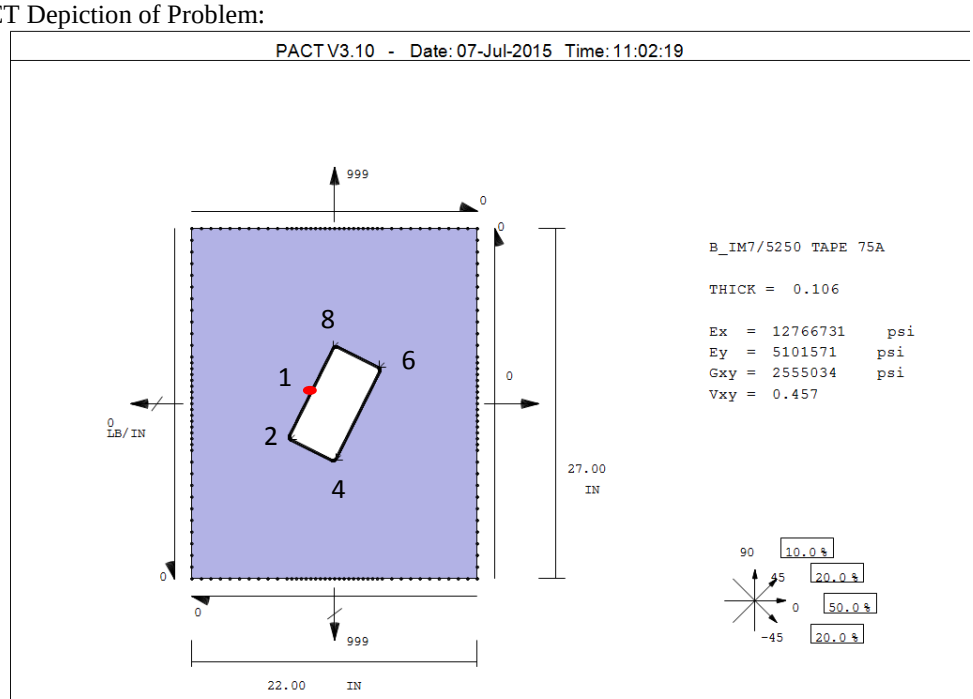

Numbers 1-8 represent analysis locations after rotation.
Critical location for Chevron Panel is Location 2.

Copyright 2015 Lockheed Martin Corporation.
Note: The current version is always the version on the Lockheed Martin network.

The output file echoes the laminate, laminate stiffness parameters, panel and hole geometry and the requested model refinement:

```
LAMINATE FILE:
c:/Users/g593189/Documents/My Documents/IDAT/hard 20 ply.ls

MATERIAL TYPE  1:  B_IM7/5250 TAPE 75A #B-BASIS FILE

STACKING SEQUENCE:  (0-DEGREE PLIES PARALLEL TO X-AXIS)
    LAYER NO.    MATL NO.    THETA    THICKNESS
         1           1        45.0       0.0053
         2           1       -45.0       0.0053
         3           1         0.0       0.0053
         4           1         0.0       0.0053
         5           1        45.0       0.0053
         6           1        90.0       0.0053
         7           1       -45.0       0.0053
         8           1         0.0       0.0053
         9           1         0.0       0.0053
        10           1         0.0       0.0053
        11           1         0.0       0.0053
        12           1         0.0       0.0053
        13           1         0.0       0.0053
        14           1       -45.0       0.0053
        15           1        90.0       0.0053
        16           1        45.0       0.0053
        17           1         0.0       0.0053
        18           1         0.0       0.0053
        19           1       -45.0       0.0053
        20           1        45.0       0.0053

SKIN MATERIAL PROPERTIES:
    EX  = 0.1277E+08
    EY  = 0.5102E+07
    GXY = 0.2555E+07
    VXY =  0.457

SKIN GEOMETRY:
    LENGTH    =  22.00
    WIDTH     =  27.00
    THICKNESS =  0.106

LOADING:
    Nx  =       0.0
    Ny  =    1000.0
    Nxy =       0.0

NUMBER OF CUTOUTS = 1

    CUTOUT 1 IS A RECTANGLE WITH ROUNDED CORNERS
    WITH DIMENSIONS:
          LENGTH =   4.000
          WIDTH  =   8.000
          CORNER RADIUS =  0.250
    LOCATED AT (X,Y) =   0.000,  0.000
    ROTATED  153.4 DEGREES FROM X-AXIS.

CUTOUT  1 CHARACTERISTIC LENGTH =  Computed

MODEL REFINEMENT:

    COMPONENT             SEGMENTS
    ----------------------------
    EXTERNAL BOUNDARY        156
    CUTOUT 1                 240
    ----------------------------
    TOTAL                    396
```

Copyright 2015 Lockheed Martin Corporation.
Note: The current version is always the version on the Lockheed Martin network.

Also in the output file, after the listing of stresses at the cutout boundary is the summary characteristic dimensions, critical stress at the characteristic dimension for each of the 8 locations, a summary of the unnotched allowables and the minimum margin of safety at each of the 8 Locations. Only location 2 is of interest for the chevron analysis.

```
CHARACTERISTIC DISTANCE (Rc) CALCULATION:

    Computed by:  Rc = min(A, B*[PTF - C] + D), where:
         A          B          C          D
      ---------------------------------------------
       0.0500  -0.000739    -7.00      0.067  Tension      - Material  1
       0.0180  -0.001957    -7.00      0.063  Compression  - Material  1

                     Tang.     Tang.
    Cutout   Pos.   Angle    Strain (T/C)     PTF      Rc
    ---------------------------------------------------------
      1       1       90      -347.1 (C)     10.00   0.0571
      1       2      -45      5682.2 (T)     20.00   0.0574
      1       3        0       967.0 (T)     50.00   0.0500
      1       4       45      -973.7 (C)     20.00   0.0376
      1       5       90      -347.1 (C)     10.00   0.0571
      1       6      -45      5682.3 (T)     20.00   0.0574
      1       7        0       967.0 (T)     50.00   0.0500
      1       8       45      -973.7 (C)     20.00   0.0376
```

Characteristic Dimension Calculation

```
STRAIN GAGE DATA:

    DATA FOR CUTOUT 1

No.     Rc       X        Y      SIG X      SIG Y      TAU XY     EPS X      EPS Y      GAM XY
  1  .0571   -0.105    4.354   -13770.9   -1876.0    -4473.7    -1011.6      124.8    -1750.9
  2  .0574   -3.550   -2.571    11011.6   56376.7    -2438.1    -1153.6    10657.0     -954.2
  3  .0500   -3.455   -2.783    23230.4   34939.5   -20737.2      570.1     6018.0    -8116.2
  4  .0376   -0.112   -4.424   -32115.8   -3717.6      296.0    -2382.6      419.8      115.9
  5  .0571    0.105   -4.354   -13770.9   -1876.0    -4473.7    -1011.6      124.8    -1750.9
  6  .0574    3.550    2.571    11011.7   56376.9    -2438.1    -1153.7    10657.1     -954.2
  7  .0500    3.455    2.783    23230.5   34939.6   -20737.2      570.1     6018.0    -8116.2
  8  .0376    0.112    4.424   -32115.8   -3717.6      296.0    -2382.6      419.8      115.8
```

Stresses at each of the 8 locations. For Chevron Analysis only Location 2 is of interest

```
FAILURE ANALYSIS:

    MATERIAL  1 ALLOWABLES: B_IM7/5250 TAPE 75A #B-BASIS FILE

       DIRECTION        PLY STRAIN ALLOWABLE
         1 TEN.                13719.6
         1 COMP.              -11406.3
         2 TEN.                10607.0
         2 COMP.              -24023.9
          1-2                  33973.9
```

Unnotched Allowables

```
    DATA FOR CUTOUT 1

     MAX-STRAIN FAILURE ANALYSIS
No.     X        Y        M.S.    PLY
 1    0.105    4.354     7.649     1
 2   -3.550   -2.571     0.287     6
 3   -3.455   -2.783     0.866     2
 4   -0.112   -4.424     3.787     3
 5    0.105   -4.354     7.649     1
 6    3.550    2.571     0.287     6
 7    3.455    2.783     0.866     2
 8    0.112    4.424     3.787     3
```

Margin of Safety – Location 2 only

The problem panel had an undercut of 60 degrees. So the straight cut margin of safety, $MS_{straightcut}$=0.287 must be modified by $K_{undercut}$. From Table 13.2-2, for a 0.25 in radius, $K_{undercut}$ = 0.90.

Using Equation 13.2-1:

$MS = [K_{undercut} \cdot (MS_{straight\ cut} + 1)]-1 = [0.90(0.287+1)]-1 = 0.15$ *(Net Tension at the Chevron Notch)*

13.3.3 Fine Grid Finite Element Detailed Analysis for Chevron Notches

If the loading is more complex than can be accommodated in IDAT/PACT then an ultra-fine grid finite element model should be constructed using shell elements. Solid elements are not required for this analysis and undercuts or chamfers along the edge are not modeled. Figure 13.3-6 shows an example of an ultra-fine FGFEM of the chevron notch detail which started with a fine grid model. The area around the notch was extracted and subdivided into smaller elements.

Copyright 2015 Lockheed Martin Corporation.
Note: The current version is always the version on the Lockheed Martin network.

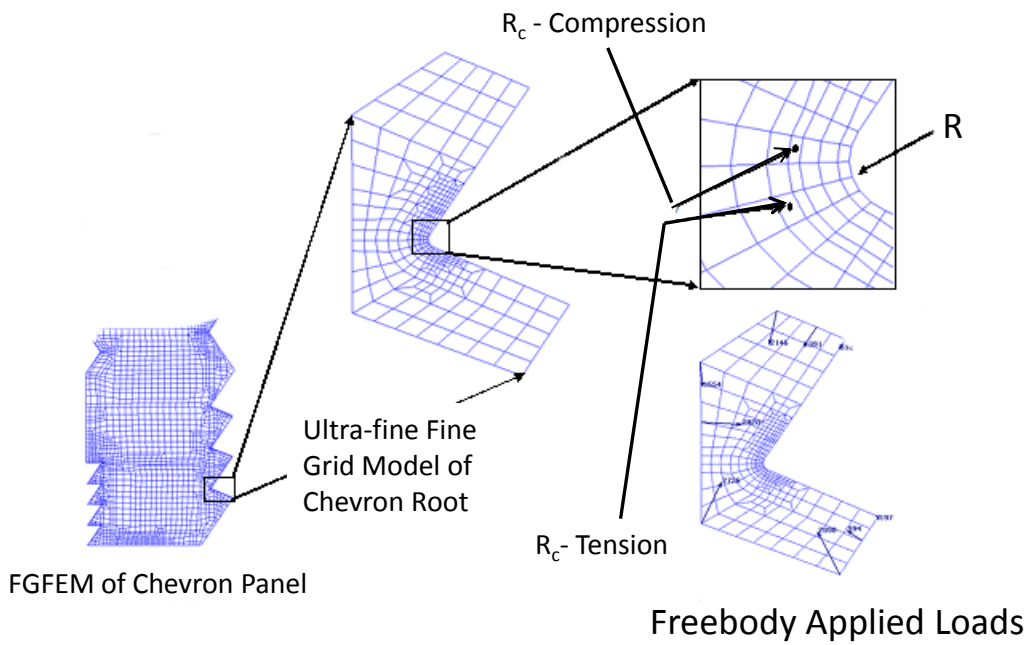

Figure 13.3-6 Sample Chevron Notch Ultra-fine Fine Grid Model

The model needs to have a sufficiently fine mesh in the area of the notch such that it captures an element at the characteristic dimension which is small enough to provide converged element forces. Note that there are different characteristic distances for tension and compression which should be calculated based on laminate orientation tangent to the root of the notch.

The model is typically loaded with balanced free body forces and moments from AVFEM or an intermediate-level FEM. The model is run for a linear NASTRAN Solution 101. The element forces are extracted from the fine grid FEM at the appropriate characteristic distance along a radial direction from the free edge for use in IDAT/SQ5. In setting up the IDAT/SQ5 run, M_x and M_y should be reduced by the appropriate bending factor as discussed in Section 7.4.1, typically 1.2. M_{xy} should be set to zero since 2D FEM output is not accurate in the immediate vicinity of joints and understructure.

Using IDAT/SQ5 results, determine the chevron notch radius minimum margin of safety. If the panel is undercut use the appropriate reduction factor, $K_{undercut}$, from Table 13.2-2 and Equation 13.2-1 to determine the final margin of safety. The minimum IDAT/SQ5 margin of safety is $MS_{straight\ cut}$.

Note that if element-level moments are negligible and the fine-grid element forces and displacements are shown to be converged, then a direct calculation of the fiber-direction margins of safety at the appropriate characteristic distances without using IDAT/SQ5 can be done. For this calculation, use FEM strain output and unnotched B-basis strain allowables at the appropriate environmental condition.

13.4 Cutouts or Holes in Webs or Panels

Holes, penetrations or cutouts in air frame structure are used for systems tubes or electrical wires to pass through, for ventilation flow, for mounting of equipment, access to the opposite side, or to make the part lighter. These holes may be any shape, but oval, elongated round or round holes are preferred. Square or rectangular holes are discouraged because the stress concentration in the corners, even if the corners are generously radiused, can lead to delaminations or early failure.

Copyright 2015 Lockheed Martin Corporation.
Note: The current version is always the version on the Lockheed Martin network.

There are two areas of concern related to the presence of holes in composite webs or skins. The first is the issue of the reduction of the buckling capability of the panel due to the presence of the hole and the second is how much of a stress concentration is created by the presence of the hole and how does that affect the strength at the hole's edge.

Typically, cutouts and holes are not modelled in an Air Vehicle level finite element model unless they are substantial. As these models grow more refined, larger cutouts may be modeled, explicitly, or by reducing the stiffness in the particular web in which they are located. This is done to determine the correct internal loads in the web and caps.

To perform the analysis, holes and cutouts are typically modeled in stand-alone finite element models of a single panel or multiple adjacent panels, running NASTRAN Solution 105 to determine the buckling eigenvalue and Solution 101 for strength analysis. The model can use unit loads or load combinations for stability or loads that have been extracted from the air vehicle model for both stability and strength. Alternately a detailed model of the panel with holes is constructed and inserted into a coarser mesh subset of the A/V FEM. This may be done for a number of reasons including the complexity of the contours of the panel or skin, unusual boundary conditions and/or the complexity of the loads. The appropriate level of refinement is required to determine the correct solution. If the model is too coarse, the FEA code may not be able to determine the correct eigenvalue. If it is too refined then the stresses at the edge of the hole may be overly influenced by the hole stress concentration when the model is used for strength checks.

IFEM/POPPI is a rapid preprocessor to develop individual bay or panel models with various hole geometries. However, at this time, it automatically runs only panels with isotropic properties, so post-processing of the model by hand to input the appropriate orthotropic properties prior to execution is required to use POPPI for composite panels.

Additionally, computer tools such as IDAT/PACT, used to determine the effect of the stress concentration is also employed. IDAT/CUTOUT is a tool which will assess the impact adding doubler plies or a doubler to the web with a cutout but it addresses only the stress concentration and not the web stability. Additionally it provides no insight into the surface area of the proposed plies or doubler, only the thickness. See Section 13.11 for a discussion of these tools.

If the cutout is made in conjunction with a joggle, see Section 13.5.

13.4.1 Web Buckling with Hole

PM4056 Section 2.4.6 discusses recommended buckling criteria, including panels and webs with holes. Specifically, Table 2.4-5 recommends that unreinforced holes in webs shall not buckle below design ultimate load as this will likely precipitate a web failure. If the hole has reinforcement then it may be allowed to buckle at 37.5% of Design Limit Load (DLL). So if a hole is present some means of determining the impact of the hole on the buckling stability must be undertaken.

The many experimental studies of aluminum beam structure undertaken to determine the impact of holes have resulted in various curves which can provide a good approximation of the impact to the buckling eigenvalue for both shear resistant and diagonal tension metallic beams. This same approach is not really applicable to composite structure unless the beam or panel is quasi-isotropic, but even with that, the curves developed for aluminum thin sheet structure don't directly apply to composite beams. Most composite beams or panels have stiffness tailoring and the buckling behavior with holes is studied through the use of FEA analysis coupled with confirmatory testing.

Figure 13.4-1 shows a comparison of a panel 8 inches wide x 20 inches tall for aluminum, a 25/50/25 IM7/5250-4 tape layup and 10/80/10 IM7/5250-4 tape layup for the impact of different size holes. The results are based on a finite element study and are shown here to illustrate the effect that adding a single unreinforced hole can have on panel buckling capability. The panel was loaded separately in shear and compression. The composite results for this can be compared with the aluminum curve and it shows that the 25/50/25 quasi-isotropic layup results in very similar reduction factors to the aluminum panel. However, the 10/80/10 panel has a higher reduction factor. The

Copyright 2015 Lockheed Martin Corporation.
Note: The current version is always the version on the Lockheed Martin network.

dashed lines represent the reduction factor for an axial running load applied along the long edge of the part for the two different layups. Again the 10/80/10 would result in a more significant reduction.

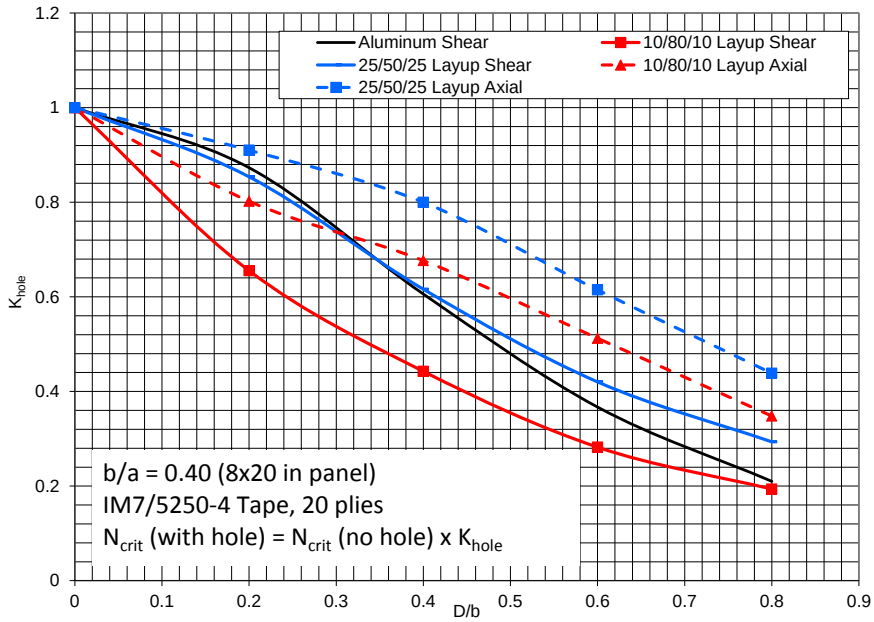

Figure 13.4-1 Comparison of Reduction in Buckling Capability of Panels with Holes

Note that even a relatively small hole on the order of 25% of the width of the web can result in a reduction in buckling capability as large as 40% for shear loading and 20% for axial loading for this specific panel size and layups. While the strength and stiffness of a composite panel varies with position around the hole in a more complex manner than that of aluminum structure, the use of some of the empirical geometric guidelines and limitations on hole size borrowed from the metallic beams seem prudent. Table 13.4-1 summarizes the pertinent guidelines, taken from PM4057, Reference 13-1, Section 6.7, which are limitations on hole size relative to web size as well as recommendations on reinforcement doubler width.

Table 13.4-1 Geometric Guidelines and Limitations for Unbuckled Webs with Cutouts

Parameter	Lightly Loaded Beams	Flanged Holes in Moderately Loaded Beams	Holes with Doublers
D/h	0.25 to 0.75	≤0.50	≤0.50
D/b	0.30 to 0.70	≤0.85-0.1(h/b)	≤0.67
b/h		0.2 to 1.0	
W/D			0.35 to 0.50
D is the diameter of the cutout (in) h is the web height of the beam (web height to centroid of caps) (in) b is the web width of the beam (fastener line or stiffener centroid if bonded) (in) W is the width of the reinforcement ring (in)			

Flanged holes in composite beams have <u>not</u> been studied in depth at Lockheed Martin; any use of flanges to stabilize the web with a hole would need to have development testing performed.

Copyright 2015 Lockheed Martin Corporation.
Note: The current version is always the version on the Lockheed Martin network.

13.4.2 Panel Hole Reinforcement

Based on testing of unreinforced holes performed on composite beams and panels at Lockheed Martin[1], holes 0.50 inch in diameter and smaller do not have a significant impact on panel strength and stability. For internal unbuckled aircraft structure, panels with holes greater than 0.50 inch in diameter are typically reinforced with additional doubler plies, or with bolted or bonded composite or metallic doublers or by adding stiffeners to reduce the bay size.

Testing performed under Reference 13-14 indicates that adding integral plies is not as effective as adding a metal or composite ring doubler. In the conclusion section, it is stated "integral ply buildups around the hole of up to 2.7 times the nominal thickness did not sufficiently stabilize the hole in any of the configurations tested where the buckle can pass through the hole" and further "shear panel with penetration holes must be stabilized through the use of ring doublers and/or externally attached stiffeners to meet hole stability requirements." This report also recommends that holes in webs be placed near the panel boundary, but away from corners and away from anticipated lines of diagonal tension for shear panels. The classical failure of a shear panel is in the corners.

Doubler reinforcement replaces the material removed by the hole, restores web stability and reduces the stresses due to the stress concentration caused by the presence of the hole. For stability, the doubler material must beam the load in the panel around the missing material. Thus, as a minimum, the area of the doubler, given by Equation 13.4-2 is equal to the cross-sectional area of the hole given by Equation 13.4-1 with the width of the doubler set by the parameters of Table 13.4-1. Some program guidance may require the area of the doubler to be 1.15 to 1.25 times the area of the material removed.

For a round hole, the cross-sectional area of the cutout is given by

$$A_{cutout}=Dt \qquad \textbf{Equation 13.4-1}$$

where D is the diameter of the hole (in)
t is the laminate thickness (in)

The cross-sectional area of the doubler is given as

$$A_{doubler}=2Wt_{dblr} \qquad \textbf{Equation 13.4-2}$$

where W is the width of the doubler(in)
t_{dblr} is the doubler thickness (in), *i.e.*, the thickness of the *added* plies

A doubler of this type is illustrated in Figure 13.4-2.

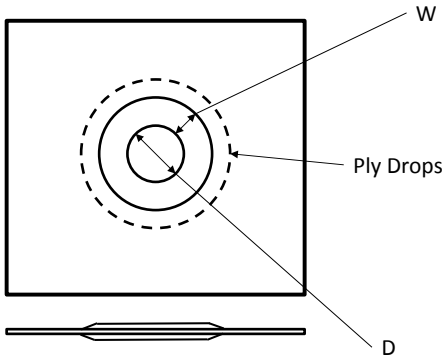

Figure 13.4-2 Geometry of Web with Integral Doubler

It is recommended that any of these reinforcements are symmetrically placed on the web, such that there is no eccentric loading and secondary bending. If stability is not a driver for panel sizing and the doubler consists of additional integral plies, then the added plies should be symmetric and balanced about the centerline of the

[1] Reference 13-14 Section 2.0 Test Summary

Copyright 2015 Lockheed Martin Corporation.
Note: The current version is always the version on the Lockheed Martin network.

composite and the plies should be interspersed in the basic laminate, rather than added as a single pack of plies on the outside. This improves the load transfer and reduces the stress concentration at the edge of the plies. Standard ply drop and taper guidelines would apply. Refer to PM4056 Section 2.3 for discussions on ply drop and taper guidelines as well as stacking sequence to minimize free edge interlaminar tension failure.

If the panel is stability critical and a separate bonded or bolted composite doubler is used, then the doubler attached on each face of the web should be balanced and symmetric about the doubler centerline to minimize residual stresses in the bond line resulting from any doubler warping. A bonded doubler should be taper-stepped and the stress in the bond line needs to be analyzed using IDAT/AE4I or IDAT/IBOND. Refer to Section 19.8.17 for a discussion of bonded doublers.

Analysis is performed by adding the doubler plies, doubler or stiffeners to the finite element model of the bay or panel. This can then be run to check for the impact on the buckling strength of the panel with the hole as well as to obtain the stress levels at the edge of the hole. Analysis for the strength of the panel is discussed in the next section.

13.4.3 Strength in Panels with Holes

In addition to the reduced buckling capability of a web with a hole which is restored through the use of the reinforcement doubler, there is a stress concentration resulting from the presence of the hole. For non-symmetric hole reinforcements the peak stresses can actually exceed the non-reinforced values as a result of secondary bending and higher stress concentration thus creating a more critical design. In addition there can be peaking of interlaminar stresses at the edge of the hole. If unsymmetrical reinforcements have to be used the interlaminar shear stresses at the edge of the hole and peak in-plane stresses at the edge of the hole must be examined using 3-D finite element analysis. Refer to Section 4.5.4 for a discussion of three dimensional failure criteria and Section 4.4.3.3 for a discussion of interlaminar free edge stresses.

To analyze the strength at the cutout, the ultimate peak stress at a characteristic dimension, R_c, from the edge of the hole is compared to unnotched allowables as discussed in Section 13.2.1. This stress can be taken from a detailed finite element model and analyzed using IDAT/SQ5 or the program IDAT/PACT can be used. The characteristic dimension or characteristic distance is dependent on material, local percent tangential fibers, and loading. Equations to calculate the R_c for IM7/5250-4 tape and fabric and for IM7/977-3 tape and fabric are based on legacy test data. Table 13.2-1 shows the minimum R_c values and the percent tangential fibers cutoff above which the R_c is assumed to be constant along with the equations to calculate R_c for the percent tangential fibers below the cutoff.

Figure 13.4-3 illustrates the impact the presence of a hole has on the strength of the panel. It was created for the same panel size/ hole size/ layup combination as used for Figure 13.4-1, using the appropriate R_c values from Table 13.2-1 and running IDAT/PACT.

Copyright 2015 Lockheed Martin Corporation.
Note: The current version is always the version on the Lockheed Martin network.

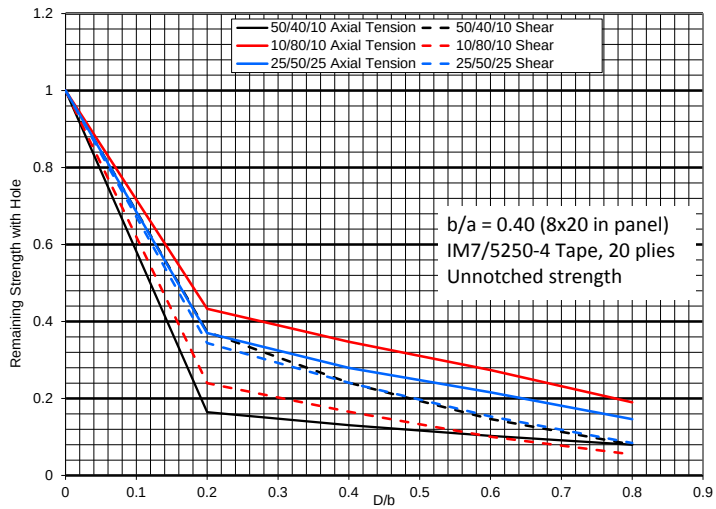

Figure 13.4-3 Remaining Strength for Panel with Unreinforced Holes for Different Layups and Loading

Note that the presence of an unreinforced hole whose diameter is 20% of the width of the panel reduces the remaining strength significantly to approximately 20-40% depending on layup and loading. As the hole gets larger relative to the panel width it continues to decrease to less than 20% for all layups and loading. Reinforcing the hole with a doubler would improve the response.

13.4.4 Durability and Damage Tolerance Considerations

If the panel with a hole is loaded in compression, then depending on the part classification, a durability and damage tolerance analysis may be required. Durability and damage tolerance analyses (DADT) are not performed at the edge of the hole but some distance from the edge of the hole as described in PM4056 Section 15.7.1 or per program guidelines. The panel and any doubler build-up should satisfy the design guidelines for laminate stacking sequence and taper as discussed in Chapter 2 to minimize interlaminar stresses due to ply drop offs and free edge effects. Although the appropriate DADT analyses need to be conducted, for a panel with a hole of any significant size, loaded in compression, typically stability considerations will limit the strains and durability and damage tolerance requirements will not size the panel.

The loads used for DADT analysis would typically come from the same fine grid FEM used to determine the buckling eigenvalues and the stresses for strength checks. Depending on the fineness of the model, element forces are averaged, as required, to represent an area approximately twice (circular) damage area predicted by the test to preclude sizing to peak FEM values that represent a fraction of the actual damage area. The elements should be chosen at a location consistent with the analysis location. Damage areas are discussed in Section 15.7.1.

DADT analysis is conducted, not at ultimate load, but at a residual strength load, P_{xx}, which will vary by program. The residual strength load may be maximum spectrum load or a load level which is defined by a factor on limit load which may vary from less than 1.0 for large transports to 1.05 to 1.25 times limit load for fighters. Also durability analysis and damage tolerance analysis may have different limit load factors for P_{xx}. Consult program guidance for the specific values.

13.4.5 Analysis Approaches for Panels with Holes

Table 13.4-2 describes the sequence in which the analysis of a panel or web with a hole should be approached based on how the presence of the hole impacts the web. Stability typically has the largest impact and, if a web is sized to satisfy the criteria for stability, it may have positive margins for all other checks.

Copyright 2015 Lockheed Martin Corporation.
Note: The current version is always the version on the Lockheed Martin network.

Table 13.4-2 Analysis Sequence for Webs with Holes

Step	Analysis Requirement	Analysis Approach	Comments
1	Check stability: stability of the web with hole per buckling criteria	Model web with hole in fine grid model for NASTRAN Solution 105 analysis to determine eigenvalue.	• IFEM/POPPI can be used to construct model but material properties will need to be modified • Model can be a single bay, appropriately constrained or multiple bays, or a fine gridded portion of the AVFEM
2	Size doubler reinforcement for stability, if required to meet buckling requirements	Determine doubler sizing per Section 13.4.2 and then add doubler to FEA model for NASTRAN Solution 105 analysis.	Adjust doubler sizing or add stiffeners to reduce bay size, if necessary.
3	Check strength: peak stress at appropriate characteristic distance from edge of hole using unnotched allowables	Use IDAT/PACT with web + doubler plies to determine margin of safety	If the fine grid model has sufficient fidelity to extract strains at the characteristic distance from the edge of the hole, use of IDAT/PACT is not required and strains from a linear run may be used for analysis
4	If doubler was not required for stability, size doubler for strength, if required	Used IDAT/CUTOUT to determine necessary additional plies for strength	
5	If part is durability critical, check durability margin of safety at $P_{xx\text{-}Durability}$	Use ¼ in protruding fastener filled hole analysis from IDAT/IBOLT or IDAT/CDADT, depending on program guidance.	Refer to Section 13.4.4 for discussion on determination of loads and Section 15.7.1 for determination of analysis location.
6	If part is fracture critical, check damage tolerance margin of safety at $P_{xx\text{-}DT}$	IDAT/CDADT	Refer to Section 13.4.4 for discussion on determination of loads and Section 15.7.1 for determination of analysis location.
7	If doubler is bonded, analyze bond line strength and interlaminar shear	IDAT/A4EI or IDAT/IBOND	Section 19.8.17 discusses bonded doubler repair for defective parts. The principles of reinforcement doublers are the same.
8	If doubler is bolted, analyze bolted joint attachments of doubler to web	IDAT/IBOLT and IDAT/SFBOLT	Section 19.8.16 discusses bolted doubler repair for defective parts. The principles of reinforcement doublers are the same. A minimum of two rows of fasteners spaced at 5D common to the doubler are required to ensure the doubler is effective.

Copyright 2015 Lockheed Martin Corporation.
Note: The current version is always the version on the Lockheed Martin network.

13.5 Joggles

Joggles are design features which allow for access doors or panels to sit flush with the surface of the aircraft. Joggles are not desirable in any structure and in particular in load bearing external composite skin panels in wings and fuselage structure due to the eccentricities created in the load line and the secondary interlaminar stresses which result; however, as with chevrons, this is a design feature that is present on modern aircraft for reasons other than structural integrity and, thus must be accommodated and the effect on weight minimized to the degree possible.

Extensive testing was performed on legacy aircraft for manufacturing development, static strength, durability and damage tolerance considerations. This included coupon and element level testing of multiple configurations, environments and materials. The materials tested included IM7/5250-4 and IM7/977-3. There were three primary geometries examined: molded with 60 degree ramp, machined with a 90 degree cut and machined with a 60 degree cut. These geometries are shown in Figure 13.5-1.

The manufacturing process and approach resulted in a good quality repeatable process after cure with negligible part distortion and minimal laminate thickness variation. It was determined that the molded design presents minimal design and fabrication risks. Confidence was also high for the machined design, but there were some areas of delamination observed at the machined step on some of the parts made.

While all three variations provided acceptable results in static strength, durability and damage tolerance testing, the molded performed better than the machined and the machined with the 60 degree ramp performed better than the machined with the 90 degree ramp. The implication of this statement is that the least impact to weight, if a joggle is necessary, would be to use a 60 degree molded design.

Durability and damage tolerance panels were impacted to 6 ft-lbs and 100 ft-lbs, respectively, cycled for a minimum of two lifetimes and then underwent residual strength testing. The residual strength requirement for the durability panels was the failure load had to meet or exceed 150%DLL. All panels passed successfully. For damage tolerance the residual strength requirement was the failure load had to meet or exceed 105% DLL. All panels went to a minimum of 150% DLL, far exceeding the requirement. The testing built confidence that the joggles were robust and there were no DADT issues.

Copyright 2015 Lockheed Martin Corporation.
Note: The current version is always the version on the Lockheed Martin network.

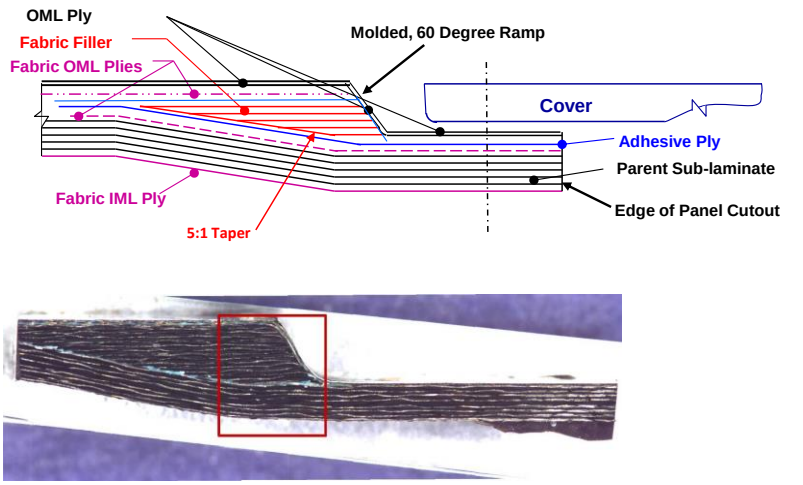

A. Molded Joggle

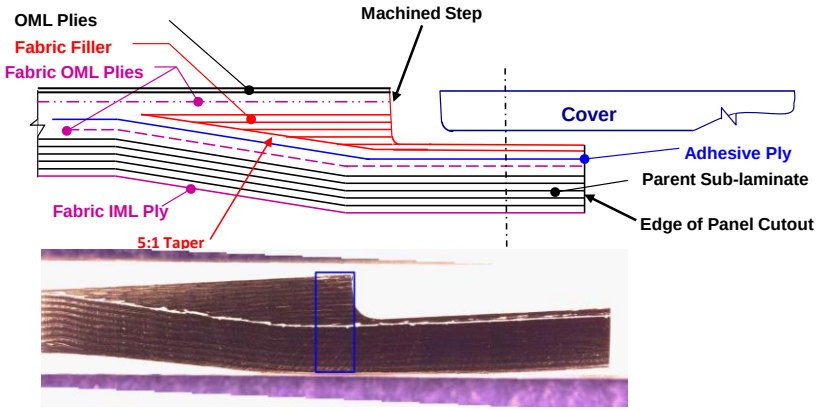

B. Machined 90 Degree Cut

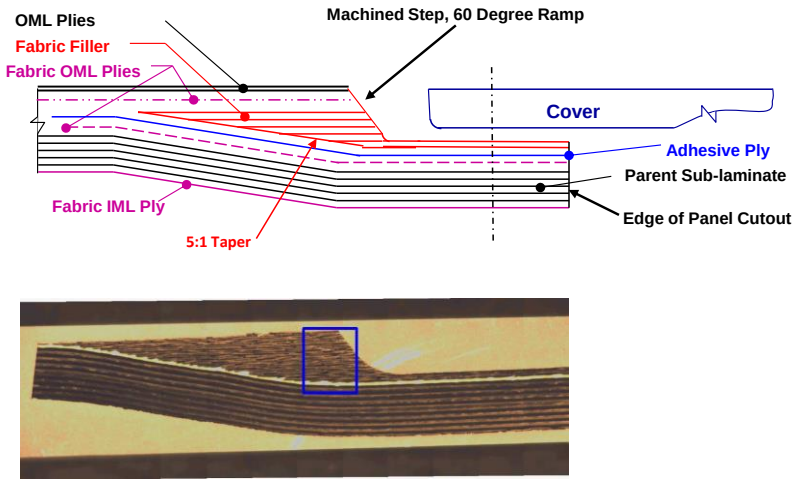

C. Machined 60 Degree Cut

Figure 13.5-1 Joggle Detail Configurations

Copyright 2015 Lockheed Martin Corporation.
Note: The current version is always the version on the Lockheed Martin network.

While the testing has shown that joggles can be used in composite panels, they do adversely impact the sizing of the panel and every effort should be made to minimize the presence of joggles as well as their depth. Table 13.5.1 provides some other design guidelines and lessons learned.

Table 13.5-1 Design Guidance and Lessons Learned for Joggle Features

Guidance Topic	Limitations / Guidance	Comments/ Discussion
Step Depth	Step ≤ 0.240 in. Testing required for new designs with a step exceeding 0.240 in.	Failure mode changed with increased step. Step and resulting eccentricity need to be minimized. Testing showed that halving the step resulted in doubling the failure load.
Taper of Ply Pack Insert	Minimum 5:1 Testing of specific configuration required if taper ratio is below 5:1	Test conducted at 5:1. Increased taper ratio is better.
Ply Pack Material and Layup	Use "soft" fabric filler pack ~(25/75/0)	Test filler packs were fabric (27/73/0).
Adhesive – Molded Design	Use adhesive commensurate with operating temperatures	Some testing used FM 300 and showed a disproportionate reduction in strength at elevated temperature wet.
Lay-up Method	Indications from limited testing are that fiber placed panels outperformed hand lay-up panels	Three fiber placed panels were tested.
NDI	Machined Panels: NDI detectible initial failure at some load level which grew to final failure Molded Panels: No NDI evidence of initial failure prior to final section failure	This could have implications in-service. If a panel is accidentally overloaded such that an initial failure has occurred, a machined panel would show evidence of this during NDI inspection. A molded panel would not.

13.5.1 Analysis of Panels with Joggles

The method of analysis provided in this section was correlated to the test results. The critical areas requiring analysis, in addition to the usual panel and joint analyses include the four locations shown in Figure 13.5-2. The presence of the hole in the joggled area also reduces the critical buckling load of the panel. In addition, if the 5:1 taper ratio is not maintained, ILT/ILS interaction needs to be analyzed at the locations indicated accompanied by specific geometry verification testing.

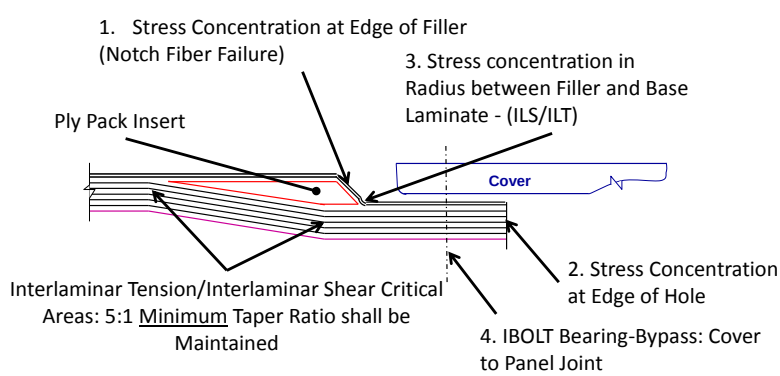

Figure 13.5-2 Critical Locations and Analysis Required for Joggle Details

The analysis methodology for the joggle details required a hybrid 2-D shell/3-D solid finite element model in order to capture the stresses at the appropriate critical locations. The ply pack insert is modeled as 8 sided CHEXA brick

Copyright 2015 Lockheed Martin Corporation.
Note: The current version is always the version on the Lockheed Martin network.

elements with 3D orthotropic smeared properties. The skin is modeled as brick elements in the area of the joggle and then transitions back to shell elements outside of this area using RBE2 elements for continuity. At the edge of the cut-out and the edge of the filler, the element size is chosen to represent the minimum characteristic distance for the material from Table 13.2-1. Additional model details and discussion are illustrated in Figure 13.5.3.

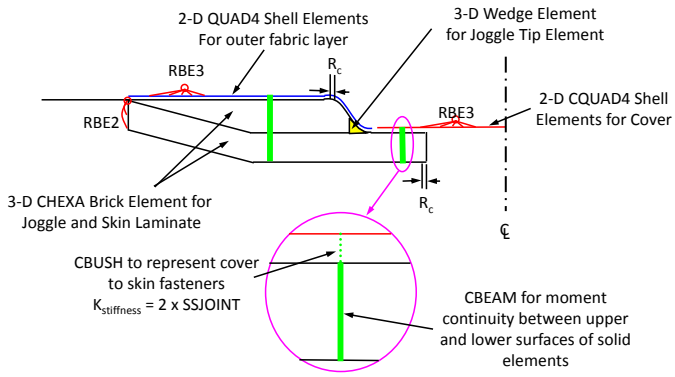

Figure 13.5-3 Model Best Practices for Hybrid 2-D/3-D Joggle Finite Element Model

Beyond the detail of the joggle area, the model can transition back to a fine/medium grid 2-D model as desired. If the joggle design is molded then the single ply of fabric on the surface is modeled by a shell element. If it is machined, then there would be no shell element on the surface. If there is substructure in the area of the solid element portion of the model it should be modeled using 2-D shell elements such as CQUAD4 and then, outside of the 3-D area can transition back to beams or bars. Substructure is connected using RBE2 elements. The model may be loaded using RBE3 elements to apply loads from the AVFEM or it may be inserted into a larger FEM. Some of these model details are illustrated in Figure 13.5-4 for a molded joggle. The model should extend far enough away from the analysis area such that the effect of applying the loads does not influence the loads and strains in the area of interest.

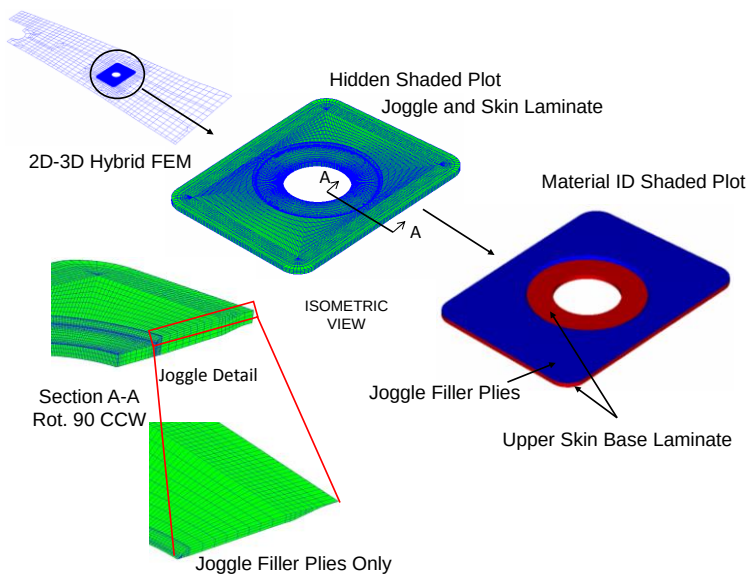

Figure 13.5-4 Sample 2-D/3-D Hybrid Model of Joggle

For a machined joggle the model needs to capture the details of the machined radius between the filler and the skin at analysis location 3. It is recommended that for this variation, the elements in the radius are no more than 0.04 in on a side x 0.16 in length around the step. This is illustrated in Figure 13.5-5.

Copyright 2015 Lockheed Martin Corporation.
Note: The current version is always the version on the Lockheed Martin network.

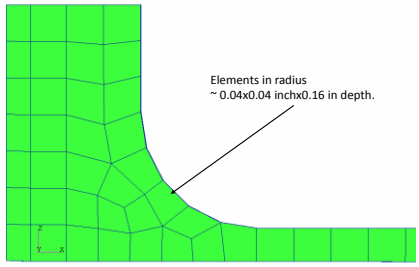

Figure 13.5-5 Solid Model Detail for Machined 90 Cut

Once the model is built and run, the analysis can proceed. Referring back to Figure 13.5-2, there are 4 analysis locations of interest. **Locations 1 and 2** are the stresses in the laminate due to the stress concentrations at the edge of the filler ramp/step and the edge of the cutout respectively. The analysis approach is the same for each and is similar to the approach described in Section 13.3.3 for chevron panel notch radius and Section 13.4.3 for hole strength. Using the element average strain values, from the 2-D/3-D model, determine the maximum in-plane tangential strains at the appropriate characteristic distance from the edge of the step (Location 1) and the edge of the hole (Location 2) respectively. These may not occur at the same location around the perimeter.

The average elemental strain values are compared to the appropriate unnotched strain allowable to calculate the margin of safety. This can be done efficiently in IDAT/SQ5. The margin of safety can also be determined from

$$MS = \frac{\varepsilon_{unnotched}}{\varepsilon_{tangential}} - 1 \qquad \textbf{Equation 13.5-1}$$

where
$\varepsilon_{unnotched}$ is the unnotched tension or compression strain allowable (in/in)
$\varepsilon_{tangential}$ is the average element strain in the tangential plies at the characteristic distance, R_c, from the edge of the hole.

Location 3 is a combined interlaminar tension/interlaminar shear calculation at the radius between the filler and the base laminate. Extract the maximum element average interlaminar tension (ILT) and interlaminar shear (ILS) stresses. Ensure that the stresses are in the appropriate coordinate system. Calculate the combined ILT/ILS margin of safety as

$$MS = \frac{1}{\sqrt{\left(\frac{\tau_{xz}}{TAU13}\right)^2 + \left(\frac{\tau_{yz}}{TAU23}\right)^2 + \left(\frac{\sigma_{zz}}{SIG33}\right)^2}} - 1 \qquad \textbf{Equation 13.5-2}$$

where
τ_{xz} is the interlaminar stress in the xz-plane (psi)
τ_{yz} is the interlaminar stress in the yz-plane (psi)
σ_{zz} is the interlaminar tension stress (psi)
TAU13 and TAU23 are the B-Basis interlaminar shear stress allowable. TAU13 is obtained from IDAT/ metdb. For a fabric TAU23 is assumed same as TAU13, while for a tape TAU23 has to be determined experimentally.
SIG33 is the B-Basis interlaminar tension stress allowable from IDAT/metdb

Location 4 is a bolted joint analysis, per Section 11.5, between the cover and the joggled skin adjacent to the cutout.

The presence of the hole in the panel, with or without the joggle has an impact on the critical buckling strength. Refer to Section 13.4.1 for discussion.

13.6 Seal Grooves

A feature sometimes used in one layer of a joint for the purpose of providing a barrier for fuel tank sealing is a seal groove. It is a radiused, machined feature, filled with a sealant material. The design of seal grooves requires careful

Copyright 2015 Lockheed Martin Corporation.
Note: The current version is always the version on the Lockheed Martin network.

analysis supported by testing that captures the complex loading state accurately. Testing done to-date on one legacy aircraft program utilized the 0.25 in. radius x 0.050-0.060 in. deep design shown in the inset of Figure 13.6-1 in a separate strap, *i.e.*, not integral with either the skin or the substructure. Functional testing has shown seal groove depth of 0.050-0.060 gives a reliable seal and a deeper groove is not required and would add weight unnecessarily. Another legacy aircraft program incorporated the seal groove into the composite cap of the substructure.

An example application of the separate strap configuration is shown in Figure 13.6-1. The strap, in the wet area, has two rows of fasteners, one on each side of the groove. They have 2.5D edge distance and 4D spacing between them. The seal groove lies midway between the two rows of fasteners. The skins also have 2.5D edge distance. Other configurations of seal groove arrangements may be possible but will require additional development testing.

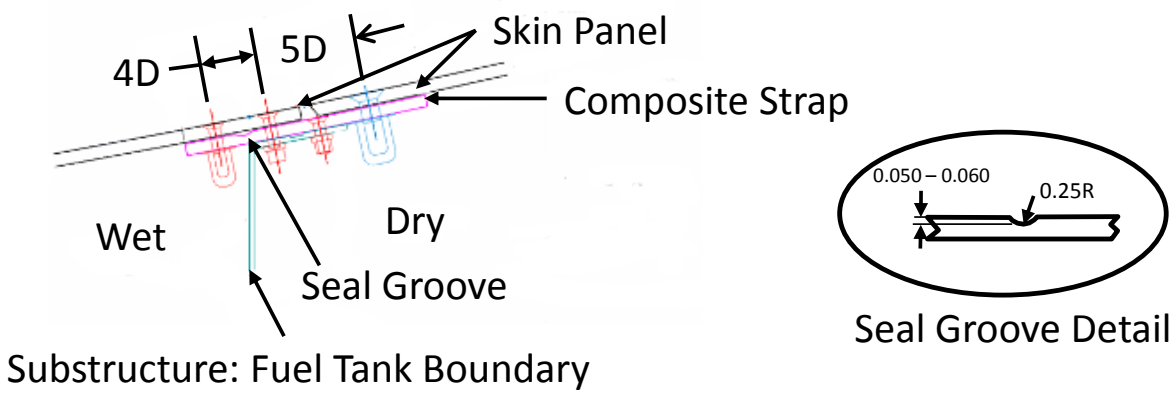

Figure 13.6-1 Seal Groove Geometry

Testing, performed in Reference 13-15, has shown that it is desirable that the seal groove be fully supported by the substructure to minimize the bending across the radius of the seal groove. If it is fully supported failure will likely occur in the fastener line due to bearing/bypass stresses. If it is not supported, the failure will occur at the groove radius due to interlaminar shear stresses which will lead to delamination.

Only one geometry of seal groove has been tested (0.25 in. radius x 0.050-0.060 in deep) and is shown in the inset of Figure 13.6-1. The specimens tested were IM7/5250-5 BMI with a total laminate thickness of 0.1491 comprised of an outer fabric ply on each surface and 25 interior tape plies. The groove depth was approximately 35% of the total laminate thickness. All tests were conducted with the loading perpendicular to the groove; however, the laminates were rotated such that some of the specimens were loaded along the 0 degree material direction and some were loaded along the 90 degree material direction. All specimens failed at similar load levels but strain gage readings at the seal groove indicated significantly different strains between those loaded along the material 0 degree direction and those loaded along the material 90 degree direction. Although the specimens were stabilized to minimize bending, bending did occur and the specimens failed in interlaminar shear at the seal groove. A double shear specimen of the same seal groove/ strap geometry failed due to bearing-bypass stresses which is the more desirable failure situation.

The test data is too limited to extrapolate to a generalized analysis methodology; however, a screening method which has been empirically correlated to existing testing, adequate for preliminary analysis of other geometries, is presented in this section. The part containing the seal groove should be designed as if there is no seal groove and then the seal groove checked as shown below. If the use of this method indicates the interlaminar shear margins of safety are positive, then the design is likely to be acceptable; however, if the ILS margins of safety reported are negative, the design may still be acceptable. Either way, <u>specific element testing is required for final verification of all seal groove designs</u>.

If the interlaminar shear margins of safety are positive, then the analysis of the joint in the part containing the seal groove can assume the plies making up the seal groove portion are a structural shim. If the interlaminar shear

Copyright 2015 Lockheed Martin Corporation.
Note: The current version is always the version on the Lockheed Martin network.

margins are negative, then for the analysis of the joint in the part containing the seal groove, an IDAT/IBOLT analysis is performed assuming that the strap has delaminated at the depth of the seal groove, 0.055 in., with the delaminated portion is acting like a non-structural shim. Figure 13.6-2 illustrates this delamination.

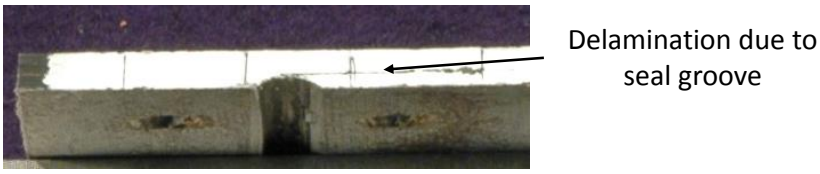

Figure 13.6-2 Seal Groove Test Coupon After ILS Failure and Delamination

Thus, to analyze the strap, there are two analyses required. An IDAT/IBOLT analysis of the joint (Analysis 1) and an interlaminar shear strength analysis of the tangency point at the bottom of the seal groove (Analysis 2). These are shown in Figure 13.6-3.

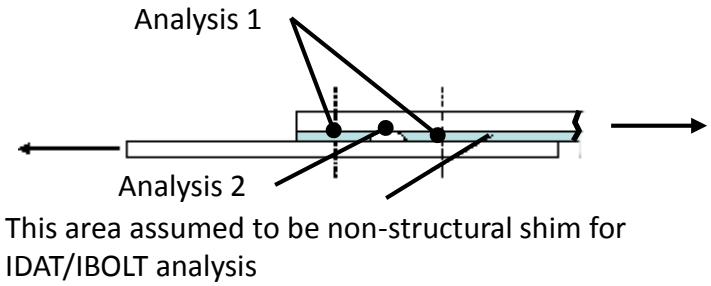

Figure 13.6-3 Analysis Locations and Assumptions

<u>Analysis 1 IDAT/IBOLT Analysis of Part Containing the Seal Groove</u>

Create a freebody diagram of the load transfer in the joint to determine the fastener and bypass loads in the part containing the seal groove. Analyze this part using IDAT/IBOLT assuming the sub-laminate is either a structural or a non-structural shim for the outer row of fasteners (0 Bypass load) per the following

If $MS_{ILS} \geq 0.0$, then groove plies form structural shim
If $MS_{ILS} < 0.0$, then groove plies form non-structural shim
where MS_{ILS} is from Step 6, Analysis 2, below

It is assumed that if an ILS failure occurs, the delamination grows to the nearest edge. For details on the use of IDAT/IBOLT, refer to PM4056 Section 11.

<u>Analysis 2 Interlaminar Shear Stress Analysis of Strap</u>

The interlaminar stress at the bottom of the seal groove which is needed for the calculation of the margin of safety will be determined from A4EI by assuming the plies which are interrupted by the seal groove (upper laminate) are a doubler attached to a base laminate (lower laminate)which is made up of the non-interrupted plies. The nominal depth of the seal groove, H_{groove}, is used in the calculations. Figure 13.6-4 shows the analysis geometry.

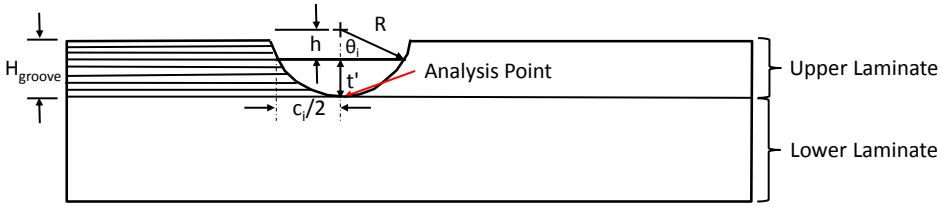

Figure 13.6-4 Geometry of the Seal Groove for Analysis

Copyright 2015 Lockheed Martin Corporation.
Note: The current version is always the version on the Lockheed Martin network.

A4EI requires the length of each tapered step to be input. The analysis assumes the height of each step is one ply. The step length input to A4EI, L_i, is the difference between adjacent ply cutout half chord lengths, $c_i/2$. To calculate L_i

$$\frac{c_i}{2} = R\sin\left(\frac{\theta_i}{2}\right)$$

$$\frac{\theta_i}{2} = \cos^{-1}\frac{h_i}{R}$$

$$R = h_i + t_i$$

$$L_i = \frac{c_{i+1}}{2} - \frac{c_i}{2} \qquad \text{Equation 13.6-1}$$

Where
c_i is the chord length at the ith step (in)
R is the radius of the seal groove (in)
θ_i is the angle as show in in Figure 13.6-4
h_i is the distance from the radius center to the ith step (in)
t_i' is the thickness of the tapered plies as measured from the deepest part of the seal groove (in)
i = 1 - n, where n represents the total number of plies interrupted by the presence of the seal groove
L_i is the length of the taper for the ith step for steps 2-n; $L_1=c_1/2$

The analysis steps for determining the preliminary margin of safety for the interlaminar failure of the seal groove are given in Table 13.6-1.

Table 13.6-1 Seal Groove Analysis Steps

Step	General Description	Instructions	Comments
1	Prepare the information necessary for A4EI	Run SQ5 with the lower laminate and the n upper laminates to determine E and the laminate allowable stresses. - Use 1000 lb/in unit load. From the SQ5 output for each laminate run, obtain the lowest margin of safety and E_x.	
1A	Calculate S1, S2	Calculate the laminate strength for each laminate from : *1000(MS+1)*	
1B	Calculate L_1-L_n	Using Equation 13.6-1 calculate the step lengths of the doubler	Each ply is a step in the doubler, thus if the seal groove cuts through 10 plies, there are 10 steps in the doubler.
1D	Determine adhesive properties	Go into IDAT/MATUTIL for the material making up the laminate at the ply which is at the bottom of the nominal seal groove depth and determine: Tau13, Gsec, Gam12 for the appropriate environment.	
1E	Set up A4EI	Choose Joint Type: Doubler Single	
		Under Adhesive Properties: - Taumax=Tau13 (Step 1D) - G=Gsec (Step 1D) - GamMAX=Gam12 (Step 1D) - Ply thickness - ALPHA1, ALPHA2 blank - DISBND=0 (100% Effective)	
		Under the Adherend Properties: -Thick 1 - is the lower laminate thickness.	Same for all steps

Copyright 2015 Lockheed Martin Corporation.
Note: The current version is always the version on the Lockheed Martin network.

Step	General Description	Instructions	Comments
		-Thick 2 - is the stepped upper laminate build-up, starting with the ply set that is the thinnest (1 ply) and incrementing until you have the total n ply set. -Step L_i is the calculated length of each step length from Step 1B -E1, E2 are the moduli of the lower and upper plyset from Step 1A. -S1, S2 are the allowable axial stress (psi) calculated in Step 1B of the lower laminate and the appropriate upper laminate plyset, respectively.	Each step will be different E1 will be the same for all steps. E2 will vary as plies are added. S1 will be the same for all steps, S2 should vary for each step.
		Input a single load case, the same unit load used in the SQ5 run, 1000 lbs/in.	
1F	Run A4EI	Look at the last output set and determine the peak shear stress, TAU, in any layer. This is τ_{max}, the interlaminar shear stress, resulting from the unit applied load.	Pertinent output has the applied load listed in the header.
2	Determine the in-plane far field strain for a unit load case	Run SQ5 with the total laminate. - Use 1000 lb/in unit load. From the SQ5 output obtain the mid-plane strain in the x direction, $\varepsilon_{xx\text{-midplane}}$	
3	Calculate the strain correlation factor, K_{CF}	$K_{CF} = \frac{\tau_{max}}{\varepsilon_{xx-midplane}}$	This factor relates the interlaminar shear stress to the midplane axial stress for the unit load case.
4	Determine the allowable in-plane laminate strain for the full laminate	$\varepsilon_{xx-max} = \frac{Tau13}{K_{CF}K_{test}}$ where Tau13 is from Step 1D K_{test} =1.33 for applied tension load K_{test} =1.20 for applied compression load	Based on the allowable interlaminar strain, an empirical factor and the ratio of the ILS at the groove to the midplane strain of the full laminate
5	Calculate the strain for the strap using the full laminate	Run SQ5 with the total laminate. - Actual in-plane load (lb/in) From the SQ5 output obtain the outer fiber strain in the x direction, $\varepsilon_{xx\text{-OML}}$	In-plane load should be determined at the seal groove, *i.e.* between the fastener rows, from the freebody diagram of the joint loads.
6	Calculate the Margin of Safety	$MS_{ILS} = \frac{\varepsilon_{xx-max}}{\varepsilon_{xx-OML}} - 1$	Preliminary Margin of Safety. **Follow-up configuration specific testing required.**

This approach doesn't attempt to model the micromechanical behavior but rather the general macroscopic behavior of the seal groove region. Because it uses one dimensional loads across the seal groove, the method does not account for Poisson's effects and the effects of transverse loads, parallel to the seal groove, are ignored. There have been different approaches utilizing ultra-fine-grid solid element finite element models proposed and used post-test; however, they are closely correlated with the limited testing and it is premature to propose that as a general methodology. As with any FEA approach, a characteristic dimension would need to be determined for analysis.

13.7 Stiffener Run-out

Tapering of material at the end of a stiffener that is not tied in to adjacent structure is important in any structural design and is crucial in the design of composites. Gradually reducing the height of the stiffener or the presence of

Copyright 2015 Lockheed Martin Corporation.
Note: The current version is always the version on the Lockheed Martin network.

caps allows the load to transition into the skin or web, minimizes the effects of load peaking on fasteners or bond line and reduces interlaminar tension and shear effects to improve the static strength.

Figure 13.7-1 illustrates the tapering of stiffener run-out and flanges. Note the flanges are typically tapered symmetrically. If the stiffener does not have flanges, as is shown in the figure, the web of the stiffener should still taper as shown. For the pi-stiffener, the pi-preform is typically extended beyond where the stiffener ends to provide additional transition. Tapering is necessary to reduce the stiffness of the stiffener and to force a shift of the neutral axis of the cross-section toward the panel on which the stiffener is mounted because at the end of the stiffener, the neutral axis is at the mid-plane of the panel. The load line change from full depth stiffener to no stiffener results in an induced bending moment which will be reacted in the skin laminate and adds to applied in-plane loads and moments resulting in peel stresses trying to pry the stiffener from the skin. Additionally, tapering the stiffener results in a more uniform load transfer through the bond or fastener line at the end of the stiffener into the skin panel and minimizes the out-of-plane peaking of load. A 20 degree taper is recommended, as shown.

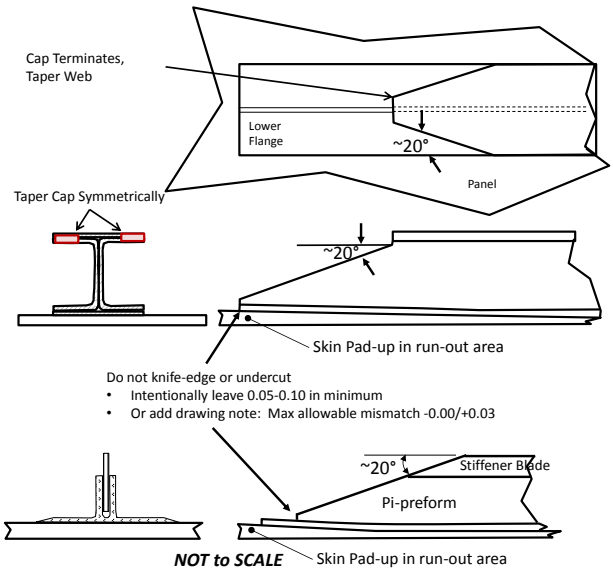

Figure 13.7-1 Example of Material Tapering at the End of Stiffeners

Possible failure modes which result from inattention to the run-out include interlaminar tension/shear at the end of the stiffener in the base laminate, bond line failure, or, for pi-stiffeners, pi failure in in-plane shear in the vertical leg. Depending on the failure mode, for run-out details that need additional strength, the addition of radius blocks or fittings can help to mitigate this failure mode.

Another area of concern is the intersection of pi-beams in highly unitized structure. This may be spanwise spars intersecting chord wise ribs as shown notionally in Figure 13.7-2. There are no details provided in the sketch concerning the structural continuity of spars and ribs or spar caps and rib caps but that is of concern for structural integrity and the stress analyst will need to be an active advocate in the decision process.

This problem is not unique for unitized composite structure. Since intersecting structure is present in all aircraft the problem has been addressed in the past. Typically the most highly loaded, critical structure is continuous and the remaining structure is segmented but attached with sufficient fidelity to provide load paths for all load components to mitigate any secondary loading. In Figure 13.7-2, the spanwise spars are likely continuous because they carry the wing loads and the chordwise ribs are discontinuous but attached at their intersection with each spar. Continuity would need to be maintained for the webs as well as the pi-caps.

Copyright 2015 Lockheed Martin Corporation.
Note: The current version is always the version on the Lockheed Martin network.

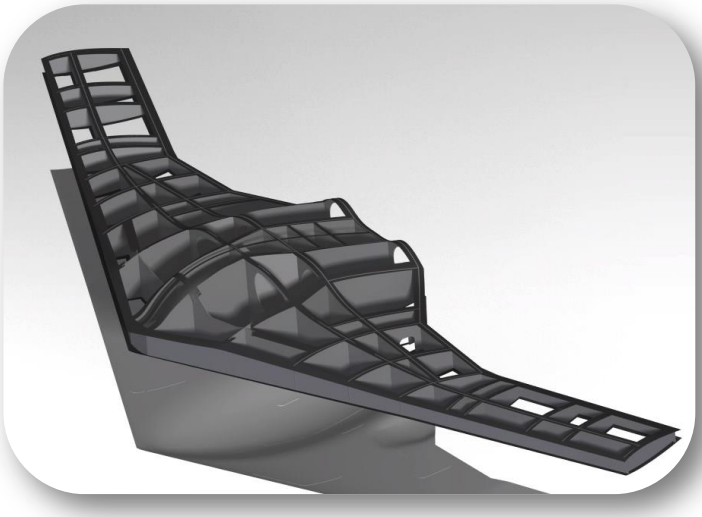

Figure 13.7-2 Intersecting Chordwise and Spanwise Structure

For web continuity the most straightforward solution is tie the intersections together using additional pi-preforms. This is illustrated in Figure 13.7-3. Typically these run full height of the spar web and act as shear connections between the rib and spar webs. They may stop just short of the caps or they may extend down and overlap the caps. This detail is dependent on the tooling concept and how continuity for the rib caps is maintained. An alternative to using the pi connections would be to use composite angles, individually or back-to-back. If the structure is hybrid, *i.e.*, one member laminated composite and one member metallic, a metallic angle might also be used.

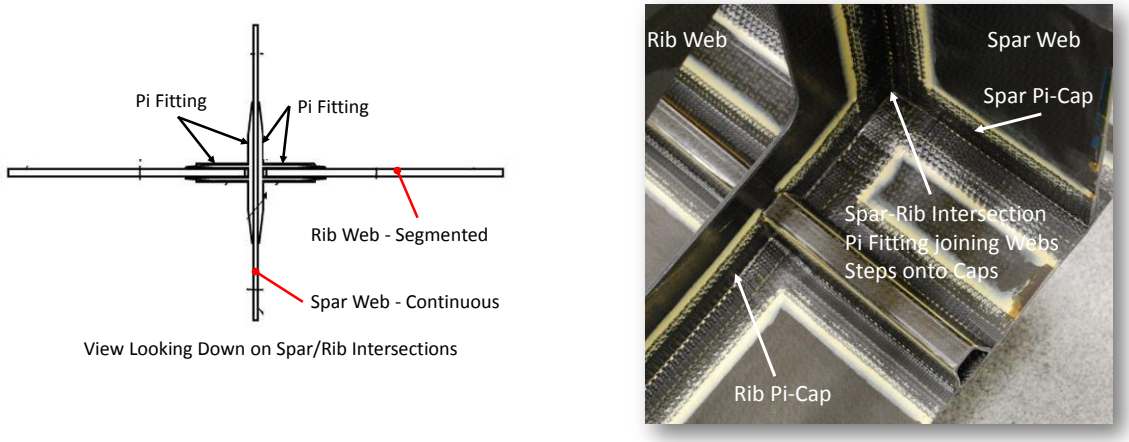

Figure 13.7-3 Details of Intersecting Structure

Cap continuity must also be maintained to transfer any axial loads that might be present in the cap. It is undesirable to terminate the cap short of the adjacent cap because it abruptly forces the section centroid to shift and requires the entire axial load to be transferred through the skin. The axial load combined with the shift of the centroid results in an induced internal moment and is likely to result in an unexpected interlaminar failure in the skin. This is discussed further below. Figure 13.7-4 illustrates this bad design detail.

Copyright 2015 Lockheed Martin Corporation.
Note: The current version is always the version on the Lockheed Martin network.

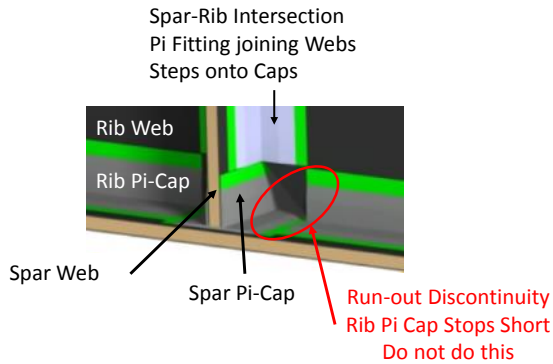

Figure 13.7-4 Spar / Rib Cap Discontinuity

Continuity can be accomplished in a number of ways, depending on the magnitude of the load. The minimum approach, useful if the loads are not significant, is to trim the web (since it is attached using the separate fittings discussed above), taper the upstanding pi legs and continue the base onto the intersecting cap. This is notionally illustrated in Figure 13.7-5 (A). Alternatively continuing the cap through the continuous web by notching the web/cap locally is another approach. This is shown for stiffeners in Figure 13.7-5 (B) but could be used for full webs as well. A final approach is to enlarge the opening in the continuous structure to allow for the entire pi cap to pass through. This type of opening is sometimes called a mouse hole and is used when complete continuity of the load path is desired / required. Figure 13.7-5 (C) shows an example of this for a hat stiffened structure. In this case the opening is very close around the hat and the rib cap is severed, including the skin flange. The rib web also has a small opening. The hat runs through and the skin flange of the cap steps up onto the skin flange of the hat.

Each of these approaches has some structural risk. Notches and openings in ribs or spars can create stress concentrations which must be investigated. Discontinuous caps, even with mitigating details, can result in interlaminar stresses in the skin in addition to the peaking of in-plane and bending stresses resulting from the load path eccentricity and the stress concentration due to the detail at the runout area. Element or subcomponent testing of these details is an important part of mitigating the risk and tuning the analysis.

Analysis of runout area involves the determination of the in-plane loads and bending moments due to the eccentricity created in the load path due to the shift in load line, typically at several locations along the taper, including where the taper stops and only the skin laminate remains. The load line shift is illustrated in Figure 13.7-6 along with the pulloff reactions. The loads and moments can be determined from a free body diagram or from a finite element model. For detail analysis the model should have sufficient fidelity to correctly capture the changing cross-sectional centroid shift. Margins of safety can be written using IDAT/SQ5 and unnotched allowables.

Copyright 2015 Lockheed Martin Corporation.
Note: The current version is always the version on the Lockheed Martin network.

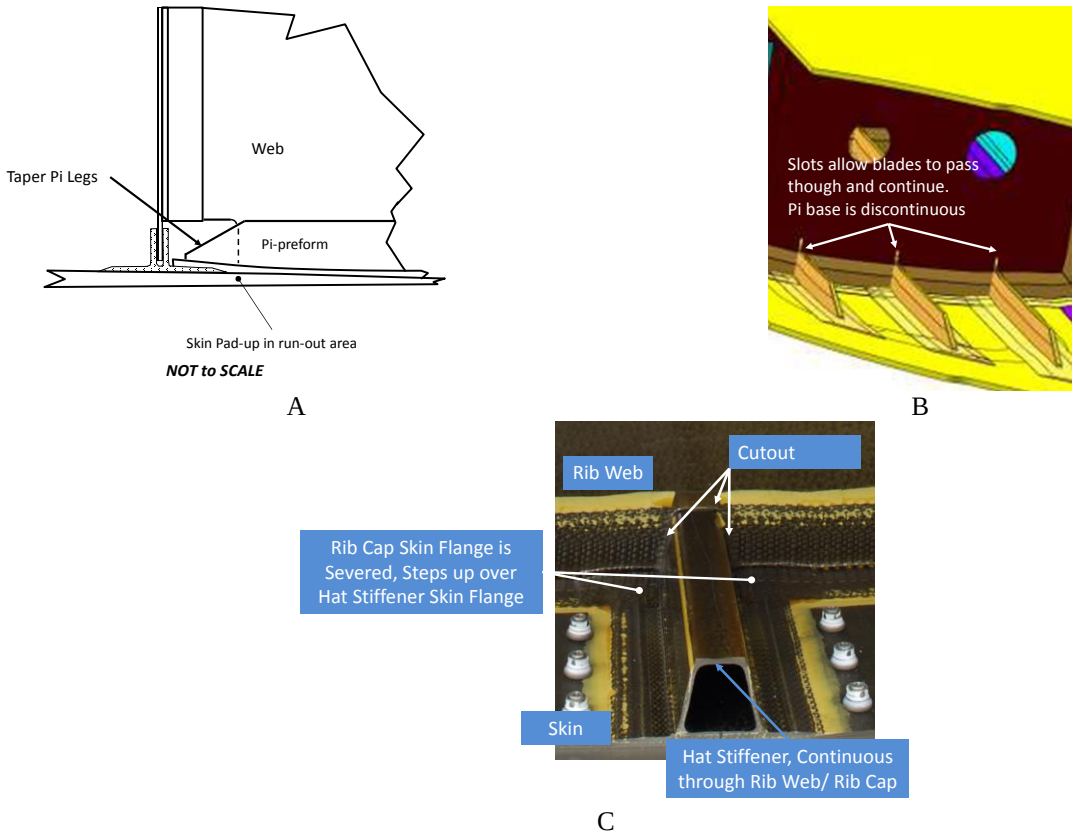

Figure 13.7-5 Alternate Means for Providing Cap Continuity

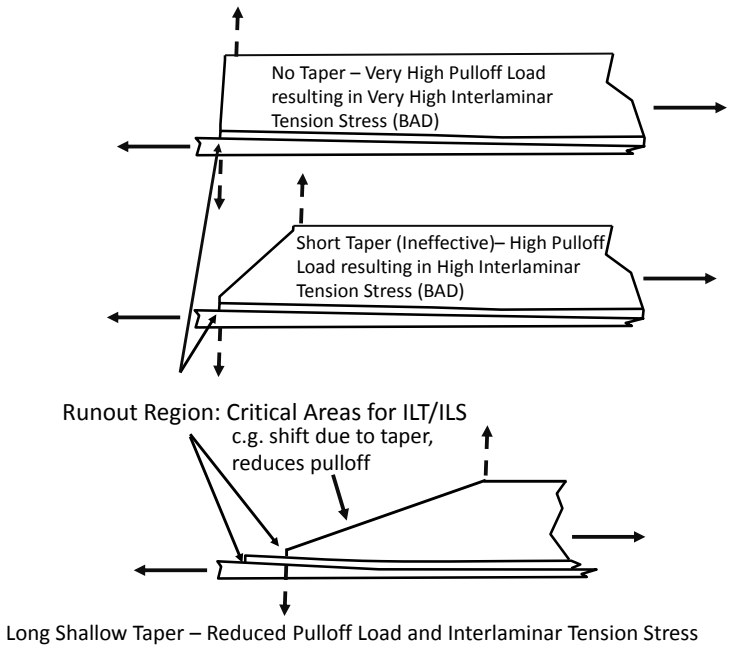

Figure 13.7-6 Stiffener Runout and ILT/ILS-Critical Areas

Copyright 2015 Lockheed Martin Corporation.
Note: The current version is always the version on the Lockheed Martin network.

In addition, the interlaminar stresses at the end of the stiffener, as shown in Figure 13.7-7, need to be determined. For a preliminary analysis, the pulloff load can be calculated by calculating the moment due to the eccentricity of the load line and reacting that as a couple over the distance from the end of the stiffener/web to the point where the stiffener reaches full height. If there is no taper, then assume the moment is coupled out over a very short distance such as 0.50 inch.

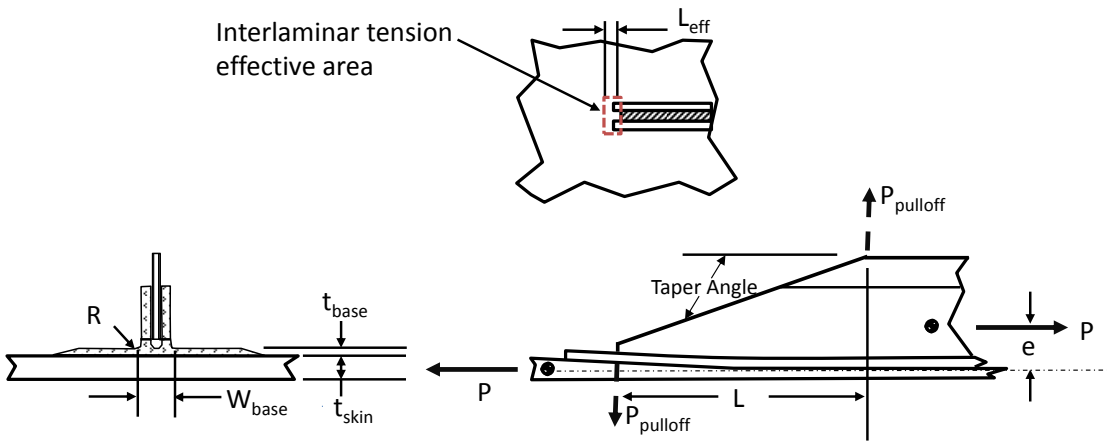

Figure 13.7-7 Geometry for Preliminary Calculation of Interlaminar Tension Stress

Once the pulloff load is determined a preliminary interlaminar tension stress margin of safety can be calculated as

$$A_{ILT}=w_{base} \cdot L_{eff}$$

$$f_{33} = \frac{P_{pulloff}}{A_{ILT}}$$

$$MS = \frac{Sig33(T)}{f_{33}} - 1$$

where
w_{base} is the width of the upstanding leg(s) + 2R + $2t_{base}$ (in)
L_{eff} is $2t_{base}$ (in)
Sig33(T) is the allowable interlaminar tension stress for the bondline (cobonded) or laminate (cocured) (psi) from IDAT/MATUTIL

A higher fidelity solution can be obtained through the use of a solid finite element model of the runout detail, similar to the one described in Section 13.5.1 on joggles. Figure 13.5-3 is particularly useful in describing the level of model detail required at the runout as the failure modes are the same. The margin of safety for ILT/ILS at each of the critical areas at the end of the stiffener can be calculated from Equation 13.5-2. The number of required checks are a function of the specific geometry of the design of the cap and taper.

13.8 Honeycomb Panel Ramps

Honeycomb panel terminations can take a number of forms from C-channel close-outs to panel ramp terminations. Ramp terminations are most commonly used at Lockheed Martin. An example of ramp termination is shown in Figure 13.8-1. The recommended ramp angle is 20 degrees with a minimum of 10 degrees. Shallower terminations, *i.e.* angles less than 10 degrees, may require core stabilization to prevent crushing during cure while steeper terminations, *i.e.* angles greater than 20 degrees, can result in a peeking of the interlaminar tension/shear stresses as well as increased bending moments due to peaking of the pulloff load. Higher angles can be used, however a careful analysis and testing of the critical areas, as discussed below, must be performed.

Copyright 2015 Lockheed Martin Corporation.
Note: The current version is always the version on the Lockheed Martin network.

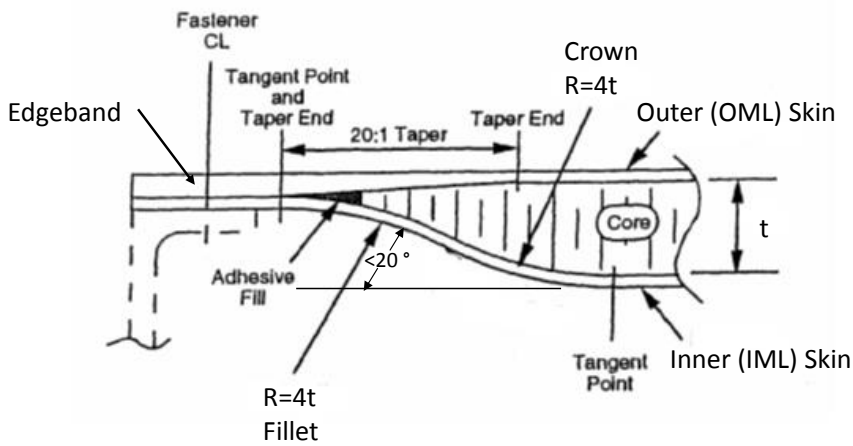

Figure 13.8-1 Honeycomb Ramp Termination Detail

Additional plies are added in the OML skin at the ramp termination/fillet area to reduce the ILT/ILS and bending stresses and to pad-up for bearing capability. Those plies should have a 20:1 taper ratio as shown in Figure 13.8-1. Depending on the loads, additional plies may also be added in the IML skin from the edge of closeout, up the ramp and over the crown where they are terminated in standard ply drops. A preliminary estimate of the required total edgeband thickness can be estimated by sizing the edgeband to the in-plane loads plus bending moment due to shear plus bending moment due to the centroid shift. Geometry assumptions for calculation of bending moments are shown in Figure 13.8-2. The moments can be estimated as

$$m_{shear}=Qa$$

$$m_{eccentricity}=N_{max}e$$

where

Q is the transverse shear load (lb/in)

N_{max} is the maximum in-plane running load for panel at the full-depth centroid perpendicular to the edgeband at the analysis location (lb/in)

a is the moment arm, defined in Figure 13.8-2 (in)

e is the distance between centroids from the full-depth core to the edgeband, shown in Figure 13.8-2.

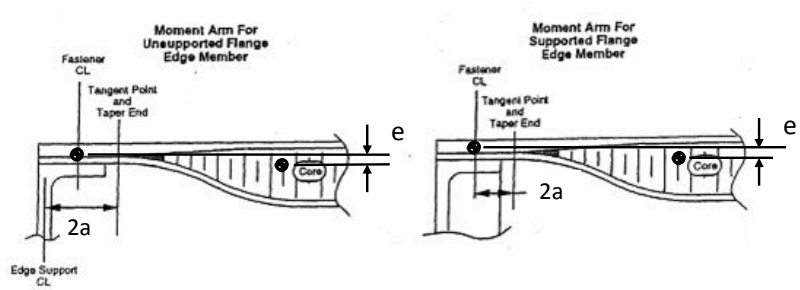

Figure 13.8-2 Honeycomb Core Ramp Geometry for Edge Moment Calculations

Testing of core ramp specimens indicate that the failure at the crown, shown in Figure 13.8-3(a), is flatwise tension failure resulting in separation of the inner face sheet from the core. At the base of the ramp termination, Figure 13.8-3(b) the failure mode is interlaminar tension failure of the IML skin.

Copyright 2015 Lockheed Martin Corporation.
Note: The current version is always the version on the Lockheed Martin network.

(a) Flatwise Tension Failure at Crown

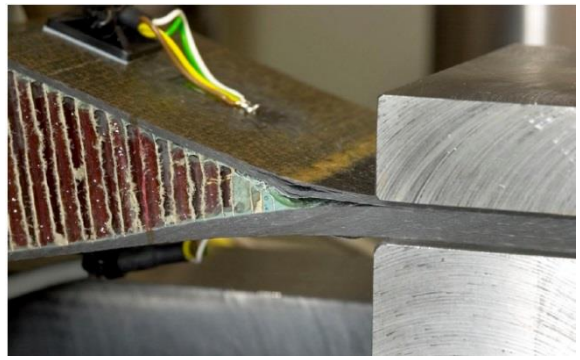

(b) Cohesive Failure of Adherend at Base of Ramp

Figure 13.8-3 Ramp Termination Failure Specimens and Modes

The radii in the corners at the crown and fillet area are typically set by manufacturing but should be as large as possible to minimize the pull-off stresses. The recommended radius is a minimum of two times the core thickness with four times core thickness recommended. As the radius gets larger, the amount of full depth core in a panel decreases resulting in a loss of stiffness and an increase in deflection. So these requirements must be balanced.

Sizing will require a fine grid model of the ramp area. It can either be a 2D plane strain strip model or a full 3D finite element model of a representative slice of the ramp area. This model can be used for core shear, bondline tension and edge bending for detailed analysis of the ramp region. The IML facesheet should be modeled with ply-by-ply element properties since testing indicates the inner facesheet failure at the ramp base is a cohesive interlaminar failure of the IML skin. The OML skin can be modeled with smeared properties. The adhesive should be modeled with nonlinear properties.

Using the results from the above models, interlaminar tension/shear in the ramp facesheet is analyzed per

$$R_t = \frac{f_{33}}{K_{radius} \cdot Sig33(T)}$$

$$R_s = \sqrt{\left(\frac{f_{13}}{Tau13}\right)^2 + \left(\frac{f_{23}}{Tau13}\right)^2}$$

$$MS = \frac{1}{\sqrt{R_s^2 + R_t^2}} - 1$$

where
f_{13}, f_{23}, f_{33} are interlaminar shear and normal stresses in the facesheet from the 2D or 3D model (psi)
Sig33(T) and Tau13 are the B-basis material property for the facesheet material from IDAT/MATUTIL
K_{radius} is an empirical correction factor from Figure 13.8-4

If the normal stress, f_{33} is in compression, then R_t is set to zero in the above formulation.

The correction factor, K_{radius} is based on legacy test data[1] and is a function of the inner facesheet radius at the ramp termination, ramp angle and core thickness and model construction. It is given in Figure 13.8-4.

[1] Reference 13-16

Copyright 2015 Lockheed Martin Corporation.
Note: The current version is always the version on the Lockheed Martin network.

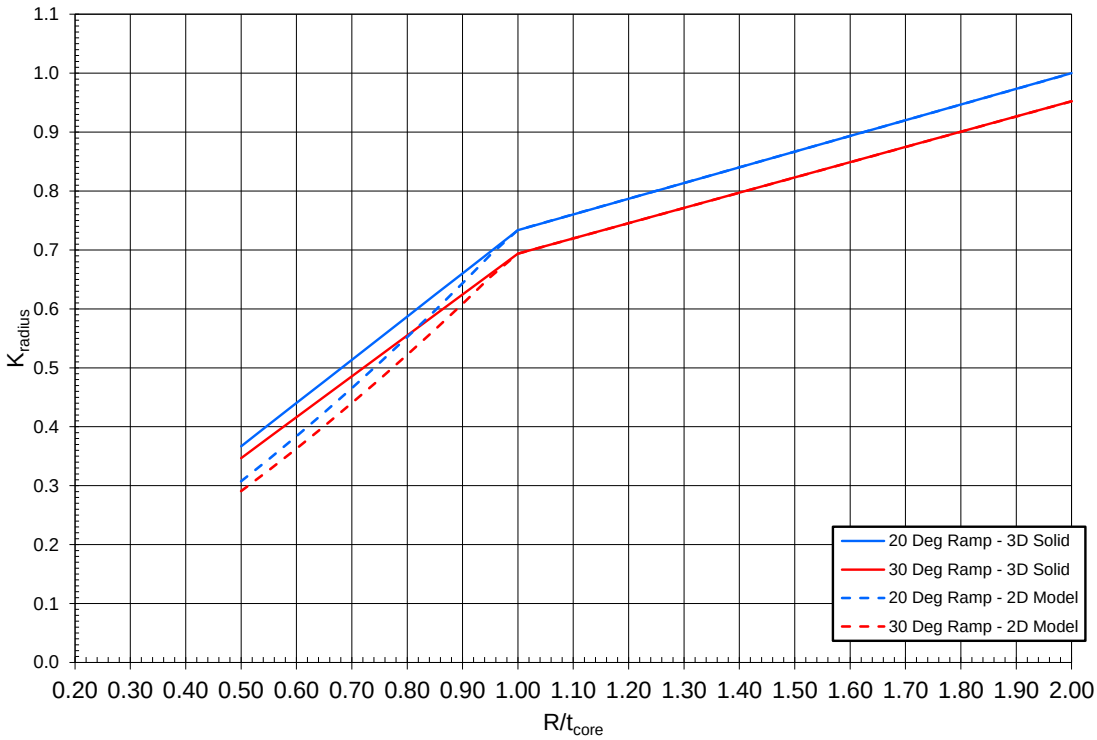

Figure 13.8-4 Allowable Strength Correction Factor as a Function of Radius, Core Thickness and Ramp Angle and Model

The shear stress in the tapered region of the core is highly sensitive to the panel boundary conditions, and in particular the rotational fixity. For honeycomb ramp regions, simply supported panels are an advantage; however, this must be balanced against the deformations and bending moments developed in mid-panel and the sizing of adjoining structure. If core shear stresses in the ramp region cannot be controlled by reduced edge fixity, then it may be necessary to splice in sections of high density core in the taper.

In addition to the analyses discussed above, the edgeband needs to be analyzed for joint strength using IDAT/IBOLT and fastener pull-through. Refer to PM4056 Section 11 for joint analysis. Depending on the edge fixity, as discussed in the previous paragraph, the edgeband may also need to be sized for bending moments as well as in-plane and transverse shear loads.

13.9 Free Edges

Any edges of composite structure, including holes, chevrons, and seal grooves may have interlaminar free edge stresses which are a boundary layer or edge effect. A free edge boundary for interlaminar stress may exist along any unsupported-unloaded laminate edge and along discontinuities such as ply drop-offs and splices. The width of the affected boundary region is approximately equal to the thickness of the laminate and the magnitude of the stresses may vary considerably with layup. PM4056 Section 4.4.3.3 discusses free edge interlaminar shear stresses in more detail.

Copyright 2015 Lockheed Martin Corporation.
Note: The current version is always the version on the Lockheed Martin network.

13.10 3-D Woven Pi-Preform Joint Analysis

3-D woven fiber preforms have been developed by Lockheed Martin for the purpose of efficiently joining composite structures by various bond processes. The 3D woven preforms come in various shapes including pi's, tee's, and airfoil shapes used in engine blades (Reference 13-26). Different types of preforms are depicted in **Figure 13.10-1**.

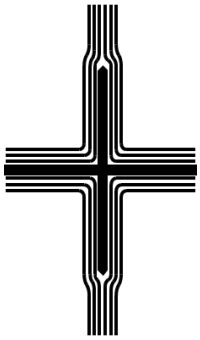

(a) Co-cured with 3-D woven X

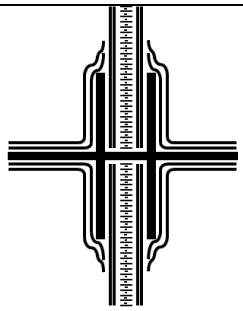

(b) Co-Bonded With 3-D Woven Double X and Sandwich Web

(c) Termination

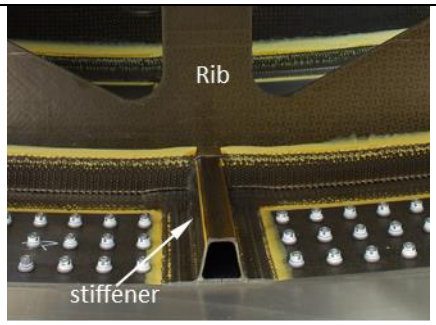

(d) Rib-stiffener Intersection

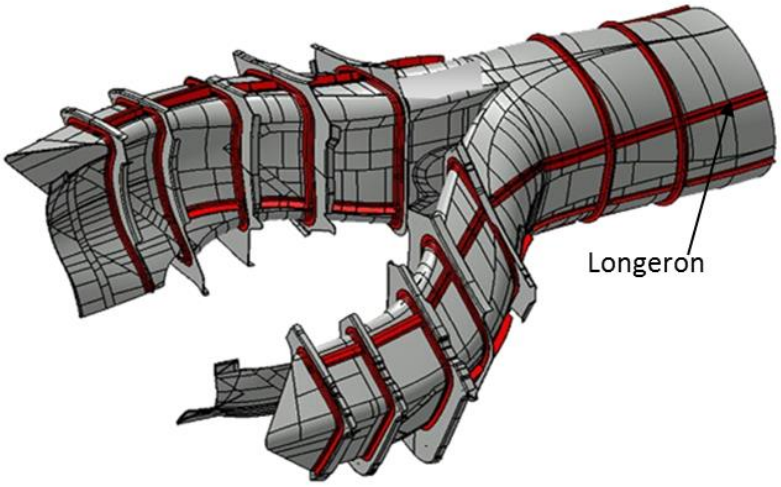

(e) Inlet Duct – Pi-preforms used to attach frames and longerons

Figure 13.10-1 Types of 3D Woven Pi-Preforms

Copyright 2015 Lockheed Martin Corporation.
Note: The current version is always the version on the Lockheed Martin network.

The focus of this section is on pi-preforms. Pi-preforms are made using a 3D weaving process. The process of 3D weaving, which is also known as Jacquard weaving, is employed to weave complex preform shapes with interlocking fibers. The interlocks may extend to two or more layers of fabric. The 0° fabric direction is the warp direction and the 90° direction is the weft direction. In the case of a 3D woven preform there are warp fibers and fibers that traverse through the thickness providing the interlock. An angle interlock fiber architecture preform is shown in **Figure 13.10-2a**. In contrast a 2D woven laminate, shown in **Figure 13.10.2b** has only warp and weft fibers in a single fabric layer, *i.e.*, it does not traverse through the thickness resulting in lower interlaminar tension (ILT) strength.

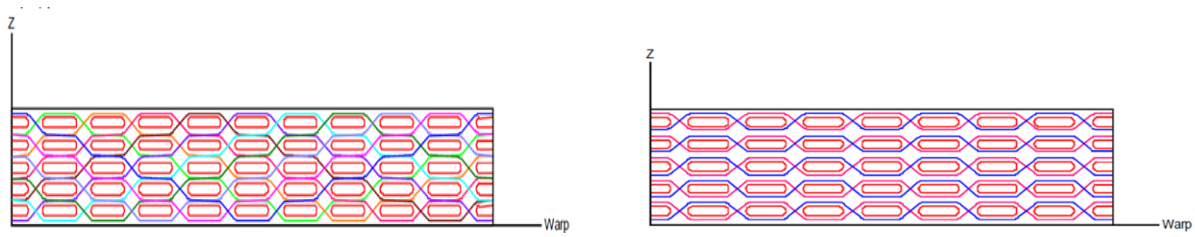

(a) Typical 3D Woven Architecture (Through thickness angle interlock fiber architecture)

(b) Conventional 2D Woven Laminate

Figure 13.10-2 A 3D Woven Architecture Compared to a 2-D Woven Laminate

A portion of a cross section of a preform unit cell level is shown in **Figure 13.10-3** to illustrate the fiber path in a 3D weave.

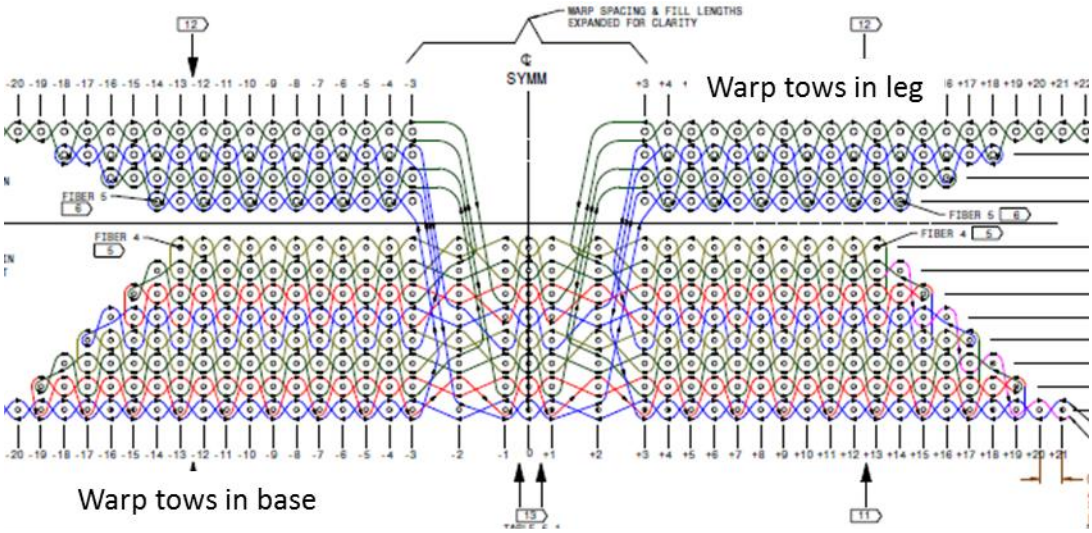

Figure 13.10-3 Fiber Path in a 3-D Weave

The analysis methods presented in this section have been correlated to specific material systems and therefore should not be used for materials not discussed here. However, for preliminary design purposes these methods may be used for similar material systems after consultation with the Composite Method Group.

13.10.1 Design Philosophy

A pi-preform is a 3D woven structure that efficiently resists out-of-plane loads, the weakness of traditional bonded joints. The out-of-plane loads arise due to pressure loads, bending of curved features, kick loads developed at

Copyright 2015 Lockheed Martin Corporation.
Note: The current version is always the version on the Lockheed Martin network.

terminations, skin buckling, bending of curved sections, and impact or ballistic threats. These out-of-plane loads are resisted through a 3D woven architecture in the curved portion of the joint where typically delamination due to interlaminar tension or shear occurs. The high peel stresses at the edges of the pi-preform terminations or at the corners of filler region (**Figure 13.10-4(a)**) are reduced since the cured preform is more compliant to flexure than the skin or web. Furthermore, the load in the web is transferred efficiently to preform through a double-lap shear joint. The flange bonded to the skin helps distribute the pull-off loads over a wider area and the tapered flange helps reduce peel stresses. A traditional bonded tee joint and its critical failure locations is compared with a pi-joint in **Figure 13.10-4**.

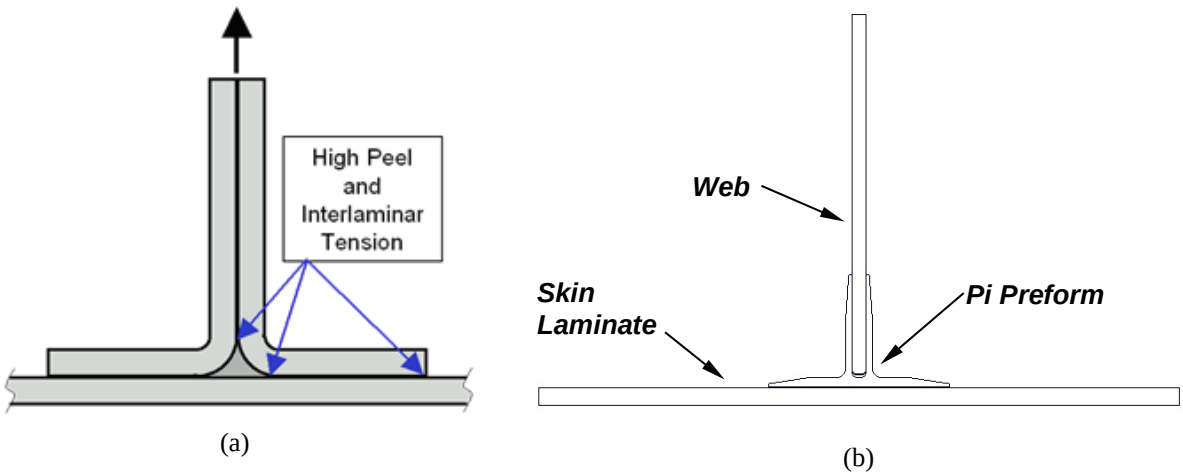

Figure 13.10-4 Conventional 2D Joint (a) Compared to Pi-Preform Joint (b)

13.10.2 Manufacturing Methods

There are three main methods of manufacturing pi-preform joints as described below.

(i) Co-bond: The skin and web are cured separately and then co-bonded with the uncured pi-preform using a film adhesive. The film adhesive is used between the web and clevis and between the bottom of the pi-preform and the skin. This is the preferred manufacturing method for pi-joints.

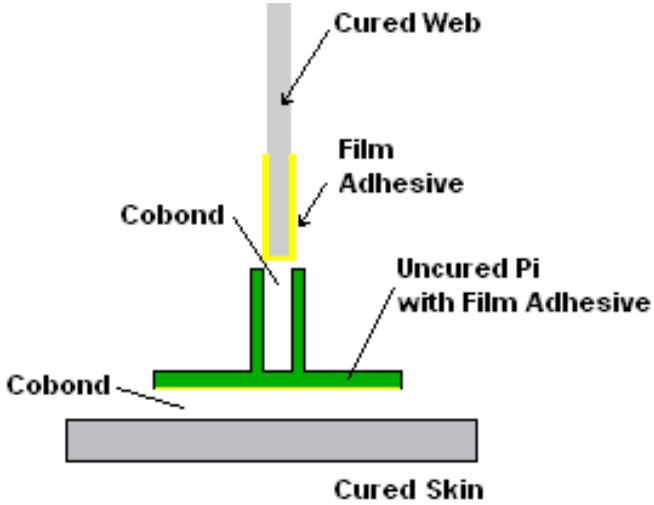

Figure 13.10-5 Co-bonded Pi-Preform Joint

Copyright 2015 Lockheed Martin Corporation.
Note: The current version is always the version on the Lockheed Martin network.

(ii) Co-cure: The skin is staged and co-cured with the cured web and un-cured pi-preform using a film adhesive between the web and clevis, and between the bottom of the pi-preform and the skin. This method generally yields lower allowables than co-bond process as shown in **Table 13.10-1** and therefore co-bond allowables cannot be used for co-cured joints. Pi-joints are co-cured when z pins are employed to reinforce the peel strength of the joint. The z pins also provide crack arresting mechanism. The uncured skin and preform are required for penetration of the z pins into the skin and preform.

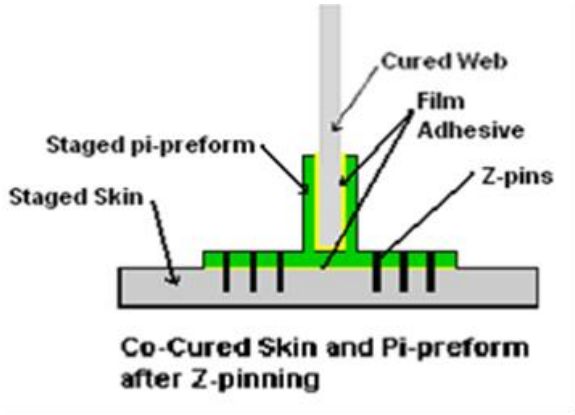

Figure 13.10-6 Co-cured Pi-Preform Joint

Table 13.10-1 Typical Pull-off value for a Co-cure and Co-bond Pi-joint (Reference 13-19)	
3-D Pi-preform co-bonded joint with no pins	1223 lbs/in
3-D Pi-preform co-cured joint with pins	1039 lbs/in

(iii) Secondary Bond: In this configuration, the web, skin and pi-preform are cured first and then bonded together using film or paste adhesive. In one method the un-cured pi is co-bonded to the skin first using a film adhesive and subsequently the web is secondarily-bonded to the clevis usually with a paste adhesive. In another method a precured pi and web are secondarily-bonded on to the skin using a film or paste adhesive. This method was adopted to bond longerons on to the outer mold line of the inlet ducts (**Figure 13.10-1**e and Reference 13-23). Secondary bond is more process dependent and additional element level testing has to be done for each material system. The reduction factors due to secondary bond are discussed for one material system in Section 13.10.9.

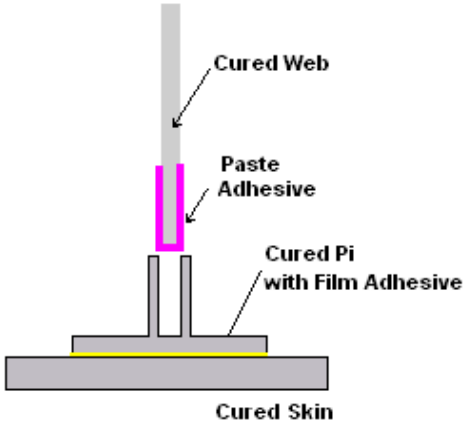

Figure 13.10-7 Secondary Bonded Pi-Preform Joint

Copyright 2015 Lockheed Martin Corporation.
Note: The current version is always the version on the Lockheed Martin network.

Further details regarding the above manufacturing methods can be found in Reference 13-19. Co-bonding is the most common form of manufacturing the pi-joint, therefore all further discussions assume that the joint is co-bonded unless otherwise specified.

The preforms are available as a pre-impregnated (prepreg) form or as dry preforms which are resin infused using the Resin Transfer Molding (RTM), autoclave infusion using neat resin, or Vacuum Assisted Resin Transfer Molding (VARTM) processes. The preforms are usually partially infused with the resin, *i.e.*, some areas of the preform are infused with the resin but not all fiber bundles. This allows the preform to be pliable during the assembly process. An impregnated uncured pi-preform is shown in **Figure 13.10-8**.

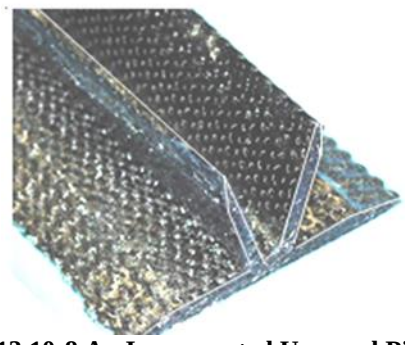

Figure 13.10-8 An Impregnated Uncured Pi-preform

13.10.3 Pi-Joint Nomenclature and Coordinate Systems

The nomenclature and material coordinate system associated with a pi-joint is shown in **Figure 13.10-9**.

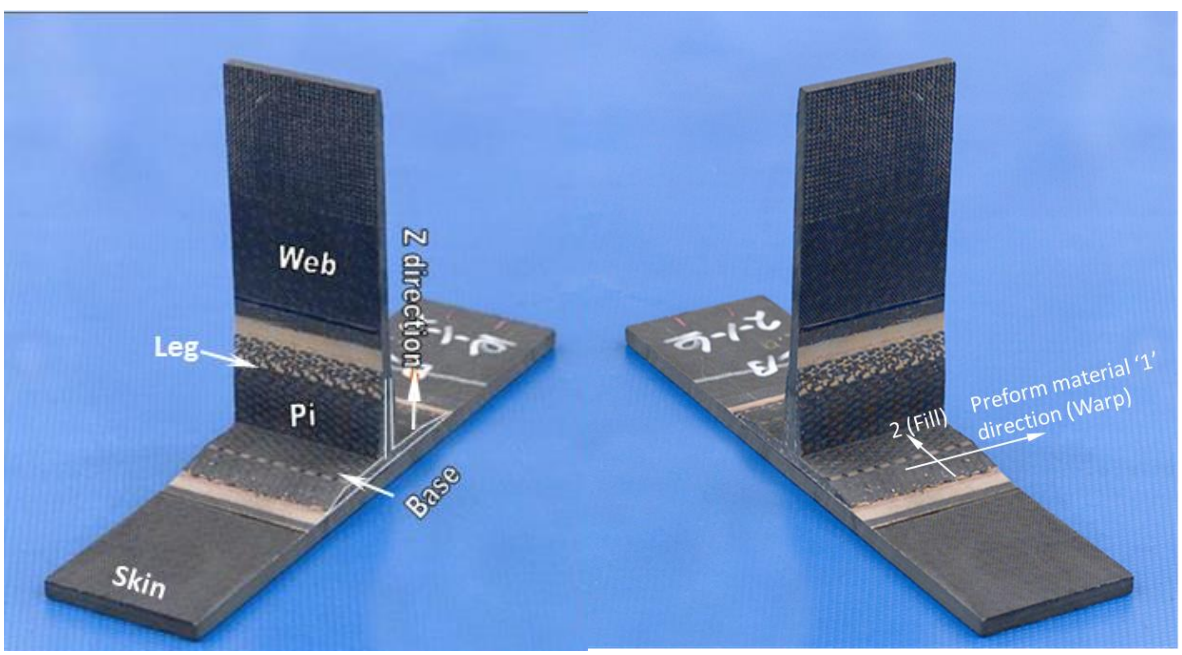

Figure 13.10-9 Pi-joint Nomenclature and Material Coordinate System

Copyright 2015 Lockheed Martin Corporation.
Note: The current version is always the version on the Lockheed Martin network.

A cross section of a pi-joint with a ±45° two-ply overwrap is shown in **Figure 13.10-10**.

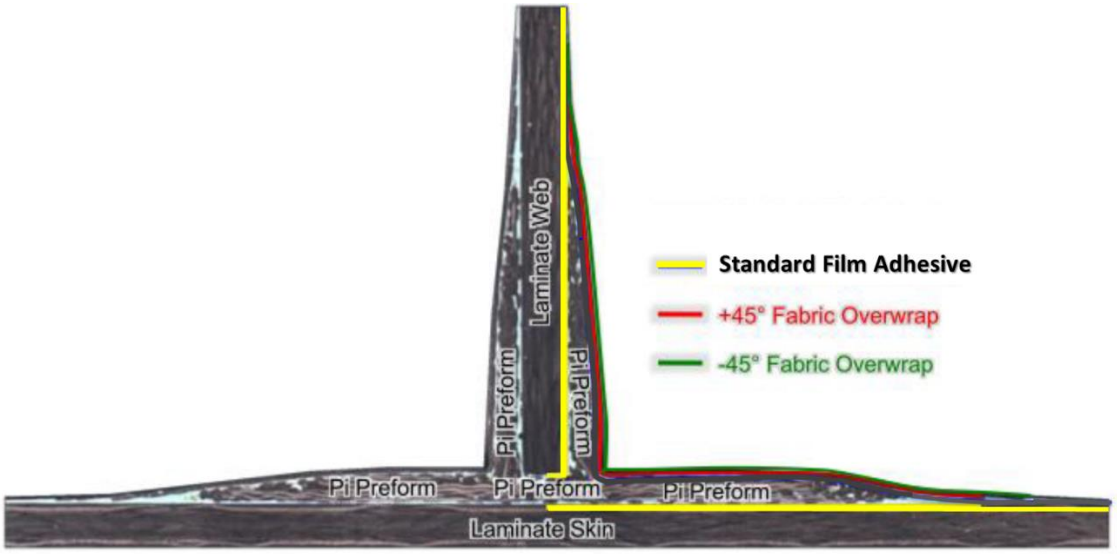

Figure 13.10-10 Cross Section of a Pi-joint

Note that the overwrap film adhesive is used only when the overwrap is over a precured pi, web, or skin. If the pi is not precured then resin in the overwrap is the adhesive bonding the overwrap to the preform. Film adhesives are still used for bonding the remaining portion of the overwrap to the precured skin and web.

13.10.4 Pi-preform Naming Convention

The pi-preforms come in different configurations and styles that are described using specific naming convention. For example a pi-preform called out as PCA2111 specifies a preform with the following features:

Digit	Value	Definition
1	P	Describes the preform cross section. Here P indicates it is a pi preform. Other shapes of preform are also available such as Delta (D), Cross (C), Flat (F), Tee (T), and H.
2	C	This indicates the preform material which in this case is carbon (C). Other preform fibers are glass (G) and nextel (N).
3	A	The 3rd digit describes the configuration and depends on the preform cross section. It indicates which legs are tapered. 'A' implies the pi-preforms base and leg are both tapered. Other configurations are described in Reference 13-24.
4	2	The fourth digit specifies the style of the preform, which is '2' in this case. The style describes the preform construction including tow type, grade, nominal linear weight, number of layers in the base and leg, preform cross section, and dimensions. Details regarding style are given in References 13-24 and 13-25.
5	1	This specifies the clevis width, which can be determined from Reference 13-24 as 0.18 inch (**Figure 13.10-11**)
6	1	This defines the dimensions of the base of the preform and is a function of the preform style. It specifies the distance from the outside of the leg to the beginning of taper (0.64 inch, **Figure 13.10-11**) and end of taper (1.18 inch, **Figure 13.10-11**). In addition it specifies the total length of the base (2.70 inches, **Figure 13.10-11**). These dimensions are provided in References 13-24 and 13-25
7	1	This value specifies dimensions for the leg of the preform that is style '1'. It specifies the length of the flat portion (0.68 inch, **Figure 13.10-11**) and the total height of the legs (1.25 inches, **Figure 13.10-11**). These dimensions are provided in References 13-24 and 13-25

Copyright 2015 Lockheed Martin Corporation.
Note: The current version is always the version on the Lockheed Martin network.

Similar details for other styles and configuration are given in Reference 13-24 .

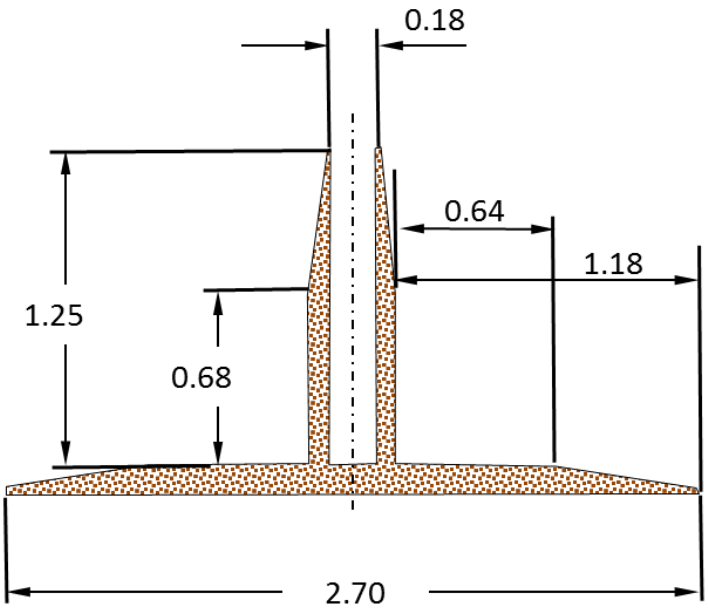

Figure 13.10-11 PCA2111, Configuration A and Style 2 Pi-preform Dimensions in Inches

13.10.5 Pi-Joint Failure Modes

The failure modes observed in a pi-joint are complex and depend on several factors including material system, type of adhesive, testing methods, skin geometry, and environment. A general discussion is provided here while failure modes unique to a specific material system are noted when that material system is discussed in later sections

Pull-off

If the loading is pull-off and if the skin is thin, and therefore flexible, the failure typically initiates in the skin near the flange tip as shown in **Figure 13.10-12**.

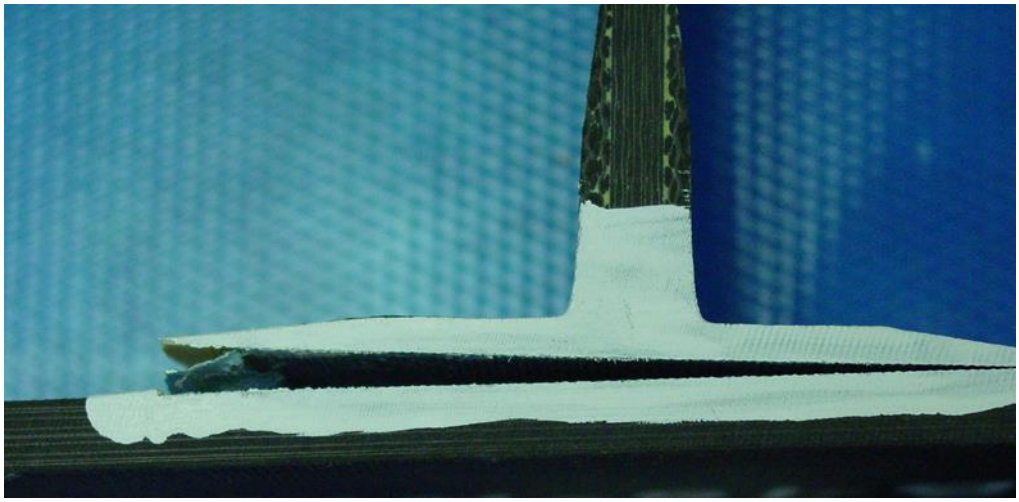

Figure 13.10-12 Pull-off Failure Mode in Skin Due to Bending Near the Flange Tip Region

Copyright 2015 Lockheed Martin Corporation.
Note: The current version is always the version on the Lockheed Martin network.

However, if the skin is thick, and therefore stiffer in bending, the failure tends to occur in the adhesive below the clevis as shown in **Figure 13.10-13** where a steel plate was fastened to the skin to make it stiff in bending for testing purposes.

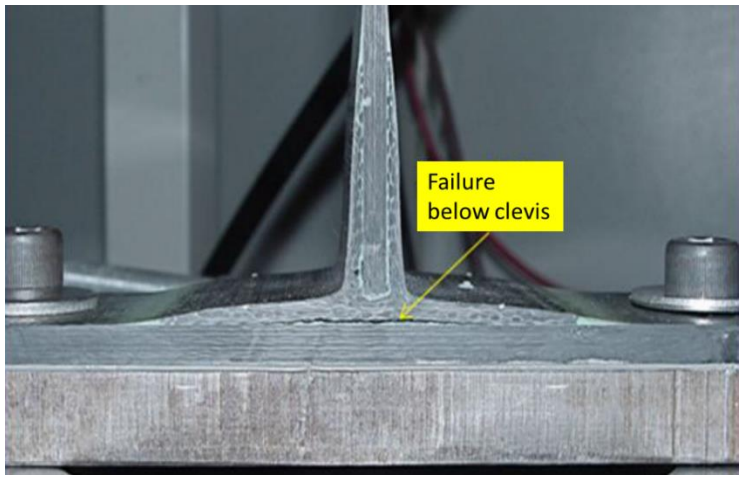

Figure 13.10-13 Pull-off Failure Mode in Adhesive Below Clevis for Skin Laminate with High Bending Stiffness

The pull-off failure modes are also dependent on the environment. For example, in an IM7/977-3, FM300-08K material system at ETW, failure tends to occurs in the adhesive region below the clevis while, at room temperature ambient, it occurs in the skin region below the flange tip.

The failure mode also depends on the resin system used for the skin. For example pull-off failure loads for IM7/977-2 occurs in the adhesive below clevis rather than in the thin skin as seen in IM7/977-3. This is attributed to the better inter-laminar properties of the 977-2 resin system that drives the failure mode to the adhesive (Reference 13-27).

When overwraps are added, especially for thin skins, the tip failure mode is mitigated due to increased bending stiffness of the skin and the failure tends to occur in the adhesive below clevis.

Joint Shear

In shear the predominant failure mode is cracks in the preform. At ETW, the failure can occur in the adhesive region between the clevis and the web.

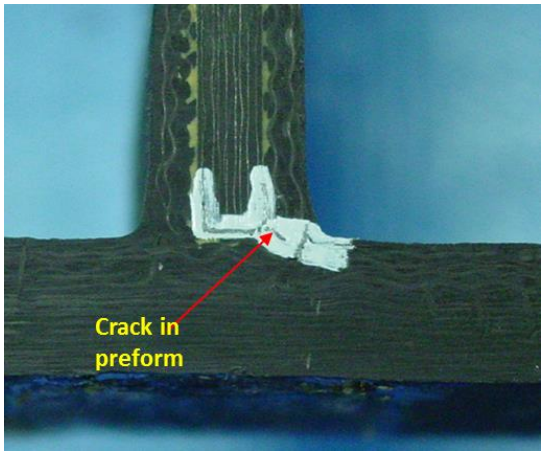

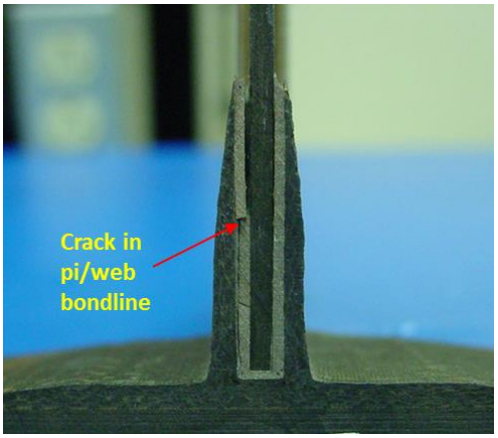

Figure 13.10-14 Joint Shear Failure Modes

Copyright 2015 Lockheed Martin Corporation.
Note: The current version is always the version on the Lockheed Martin network.

Lateral Bend

The lateral bend failure occurs predominately in the bond line below the clevis or, at CTD and RTA, sometimes in the preform filet. However, at ETW, the failure could occur in the adhesive below the flange tip due to peel.

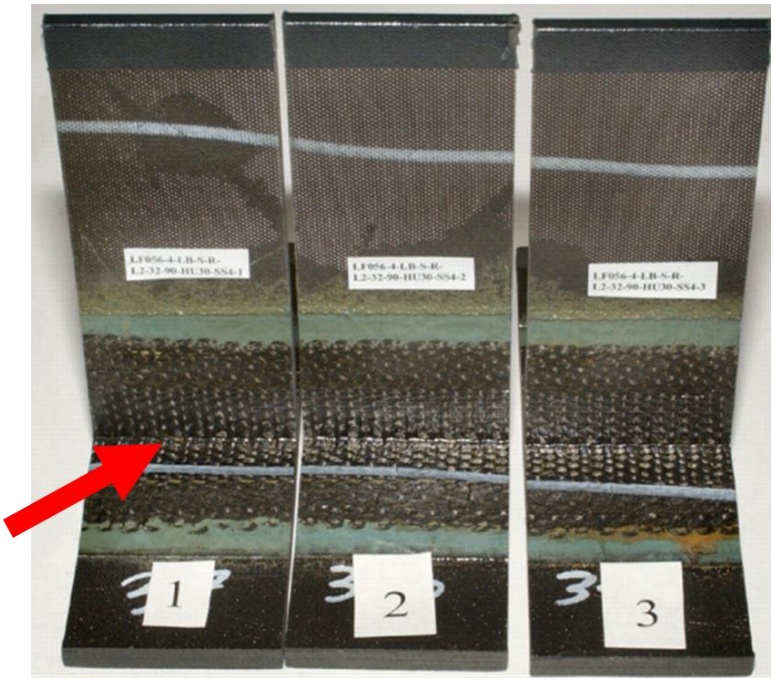

Figure 13.10-15 Preform Failure in the Preform Filet Region Due to Lateral Bend

13.10.6 Design Guidelines

(i) When large pull-off loads are present, 3D woven preforms should be used in composite structures.

(ii) Stiffener terminations should have a ply drop-off slope of 20:1 to avoid high peel stresses at the ends. If this ratio cannot be maintained additional analysis and/or testing is required to show positive margins for the interlaminar tension and shear stresses

(iii) To improve post-impact peel strength anti-peel devices or radius block may be required at stiffener terminations.

(iv) The paste adhesive bond line thickness should be between 0.005 inch and 0.09 inch. Paste adhesives may have inclusions, micro-balloons or fillers that fix the minimum thickness. Paste adhesives are generally used for repair purposes. They are brittle and should not be used for skin to pi-preform connections.

(v) Film adhesive thickness can vary between the carrier cloth thickness, usually 0.0025 in, to 0.01 inches when used over a solid laminate. Thicker adhesive may require a reduction factor on the pull-off allowable.

(vi) Film adhesive should extend no less than 0.03 inch and no more than 0.25 inch past the edge of the pi-preform or overwraps in the uncured state.

(vii) The gap between the web and the base of the clevis must be carefully maintained per specification and if the manufacturing process is unable to maintain that gap, tests should be performed to determine the effects of variation of the gap on allowables.

(viii) For terminations the upstanding leg can be terminated while the base of the pi-preform extends further as shown in **Figure 13.10-1**c. This is referred to as notching.

Copyright 2015 Lockheed Martin Corporation.
Note: The current version is always the version on the Lockheed Martin network.

(ix) Fabric ply should be the outermost ply for skin and web laminates. This is to reduce breakout during drilling and delaminations during trimming of edges. It is also easier to remove peel plies if fabric is the outer-most layer.

(x) 0° and 90° plies on the bond surface should be avoided. Instead use a 45° ply to reduce peel stress.

(xi) At least two outermost structural plies should be continuous. If this is not possible then the outermost plies should be continuous in the bond interface region.

(xii) The faying surfaces should be clean prior to bonding.

(xiii) Typically, the fillet radius should not be less than 0.125 inches for inspectability. However, on pi-joints the radii is typically 0.06 in. Therefore, effects of defects static and fatigue testing should be performed to pre-determine strength reduction factor associated with the variability in manufacturing process (**Table 13.10-38**, Specimen type #11).

(xiv) Two to six ±45° fabric overwrap plies can be added to increase pi-joint shear strength. Each ply overwrap should be stair stepped in a 0.20 to 0.25 inch increment. The step may increase to 0.30 inch for Out-of-Autoclave (OoA) cure system.

The following guidelines are specific to OoA material system.

(i) Pi infusion in an autoclave should be performed per specification Palmdale Bulletin #427 with a straight infusion bar.

(ii) Manufacturing cauls should be stiff and either rotamolds or stepped to match the pi shape desired.

(iii) Two plies of FM309-1M should be used for web bond.

(iv) All adhesive should be perforated prior to installation to allow venting during the debulk period.

(v) A minimum debulk period of 12 hours is required prior to the start of a cure. Minimum vacuum required is 24 inch upto 300°F.

(vi) All pi terminations should utilize an Eddie bolt, countersink for the skin and protruding head for the web, to prevent premature failures. Two fasteners on each flange for a total of four fasteners at the termination is recommended. The fastener size can vary from 3/16 to ¼ inch depending on the width of the flange.

13.10.7 Summary of LM Documents with Pi-Preform Properties, Allowables and Pi-Joint Allowables

A summary of the various documents that contain pi-joint allowables for various material systems, and environment are provided in **Table 13.10-2**.

Copyright 2015 Lockheed Martin Corporation.
Note: The current version is always the version on the Lockheed Martin network.

Table 13.10-2 Summary of Reports Documenting Pi-Preform Material Properties, Allowables, and Pi-joint Allowables

Document	Ref.	Material System	Test Objective	Environment	Properties/ Allowables	Comments
EL-ST-EL-09	13-10	IM7/977-3 pi-preforms, IM7/977-3 prepreg thick tapes and fabric, and FM300-08 adhesive.	Develop allowables for design of co-bonded joints applying 3D woven pi-preforms in primary structure applications. - Skin Thickness: 0.190 to 0.332 in - Spans: 4 and 7 in. - Web Angle Effect: 45° and 67° - Fixity: Simple and Clamped - Skin Lay-up: Quasi-isotropic and Soft Laminate for Pull-off	RTA CTD ETW (220 and 250°F)	Tensile Pull-off Lateral Bend Shear Combined Pull-off and Lateral Bend Combined Pull-off and Shear Combined Shear and Lateral Bending Effects of defects	Bondline Thickness: 0.005 in
XG-ST-EL-22	13-16	IM7/977-3 pi-preforms, IM7/977-3 prepreg thick tapes and fabric, and FM300-08 adhesive.	This test series dealt with the qualification of the secondarily bonded joints specifically: - Bond strength of the secondarily bonded pi-preform joint exhibiting the baseline bondline configuration: one layer of FM-300 film adhesive. - The bond strength of secondarily bonded pi-preform joints exhibiting thick bondlines (multiple layers of FM-300)	RTA ETW (250°F)	Tensile Pull-off Lateral Bend Shear	Resulted in reduction factors for secondarily bonded joints The pre-cured pi-preform and the web were secondarily-bonded to the base laminate.
XG-ST-CO-13	13-14	IM7/977-3 flat weave	To characterize the mechanical and physical properties of the 3D IM7/977-3angle-interlock weave used to fabricate the pi-shaped textile preform.	RTA CTD ETW (250°F)	$E_{tension}$ $E_{compression}$ OHT, OHC, FHT, FHC Bearing with various reactions, Notched Flexure ILS Pull-thru	Joint allowables for the same material system were documented in EL-ST-EL-09.

Copyright 2015 Lockheed Martin Corporation.
Note: The current version is always the version on the Lockheed Martin network.

Document	Ref.	Material System	Test Objective	Environment	Properties/ Allowables	Comments
XG-ST-CO-14	13-22	IM7/977-3 pi-preforms, IM7/977-3 prepreg thick tapes and fabric, and FM300-08 adhesive.	The local effects of microdarting and stretching on strength properties of the preform material are	RTA CTD ETW (250°F)	Tensile, pull-off, lateral bend and shear	Reduction factors for
FZM-9025	13-12	IM7/977-3 pi-preforms, IM7/977-3 prepreg tapes and fabric, and AF191 adhesive.	Documents the tests performed on pi-joints during Composites Affordability Initiative (CAI).			Report discusses the pi-preform joint configurations, manufacturing steps, overwraps, tooling, inspection techniques, and repair.
XG-ST-EL-29.1	13-37	IM7/977-3 pi-preforms, IM7/977-3 prepreg thick tapes and fabric, and FM300-08 adhesive.	To investigate the effects of 40 ft-lb impact damage in and around the preform terminations of the bonded duct structure.			There were twenty-one impact points in total.
FZM-10160	13-29	IM7/MTM45-1 FM309-1M	IM7/MTM45-1 Pi Weave Allowables (including UNT, UNC, OHC, OHT)	RTA, CTD (-100ºF, -65ºF), ETW (200ºF, 250ºF)		In work – not released
FZM-10161	13-30	IM7/MTM45-1 FM309-1M	IM7/MTM45-1 Pi-Preform Joint Allowables - Standard Weight	RTA, CTD (-100ºF), ETW (220ºF)	Pull-off, joint shear, lateral bend, effects of defects, durability and damage tolerance.	In work – not released
FZM-10162	13-31	IM7/MTM45-1 FM309-1M	IM7/MTM45-1 Pi-Preform Joint Allowables - Light Weight	RTA, CTD (-100ºF), ETW (220ºF)	Pull-off, joint shear, lateral bend, effects of defects.	In work – not released

References to additional material forms and reports can be found in Ref. 13-38.

Copyright 2015 Lockheed Martin Corporation.
Note: The current version is always the version on the Lockheed Martin network.

13.10.8 Joint Element Configurations

The pi-joint elements employed to develop the allowables are shown in **Table 13.10-3**. The center column of the table summarizes the various test element configurations employed to develop the allowables

Table 13.10-3 Various Joint Element Test Configurations Used for Determining Joint Allowables

Loading Configuration	Drawing/Figure	Comments
Tensile pull-off load .	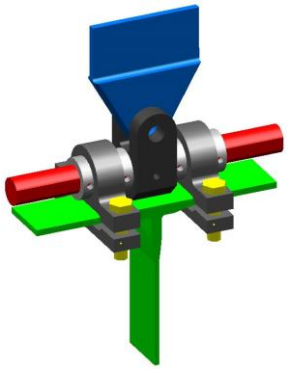 Two Roller Test Configuration	This test configuration was used to determine the pull-off allowable for the IM7/977-3 thick tape FM300-08 (adhesive) material system and IM7/977-3 AF191 (adhesive) material system. It was also used to develop allowables for IM7/5250, IM7/M65, and some of the IM7/MTM45-1 FM300-2K (adhesive) material system (Reference 13-28). Not preferred for future design
	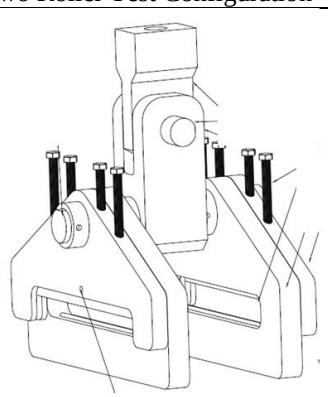 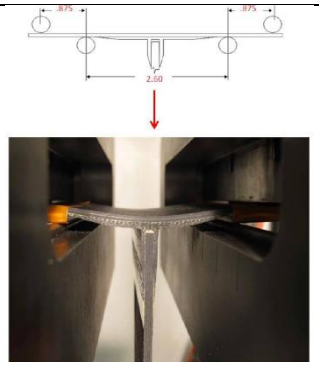 Four Roller Test Configuration	This test configuration was used to determine pull-off allowable for some IM7/977-3, FM300-2k material system (Reference 13-28) and pull-off allowable for IM7/MTM45-1 FM309-1M (adhesive) material system. The four roller test configuration reduces the bending at the flange tip compared to the two roller test configuration. Preferred for future design

Copyright 2015 Lockheed Martin Corporation.
Note: The current version is always the version on the Lockheed Martin network.

Loading Configuration	Drawing/Figure	Comments
Shear load	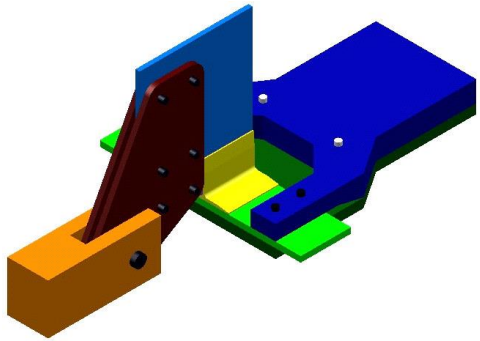	This test configuration was used to develop joint shear allowable for IM7/977-3 FM300-08K (adhesive), IM7/977-3 AF191 (adhesive), IM7/5250 2550G (adhesive), and IM7/M65 2550G (adhesive) material systems. A drawback of this method is that it does not accurately represent load introduction into the specimen and is more severe than what is observed in an actual structure. Alternative test fixture such as the I-beam shear configuration was developed to overcome this drawback. Not preferred for future design.
	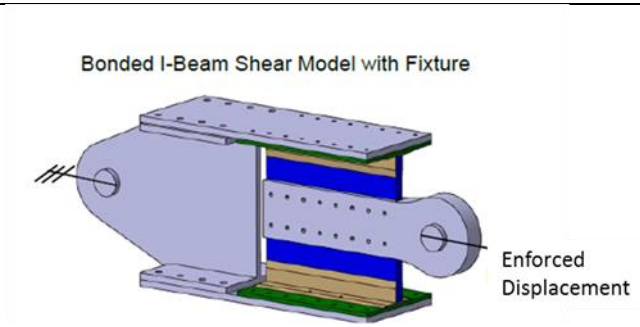	Preferred for future design. However, this fixture costs more than the one shown above.

Copyright 2015 Lockheed Martin Corporation.
Note: The current version is always the version on the Lockheed Martin network.

Loading Configuration	Drawing/Figure	Comments
Lateral bend	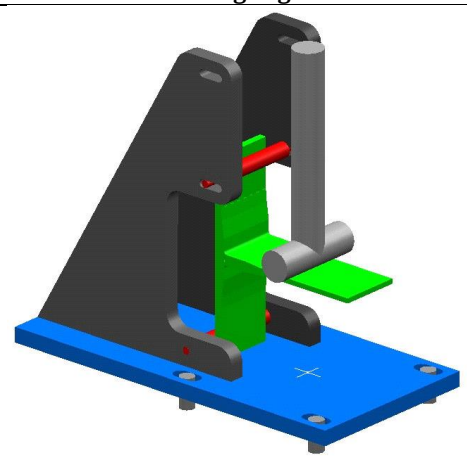	Not preferred for future design
	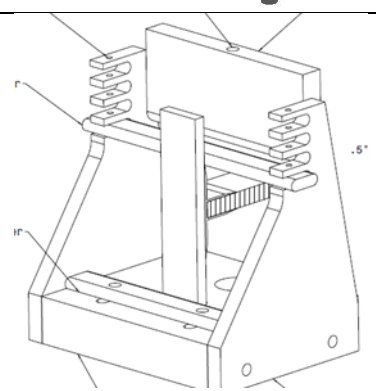	Prefered future design since this can handle wider specimen and accommodate multiple pi widths.

Copyright 2015 Lockheed Martin Corporation.
Note: The current version is always the version on the Lockheed Martin network.

Loading Configuration	Drawing/Figure	Comments
Preform pull-off and joint shear	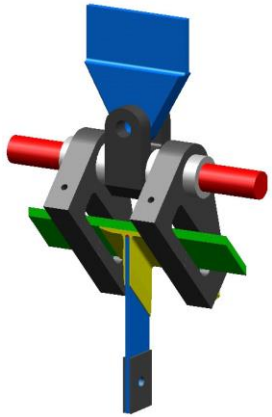 Straight Beam Specimen	The straight beam specimen was used for determining interaction equations for IM7/977-3 FM300-08 and IM7/977-3 AF191 material systems. However, the data obtained for the FM300-08 was not correct for the reason: It is important to ensure that the specimen is gripped correctly and not constrained improperly during the test. Ignoring this resulted in the invalidation of the entire combined pull-off/shear test in a recent program (Reference 13-17). The straight beam configuration also results in higher pull-off/shear ratio. Not preferred for future design
	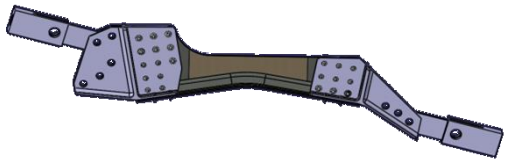 Curved Beam Specimen	The curved beam configuration facilitates better load introduction to the specimen and provides for lower pull-off/shear ratio. Preferred for future design
Pull-off and lateral load	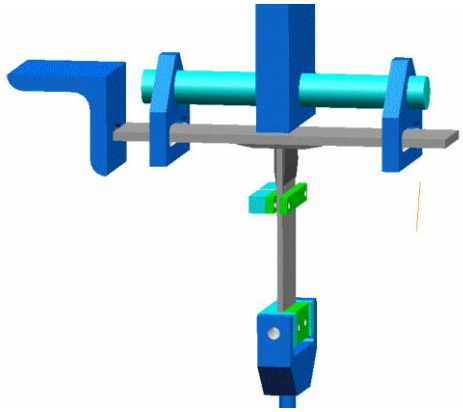	This test configuration was emplyed to obtain the interaction equation for the IM7/977-3 FM300-08 material system. First a pull-off load is applied upto a certain percent of pull-of allowable and then a lateral load is applied. The accuracy of results from this test is questionable since the loading is not proportional and therefore not representative of the combined loads on the actual structure. Not preferred for future design. See 13.10.9.4 for details on how to handle this loading scenario.

Copyright 2015 Lockheed Martin Corporation.
Note: The current version is always the version on the Lockheed Martin network.

Loading Configuration	Drawing/Figure	Comments
Shear and lateral load	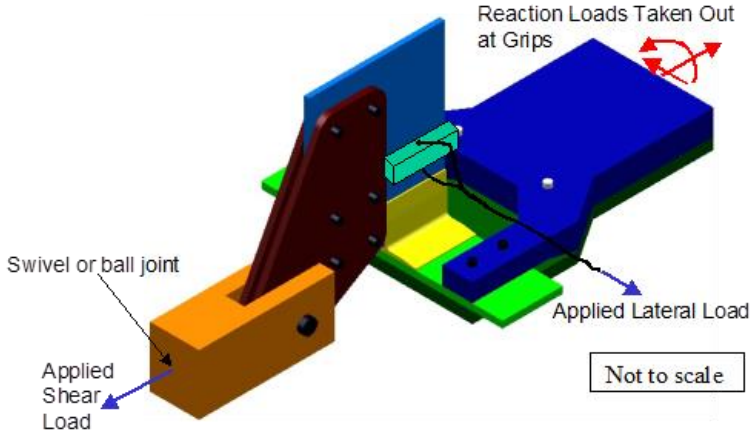	This test configuration was used for IM7/977-3 FM300-08 material system. A shear load is first applied upto a certain percent of the joint shear allowable and subsequently a lateral bend is applied. This method has the same drawback as the shear test and furthermore the loading is not proportional and therefore not representative of the actual structure. Not preferred for future design. See 13.10.11.6 for details on how to handle this loading scenario.

Copyright 2015 Lockheed Martin Corporation.
Note: The current version is always the version on the Lockheed Martin network.

13.10.9 IM7/977-3 & FM-300-08K Adhesive, 350ºF Autoclave Cure Material System

The pi-preform and the material system for which the allowables are developed is described in **Table 13.10-4** and **Table 13.10-5** respectively. Note that the pi-preform allowables developed in this section are specific to the configuration depicted in **Table 13.10-4**.

Table 13.10-4 Pi-Preform Dimensions

Preform Supplier	LM Spec	Preform Material, Style & Configuration	Preform Cross Section
Bally Ribbon Mills	LMB003C	IM7/977-3 3D Weave Fabric Prepreg, PCA1111	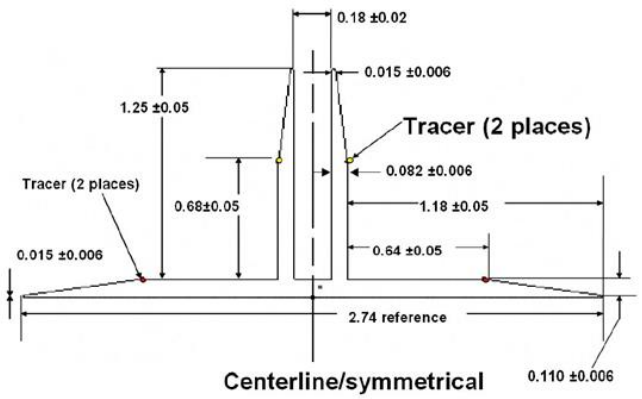

Table 13.10-5 IM7/977-3 & FM-300-08K 350ºF Cure Material System

Skin	Web	Web Thickness (in)	Adhesive
IM7/977-3 Thick Tape Prepreg	IM7/977-3 2D Weave Fabric Prepreg	0.166	FM-300-08K 0.08 lb/ft^2 open knit polyester carrier film, -65ºF to 250ºF service temperature

13.10.9.1 Failure Modes Observed

The failure modes observed in IM7/977-3 thick tape and FM300-08 adhesive material system were complex and depicted in **Figure 13.10-16**.

Copyright 2015 Lockheed Martin Corporation.
Note: The current version is always the version on the Lockheed Martin network.

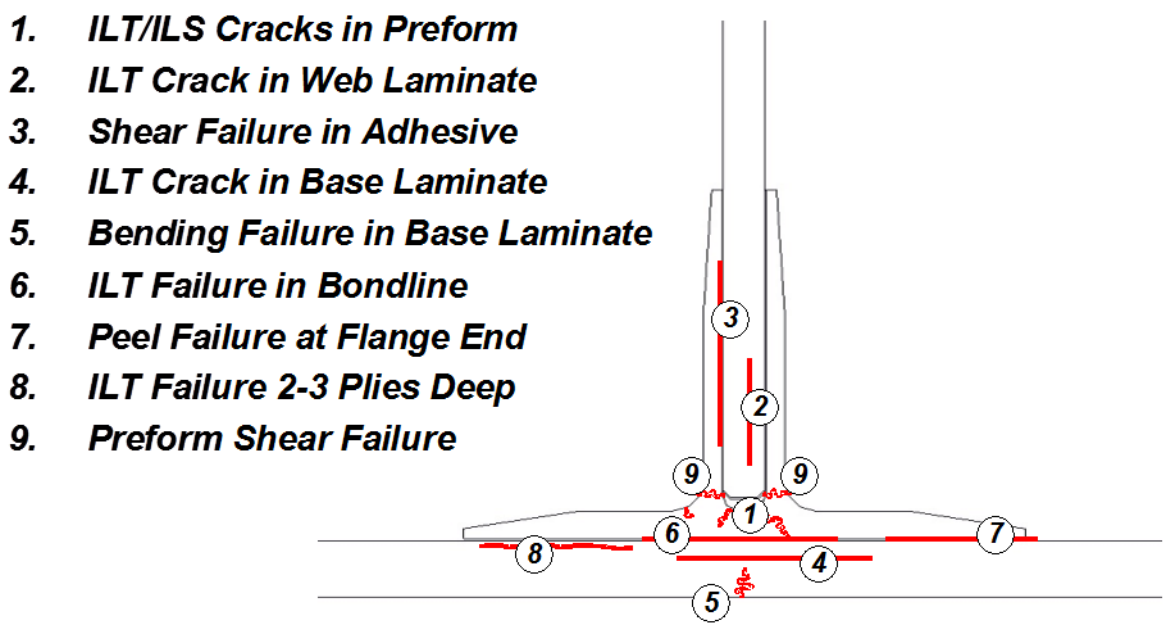

Figure 13.10-16 Typical Failure Modes Seen in a Pi-joint Without Fastener and Overwrap

The critical failure modes are dependent on the loading and environment. These modes are summarized in **Table 13.10-6** for different loading conditions.

Table 13.10-6 Summary of Observed Failure Modes

Material	Loading Condition	Description	Failure Modes (Figure 13.10-16)
Skin: IM7/977-3 thick tape Web: IM7/977-3 fabric Adhesive: FM300-08K See **Figure 13.10-16** for a schematic of different failure modes	Pull-off	Failure occurred below preform tip and/or in the adhesive below the upstanding leg (especially at ETW). The failure load is dependent on laminate thickness, laminate lay-up, span, and web angle.	7, 8, 5
	Joint Shear	At RTA and CTD failure occurs at the curved portion of the pi-preform, i.e., intersection of the leg and flange. At ETW shear failure occurred in the web adhesive. Failure loads does not depend on the laminate thickness, lay-up, and span.	9, 3
	Lateral Bend	Failure occurs at preform radius at RTA and CDT and in the skin or the adhesive directly below the upstanding leg at ETW. Failure load is independent of thickness, lay-up, and span.	6, 7, 1, 3
	Pull-off and Joint Shear	Failure is dominated by pull-off mode for high pull-off/shear loading ratios. Failure occurs at preform tip at RTA and CDT, and in the adhesive beneath the upstanding leg at ETW.	7, 8, 9, 3
	Pull-off and Lateral Load	If pull-off dominated, failure occurs at the preform tip. If lateral bending dominated, failure occurs at preform fillet radius. If they are both equal and at ETW failure occurs in the adhesive beneath the upstanding leg	6, 7, 8, 2, 4
	Shear and Lateral Load	Failure occurs in preform radius and/or in the adhesive below the upstanding leg.	9, 3, 6

Copyright 2015 Lockheed Martin Corporation.
Note: The current version is always the version on the Lockheed Martin network.

13.10.9.2 Stress Method and Pull-off Allowables

The B-basis pull-off allowable as a function of thickness and environment is given in **Table 13.10-7**.

Table 13.10-7 Pull-off Allowables P_{po-a} (lb/in) for a Simply Supported 4 inch Span Quasi Layup [25/50/25] with a Web Angle = 90º (Reference 13-17).

Plies	Skin Thickness (in)	Temperature			
		-65ºF	75ºF	220ºF	250ºF
24	0.199	720	690	598	554
32	0.266	1078	1045	844	728
40	0.332	1241	1247	944	814

Based on the above table the pull-off values are expressed in equation form as shown below.

$$P_{po-a} = (m_t \times t + C_t) \qquad \text{Equation 13.10-1}$$

where
P_{po-a} = pull-off allowable (lb/in)
m_t = slope (lb/in^2)
C_t = intercept (lb/in)
t_{skin} = skin thickness (in)
The intercept and slope are given in **Table 13.10-8**.

Table 13.10-8 Pull-off Allowables P_{po} (lb/in) as a Function of Skin Thickness in Equation Form and Environment for a Simply Supported 4 in Span Quasi Layup [25/50/25] with a Web Angle = 90º.

Skin Thickness (in)	Temperature							
	-65ºF		75ºF		220ºF		250ºF	
	m_t	C_t	m_t	C_t	m_t	C_t	m_t	C_t
≤0.199	3618.09	0.0	3467.34	0.0	3005.03	0.0	2783.92	0.0
0.199 – 0.266	5785.00	-435.57	5622.79	-432.15	4027.99	-207.11	2834.59	-12.41
0.266 – 0.332	3423.46	105.23	3806.55	-16.24	2226.12	205.52	1725.90	241.48

The pull-off allowable margin of safety for the pull-off load can be calculated as follows.

$$MS_{po} = \frac{K_{po} P_{po-a}}{P_{po}} - 1 \qquad \text{Equation 13.10-2}$$

where
P_{po} = applied pull-off load (lb/in)
P_{po-a} = pull-off allowable (lb/in)
K_{po} = pull-off factor, described in **Table 13.10-9**
MS_{po} = pull-off margin of safety

The values in the table can be interpolated between temperatures to estimate the allowable when operating temperature is different than the test temperatures. The pull-off factor, which depends on the span, web angle, ply percent, repair fastener, presence of splice, and secondary bond is described in **Table 13.10-9**. These factors are based on the test data for IM7/977-3 thick tape, FM300-08 material system (Reference 13-17) and should not be used for other material systems.

Copyright 2015 Lockheed Martin Corporation.
Note: The current version is always the version on the Lockheed Martin network.

Table 13.10-9 Pull-off Factors Defined (K_{po})

$K_{po} = K_{span} \times K_{web\text{-}angle} \times K_{ply\%} \times K_{po\text{-}overwrap} \times K_{po\text{-}EOD} \times K_{po\text{-}splice} \times K_{po\text{-}secbond}$		Equation 13.10-3
Factors	**Symbol**	**Table Reference**
Span length factor	K_{span}	**Table 13.10-10**
Web angle factor	$K_{web\text{-}angle}$	**Table 13.10-12**
0° ply percent factor (quasi, soft, hard)	$K_{ply\%}$	**Table 13.10-13**
Pull-off overwrap factor	$K_{po\text{-}ovewrap}$	**Table 13.10-14**
Pull-off effects of defects	$K_{po\text{-}EOD}$	**Table 13.10-15**
Pull-off splice factor	$K_{po\text{-}splice}$	**Table 13.10-16**
Pull-off secondary bond factor	$K_{po\text{-}secbond}$	**Table 13.10-17**

Span Length Factor (K_{span})

The span length factor correlates the pull-off allowable determined for a 4in span test specimen to the actual structural span as depicted in **Figure 13.10-17**. Span 'S' is the span between the supports in the actual structure.

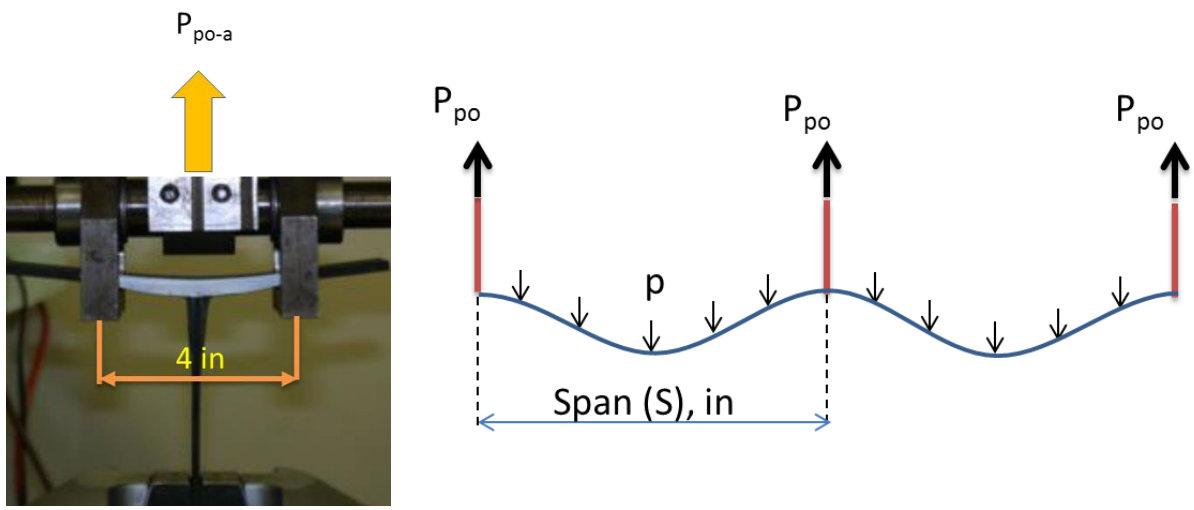

Test Configuration Actual Structural Configuration

Figure 13.10-17 Span Length (in) Defined

The pressure p is a function of the pull-off load and is expressed as:

$$p = \frac{P_{po}}{S} \qquad \text{Equation 13.10-4}$$

where,

p = pressure (psi, e.g. fuel pressures)
S = span length (in, e.g. spar spacing)

The applied pull-off load $P_{po} \leq P_{po\text{-}a}$, where $P_{po\text{-}a}$ is the pull-off allowable. The span length factor (K_{span}) is given in **Table 13.10-10**.

Copyright 2015 Lockheed Martin Corporation.
Note: The current version is always the version on the Lockheed Martin network.

Table 13.10-10 Span Factor as a Function of Span (S) and Skin Thickness (t_{skin}) for Quasi [25/50/25], and Soft [10/80/10] Laminates, p < 30psi.

t_{skin} (in)	p (psi)	K_{span}	
≤0.199	≤ 30	1.0	
0.199 to 0.332	≤ P_q	1.0	
	> P_q	$\frac{\lambda_q - 1}{30 - P_q} \times \Delta p_q + 1$	Equation 13.10-5
P_q =-0.45×S+39.018 psi $\Delta p_q = p - P_q\ psi$ $\lambda_q = 0.9992 - 0.00741 \times (S - 21) - 0.038346 \times (t_{skin} - 0.199) - 0.06483 \times (t_{skin} - 0.199) \times (S - 21)$ t_{skin} = skin thickness (in)			Equation 13.10-6 Equation 13.10-7 Equation 13.10-8

Table 13.10-11 Span Factor as a Function of Span (S) and Skin Thickness (t_{skin}) for Hard [50/40/10] Laminates, p < 30psi.

t_{skin} (in)	p (psi)	K_{span}	
≤0.199	≤ 30	1.0	
0.199 to 0.332	≤ P_h	1.0	
	> P_h	$\frac{\lambda_h - 1}{30 - P_h} \times \Delta p_h + 1$	Equation 13.10-9
P_h =-0.981×S+44.706 psi $\Delta p_h = p - P_h$ psi $\lambda_h = 0.9999 - 0.02728 \times (S - 15) + 0.000606 \times (t_{skin} - 0.199) - 0.040939 \times (t_{skin} - 0.199) \times (S - 15)$			Equation 13.10-10 Equation 13.10-11 Equation 13.10-12

The span length (S) is limited to 30 inches in **Table 13.10-10** and **Table 13.10-11**.

Web Angle Factor ($K_{web\text{-}angle}$)

The web-angle is defined in **Figure 13.10-18**.

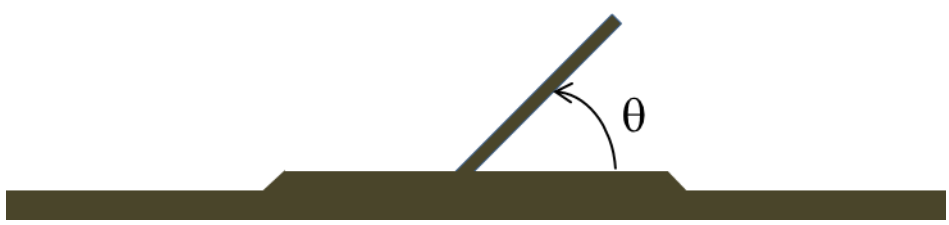

Figure 13.10-18 Web-Angle (θ) Defined

The web angle factor ($K_{web\text{-}angle}$) as a function of thickness is given in **Table 13.10-12**.

Table 13.10-12 Web Angle Factor ($K_{web\text{-}angle}$) as a Function of Skin Thickness and Web Angle, Reference 13-17.

	0.199in≤t≤0.332in	
θ=90°	1.0	Equation 13.10-13
67°≤θ<90°	$K_{web-angle} = 0.150376 \times t_{skin} + 0.970075$	

Copyright 2015 Lockheed Martin Corporation.
Note: The current version is always the version on the Lockheed Martin network.

0° ply percent factor ($K_{ply\%}$)

The effect of 0° ply percent on pull-off allowable is given by the factor $K_{ply\%}$, which is given below:

Table 13.10-13 0° Ply Percent Factor ($K_{ply\%}$) as a Function of 0° Ply Percent, Reference 13-17.

0° ply%	$K_{ply\%}$	
< 25% (Soft)	$1 + 2.47 \times \left(\frac{0^o ply\%}{100} - 0.25\right) - 17.37 \times (t_{skin} - 0.190) \times (\frac{0^o ply\%}{100} - 0.25)$	Equation 13.10-14
≥25% (Quasi and Hard)	1.0	

Pull-off overwrap Factor ($K_{po\text{-}Overwrap}$)

The effect of overwraps on pull-off as a function of skin thickness is given in **Table 13.10-14**. Test data shows no significant increase in pull-off strength beyond two overwrap plies.

Table 13.10-14 Pull-off Overwrap Factor ($K_{po\text{-}Overwrap}$) as a Function of Skin Thickness, References 13-19, 13-28.

	Skin Thickness (t_{skin})	$K_{po\text{-}Overwrap}$	
≥ 2 overwrap plies	t_{skin}<0.199 in	1.41	Equation 13.10-15
	0.199 in ≤ t_{skin} ≤ 0.3 in	-3.6363× t_{skin} + 2.1	
	t_{skin} > 0.3 in	1.0	

Pull-off Effect of Defect Factor ($K_{po\text{-}EOD}$)

When a fastener is used to repair disbond between the pi-preform and skin the pristine pull-off strength is not completely restored. This reduction in pristine strength depends on the type of fastener used and is defined as an effects-of-defect factor ($K_{po\text{-}EOD}$) in **Table 13.10-15**. Note that the joint should be designed for repairability and hence the pristine pull-off allowable should be reduced by this factor.

Table 13.10-15 Pull-off Effects of Defect Factor ($K_{po\text{-}EOD}$) for All Environment, References 13-17,13-19,13-32

Fastener Type	$K_{po\text{-}EOD}$	
Ti/CRES Blind Bolt 100° CSK (Reference 13-19)	0.84	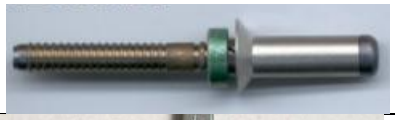
Eddie Bolt (Reference 13-17) Countersunk	0.91	
Protruding head fastener (Reference 13-19)	1.0	

Pull-off Splice factor ($K_{po\text{-}splice}$)

If the preform is spliced the pull-off allowable should be reduced. If required, arresting feature such as fasteners can be added to reduce peel. Preform splices are formed by overlapping darted strips of preform. Details of the methods for forming contours with preforms and preform splices are given in Reference 13-20. A spliced preform is shown in **Figure 13.10-19**.

Copyright 2015 Lockheed Martin Corporation.
Note: The current version is always the version on the Lockheed Martin network.

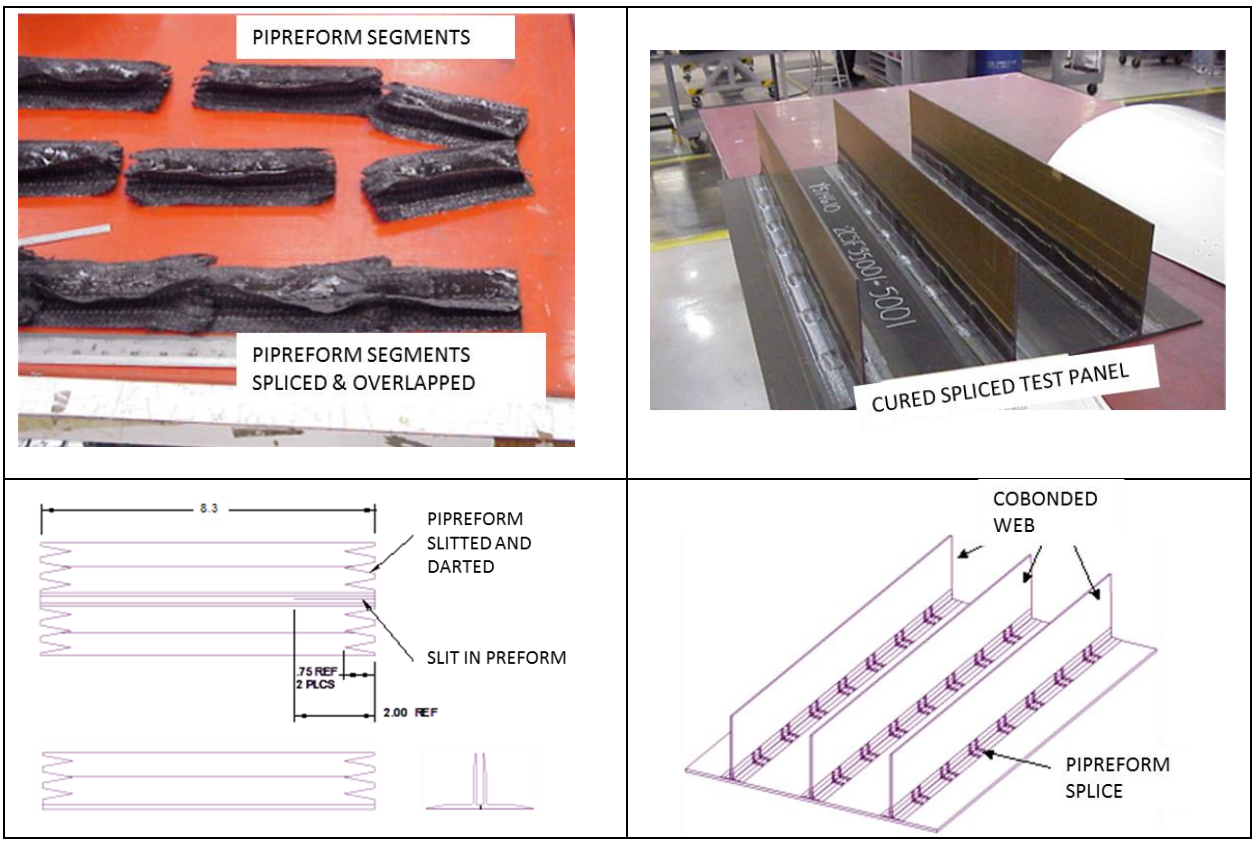

Figure 13.10-19 Spliced Preform Joint

Factor for splices for the pull-off loading configuration is given in **Table 13.10-16**.

Table 13.10-16 Pull-off Splice Factor ($K_{po\text{-}splice}$), Reference 13-22.

Configuration	-65ºF - 250ºF
Pull-off	0.88
No Splice	1.0

The above method of splicing, overlapping, and joining the pi-preform is suitable where high axial loads are to be transferred by the pi-preform.

Pull-off Secondary-bond Factor ($K_{po\text{-}secbond}$)

For secondarily-bonded pi-joints additional reduction to pull-off allowable is required. This factor is shown in **Table 13.10-17**. Areas of application of secondary bond is discussed in Section 13.10.2.

Table 13.10-17 Pull-off Secondary Bonded Factor ($K_{po\text{-}secbond}$), Reference 13-23.

Configuration	-65ºF - 250ºF
Secondary-bond	0.71
No Secondary Bond	1.0

The above table includes the effect of adhesive thickness (<0.1 in). Thicker adhesives are generally employed when the gap between the faying surfaces cannot be tightly controlled. If the bond is not a secondary bond then $K_{po\text{-}secbond}$=1.0. These factors cannot be applied for other adhesive systems.

Copyright 2015 Lockheed Martin Corporation.
Note: The current version is always the version on the Lockheed Martin network.

13.10.9.3 Stress Method and Joint Shear Allowables

The joint shear allowable is dependent only on temperature and is independent of web angle, span length, skin lay-up, and skin thickness. However, it is affected by overwraps, repair fasteners, secondary bond, and presence of splice. The shear allowables as a function of temperature are given in **Table 13.10-18**.

Table 13.10-18 Joint Shear Allowable as a Function of Environment, Reference 13-17.

	-65ºF	75ºF	220ºF	250ºF
Joint Shear (lb/in)	1852	1574	1218	1066

The values in the table can be interpolated between temperatures to estimate the allowable when operating temperature is different than the test temperature. Employing the joint shear allowable the margin of safety for the joint shear load can be calculated as follows.

$$MS_{js} = \frac{K_{js} P_{js-a}}{P_{js}} - 1 \qquad \text{Equation 13.10-16}$$

where

P_{js} = applied joint shear load (lb/in)
P_{js-a} = joint shear allowable (lb/in)
K_{js} = joint shear factor, described in **Table 13.10-19**
MS_{js} = joint shear margin of safety

The joint shear factor (K_{js}), which depends on the overwrap, repair, secondary bond, and splice, is described in **Table 13.10-19**. These factors are based on the test data for IM7/977-3 thick tape, FM300-08 material system and should not be used for other material system.

Table 13.10-19 Joint Shear Factors Defined (K_{js})

$K_{js} = K_{js\text{-}overwrap} \times K_{js\text{-}EOD} \times K_{js\text{-}splice} \times K_{js\text{-}secbond}$		**Equation 13.10-17**
Factors	Symbol	Table Reference
Joint shear overwrap factor	$K_{js\text{-}ovewrap}$	**Table 13.10-20**
Joint shear Effect of Defect factor	$K_{js\text{-}EOD}$	**Table 13.10-21**
Joint shear splice factor	$K_{js\text{-}splice}$	**Table 13.10-22**
Joint shear secondary bond factor	$K_{js\text{-}secbond}$	**Table 13.10-23**

Joint Shear overwrap Factor ($K_{js\text{-}Overwrap}$)
The effect of overwraps on joint shear is given in **Table 13.10-20**.

Table 13.10-20 Joint Shear Overwrap Factor ($K_{js\text{-}overwrap}$), References 13-19.

	-65ºF to 250ºF
≥ 2 overwrap plies	1.3

The Joint Shear Effect of Defect Factor ($K_{js\text{-}EOD}$)
When a fastener is used to repair disbond between the pi-preform and the skin the pristine shear strength is not restored. This reduction in pristine strength is defined as an effects-of-defect factor ($K_{js\text{-}EOD}$) in **Table 13.10-21** and is applied to the joint shear allowable dependent on the type of repair fastener used. Note that the joint should be designed for repairability and hence the pristine joint shear allowable should be reduced by this factor before using it in design. Furthermore the skin should be sized for this bearing load in the initial design.

Copyright 2015 Lockheed Martin Corporation.
Note: The current version is always the version on the Lockheed Martin network.

Table 13.10-21 Joint Shear Effects of Defect Factor ($K_{js\text{-}EOD}$) for All Environment, References 13-17 & 13-19.

Fastener Type	$K_{js\text{-}EOD}$	
Eddie Bolt (Reference 13-17)	0.86	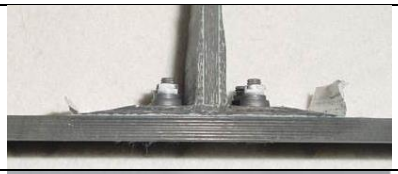
Protruding head fastener (Reference 13-19)	0.9	

Joint Shear Splice factor ($K_{js\text{-}splice}$)
If the preform is spliced the shear allowable should be reduced. Details of the splicing method used is discussed in Section 13.10.9.2. Factors for splices for the joint shear loading configurations is given in **Table 13.10-22**.

Table 13.10-22 Joint Shear Splice Factors ($K_{js\text{-}splice}$), Reference 13-22.

Configuration	-65ºF - 250ºF
Pull-off	0.88
No splice	1.0

Joint Shear Secondary-bond Factor ($K_{js\text{-}secbond}$)
For secondarily-bonded pi-joints additional reduction to joint shear allowable is required. This factor is shown in **Table 13.10-23**. The areas of application of secondary bond is discussed in Section 13.10.2.

Table 13.10-23 Joint Shear Secondary Bonded Factor ($K_{js\text{-}secbond}$), Reference 13-23.

Configuration	-65ºF - 250ºF
Pull-off	0.71
No Secondary Bond	1.0

The above table includes the effect of adhesive thickness (<0.1 in). Thicker adhesives are generally employed when the gap between the faying surfaces cannot be tightly controlled. These factors must not be applied for other adhesive systems.

13.10.9.4 Stress Method and Lateral Bend Allowables

The lateral bend allowable is dependent only on temperature and is independent of web angle, span length, skin lay-up, and skin thickness. The lateral bend allowables as a function of temperature are given in **Table 13.10-24**.

Table 13.10-24 Lateral Bend Allowable as a function of Environment, Reference 13-17.

	-65ºF	75ºF	220ºF	250ºF
Lateral Moment (in-lb/in)	228	240	199	195

The values in the table can be interpolated between temperatures to estimate allowable when operating temperature is different than the test temperature. Employing the lateral bend allowable the margin of safety for the lateral bend can be calculated as follows.

Copyright 2015 Lockheed Martin Corporation.
Note: The current version is always the version on the Lockheed Martin network.

$$MS_{lb} = \frac{K_{lb} M_{lb-a}}{M_{lb}} - 1$$ Equation 13.10-18

where

M_{lb} = applied lateral bend moment (in-lb/in)
M_{lb-a} = lateral bend moment allowable (in-lb/in)
K_{lb} = lateral bend factor, described in **Table 13.10-25**
MS_{lb} = lateral bend margin of safety

The lateral bend factor (K_{lb}), which depends on the overwrap, repair, secondary bond, and splice is described in **Table 13.10-25**. These factors are based on the test data for IM7/977-3 thick tape, FM300-08 material system and should not be used for other material system.

Table 13.10-25 Lateral Bend Factors Defined (K_{lb})		
$K_{lb} = K_{lb\text{-}overwrap} \times K_{lb\text{-}EOD} \times K_{lb\text{-}splice} \times K_{lb\text{-}secbond}$		**Equation 13.10-19**
Factors	**Symbol**	**Table Reference**
Lateral bend overwrap factor	$K_{lb\text{-}ovewrap}$	**Table 13.10-26**
Lateral bend Effect of Defect factor	$K_{lb\text{-}EOD}$	**Table 13.10-27**
Lateral bend splice factor	$K_{lb\text{-}splice}$	**Table 13.10-28**
Lateral bend secondary-bond factor	$K_{lb\text{-}secbond}$	**Table 13.10-29**

Lateral Bend Overwrap Factor ($K_{lb\text{-}Overwrap}$)
The effect of overwraps on lateral bend is given in **Table 13.10-20**.

Table 13.10-26 Lateral Bend Overwrap Factor ($K_{lb\text{-}overwrap}$), Reference 13-28	
	-65ºF to 250ºF
≥ 2 overwrap plies	1.0

Lateral Bend Effect of Defect Factor ($K_{lb\text{-}EOD}$)
When a fastener is used to repair disbond between the pi-preform and the skin the pristine shear strength is not restored. This reduction in pristine strength is defined as an effects-of-defect factor ($K_{lb\text{-}EOD}$) **Table 13.10-27** and is applied to the lateral bend allowable dependent on the type of repair fastener used. Note that the joint should be designed for repairability and hence the pristine lateral bend allowable should be reduced by this factor.

Table 13.10-27 Lateral Bend Effects of Defect Factor ($K_{lb\text{-}EOD}$) for All Environment, References 13-17.		
Fastener Type	**$K_{lb\text{-}EOD}$**	
For any fastener type (Reference 13-17)	0.97	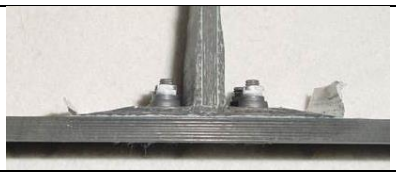

Lateral Bend Splice Factor ($K_{lb\text{-}splice}$)
If the preform is spliced the lateral bend allowable should be reduced. Details of the splicing method used is discussed in Section 13.10.9.2. Factor for splices for the lateral bend loading configurations is given in **Table 13.10-28**.

Table 13.10-28 Lateral Bend Splice Factor, Reference 13-22 ($K_{lb\text{-}splice}$)

Configuration	**-65ºF - 250ºF**
Lateral Bend	0.88
No Splice	1.0

Copyright 2015 Lockheed Martin Corporation.
Note: The current version is always the version on the Lockheed Martin network.

Lateral Bend Secondary Bond Factor ($K_{lb\text{-}secbond}$)
For secondarily-bonded pi-joint additional reduction to lateral bend allowable is required. This factor is shown in **Table 13.10-29**. The areas of application of secondary bond is discussed in Section 13.10.2.

Table 13.10-29 Lateral Bend Secondary Bonded Factor, Reference 13-23 & 13-20 ($K_{lb\text{-}secbond}$)

Configuration	-65ºF - 250ºF
Lateral Bend	0.71
No Secondary Bond	1.0

The above table includes the effect of adhesive thickness (<0.1 in). Thicker adhesives are generally employed when the gap between the faying surfaces cannot be tightly controlled. These factors cannot be applied for other adhesive systems.

13.10.9.5 Combined Pull-off and Joint Shear Interaction

The combined pull-off and joint shear interaction can be expressed in terms of a quadratic interaction curve as shown below

$$\left(\frac{P_{po}}{K_{po}P_{po-a}}\right)^2 + \left(\frac{P_{js}}{K_{js}P_{js-a}}\right)^2 = 1$$ Equation 13.10-20

where
P_{po} = applied pull-off load (lb/in)
$P_{po\text{-}a}$ = pull-off allowable (lb/in)
P_{js} = applied joint shear load (lb/in)
$P_{js\text{-}a}$ = joint shear allowable (lb/in)

Note that the pull-off allowable is a function of span, web angle, skin bending stiffness, fixity, skin laminate thickness, and skin laminate stacking sequence.

The margin of safety for pull-off and joint shear interaction is given as

$$MS_{po-js} = \frac{1}{R_{po-js}} - 1$$ Equation 13.10-21

Where
$MS_{po\text{-}js}$ = combined pull-off and joint shear margin of safety

$$R_{po-js} = \sqrt{\left(\frac{P_{po}}{K_{po}P_{po-a}}\right)^2 + \left(\frac{P_{js}}{K_{js}P_{js-a}}\right)^2}$$ Equation 13.10-22

13.10.9.6 Combined Pull-off and Lateral Bend Interaction

The combined pull-off and lateral bend interaction can be expressed in terms of a linear interaction curve as shown below

$$\left(\frac{P_{po}}{K_{po}P_{po-a}}\right) + \left(\frac{M_{lb}}{K_{lb}M_{lb-a}}\right) = 1$$ Equation 13.10-23

where

Copyright 2015 Lockheed Martin Corporation.
Note: The current version is always the version on the Lockheed Martin network.

P_{po} = applied pull-off load (lb/in)
$P_{po\text{-}a}$ = pull-off allowable (lb/in)
M_{lb} = applied lateral bend moment (in-lb/in)
$M_{lb\text{-}a}$ = lateral bend moment allowable (in-lb/in)

Note that the pull-off allowable is a function of span, web angle, skin laminate thickness, and skin laminate stacking sequence.

The margin of safety for pull-off and lateral bend interaction is given as

$$MS_{po-lb} = \frac{1}{R_{po-lb}} - 1$$ Equation 13.10-24

where
$MS_{po\text{-}lb}$ = combined pull-off and lateral bend margin of safety

$$R_{po-lb} = \left(\frac{P_{po}}{K_{po}P_{po-a}}\right) + \left(\frac{M_{lb}}{K_{lb}M_{lb-a}}\right)$$ Equation 13.10-25

13.10.9.7 Combined Joint Shear and Lateral Bend Interaction

The combined joint shear and lateral bend interaction can be expressed in terms of a quadratic interaction curve as shown below

$$\left(\frac{P_{js}}{K_{js}P_{js-a}}\right)^2 + \left(\frac{M_{lb}}{K_{lb}M_{lb-a}}\right)^2 = 1$$ Equation 13.10-26

where
P_{js} = applied joint shear load (lb/in)
$P_{js\text{-}a}$ = joint shear allowable (lb/in)
M_{lb} = applied lateral bend moment (in-lb/in)
$M_{lb\text{-}a}$ = lateral bend moment allowable (in-lb/in)

The margin of safety for joint shear and lateral bend interaction is given as

$$MS_{js-lb} = \frac{1}{R_{js-lb}} - 1$$ Equation 13.10-27

where
$MS_{js\text{-}lb}$ = combined joint shear and lateral bend margin of safety

$$R_{js-lb} = \sqrt{\left(\frac{P_{js}}{K_{js}P_{js-a}}\right)^2 + \left(\frac{M_{lb}}{K_{lb}M_{lb-a}}\right)^2}$$ Equation 13.10-28

Copyright 2015 Lockheed Martin Corporation.
Note: The current version is always the version on the Lockheed Martin network.

13.10.9.8 Combined Pull-off, Lateral Bend, and Joint Shear Interaction

The margins of safety for the combined pull-off, lateral bend, and joint shear interaction is determined by selecting the minimum of the six margins as shown below.

$$MS_{po-js-lb} = \frac{1}{R_{po-js-lb}} - 1 \qquad \text{Equation 13.10-29}$$

where

$MS_{po-js-lb}$ = combined joint pull-off, shear, and lateral bend margin of safety.

$$R_{po-js-lb} = \sqrt{\left(\frac{P_{po}}{K_{po}P_{po-a}} + \frac{M_{lb}}{K_{lb}M_{lb-a}}\right)^2 + \left(\frac{P_{js}}{K_{js}P_{js-a}}\right)^2} \qquad \text{Equation 13.10-30}$$

The critical margin is the minimum margin and is given as

$$MS_{crit} = Minimum\{MS_{po}, MS_{lb}, MS_{js}, MS_{po-js}, MS_{po-lb}, MS_{js-lb}, MS_{po-js-lb}\} \qquad \text{Equation 13.10-31}$$

13.10.9.9 Effect of Defects and Repair

A summary of the different defects that are possible during manufacturing process of a pi-joint is summarized in **Table 13.10-38**. Of these only the critical defects that result in a decrease in strength are described below in **Table 13.10-30** to **Table 13.10-32** for different loading conditions. All the other defects did not cause significant reduction in strengths and were included in the B-basis allowable calculations (Reference 13-17).

Table 13.10-30 Effects of Critical Defect for Pull-off Loading

Table 13.10-38 Reference No.	Defect	Resolution
15	Forgetting to remove the peel ply from the base laminate.	Repair with fasteners. This results in additional reduction to the allowable, K_{po-EOD} (Section 13.10.9.2)
9,10	Large inclusion/porosity between preform and base or between preform and upstanding leg. Poor quality bond between preform and base or between preform and web.	Repair with fasteners. This results in additional reduction to the allowable, K_{po-EOD} (Section 13.10.9.2)
1	Flaw directly below web, between preform base and adhesive	Repair with fasteners. This results in additional reduction to the allowable, K_{po-EOD} (Section 13.10.9.2)
13	Web installed at 0.09 inches or above preform nominal thickness	***Process control must prevent this flaw from occurring.***

Copyright 2015 Lockheed Martin Corporation.
Note: The current version is always the version on the Lockheed Martin network.

Table 13.10-31 Effects of Critical Defect for Joint Shear Loading

Table 13.10-38 Reference No.	Defect	Resolution
15	Forgetting to remove the peel ply from the base laminate.	Repair with fasteners. This results in additional reduction to the allowable, $K_{js\text{-}EOD}$ (Section 13.10.9.2)
9,10	Large inclusion/porosity between preform and base or between preform and upstanding leg. Poor quality bond between preform and base or between preform and web.	Repair with fasteners. This results in additional reduction to the allowable, $K_{po\text{-}EOD}$ (Section 13.10.9.2)

Table 13.10-32 Effects of Critical Defect for Lateral Bend Loading

Table 13.10-38 Reference No.	Defect	Resolution
9,10	Large inclusion/porosity between preform and base or between preform and upstanding leg. Poor quality bond between preform and base or between preform and web.	Repair with fasteners. This results in additional reduction to the allowable, $K_{lb\text{-}EOD}$ (Section 13.10.9.2)
4	Edge flaw between the preform and base laminate	Repair with fasteners. This results in additional reduction to the allowable, $K_{lb\text{-}EOD}$ (Section 13.10.9.2)
13	Web installed at 0.09 inches or above preform nominal thickness	P***rocess control must prevent this flaw from occurring.***

13.10.10 Example Problem

Consider an IM7/977-3 3D woven preform pi-joint with IM7/977-3 thick tape skin (0.199 in thick) and IM7/977-3 fabric web. The preform style used is PCA1111. The adhesive used is FM300-08. Eddie bolts are to be used for fastener repairs. The different ultimate loads acting on the joints are shown below:

p	Pull-off (P_{po})	Joint Shear (P_{js})	Lateral bend Moment (M_{lb})
psi	lb/in	lb/in	in-lb/in
20	421	560	60

Calculate the Margins of Safety for this joint for the following cases.

Case	Web Angle	Temp (°F)	Span Length, S (in)	Skin Thickness, t_{skin} (in)	Preform Spliced	Layup	Overwrap	Secondary Bond
1	90°	75	21	0.19	No	[25/50/25]	No	No

<u>Pull-off Margin</u>

First the pull-off factor is calculated. The pull-off factor is given by **Equation 13.10-3**

$K_{po} = K_{span} \times K_{web\text{-}angle} \times K_{ply\%} \times K_{po\text{-}overwrap} \times K_{po\text{-}EOD} \times K_{po\text{-}splice} \times K_{po\text{-}secbond}$

<u>Span Factor (K_{span})</u>

P_{po} = 421 lb/in

Copyright 2015 Lockheed Martin Corporation.
Note: The current version is always the version on the Lockheed Martin network.

From **Table 13.10-10**
Since t_{skin} = 0.19 in, K_{span} = 1.0.

Web Factor ($K_{web\text{-}angle}$)
From **Table 13.10-12** since web angle = 90°, $K_{web\text{-}angle}$ = 1.0

0° ply % Factor ($K_{ply\%}$)
From **Table 13.10-13** since 0° ply % = 25%, $K_{ply\%}$ = 1.0

Pull-off overwrap factor ($K_{po\text{-}overwrap}$)
Since there are no overwraps $K_{po\text{-}overwrap}$ = 1.0

Pull-off EOD Factor ($K_{po\text{-}EOD}$)
From **Table 13.10-15** for a Eddie bolt repair fastener $K_{po\text{-}EOD}$ = 0.91

Pull-off splice factor ($K_{po\text{-}splice}$)
From **Table 13.10-16**, since no splices are present $K_{po\text{-}splice}$ = 1.0

Pull-off secondary bond factor ($K_{po\text{-}secbond}$)
From **Table 13.10-17**, since no secondary bonds are present $K_{po\text{-}secbond}$ = 1.0

$K_{po} = K_{span} \times K_{web\text{-}angle} \times K_{ply\%} \times K_{po\text{-}overwrap} \times K_{po\text{-}EOD} \times K_{po\text{-}splice} \times K_{po\text{-}secbond}$
$K_{po} = 1 \times 1 \times 1 \times 1 \times 0.91 \times 1 \times 1$
$= 0.91$

Using Equation 13.10-1 pull-off allowable is given as
$P_{po-a} = (m_t \times t_{skin} + C_t)$
From **Table 13.10-8** for 75° F and t=0.190
m_t = 3467.34
C_t = 0.0
$P_{po-a} = 3467.34 \times 0.19 + 0.0$
$P_{po-a} = 659\ lb/\text{in}$

From Equation 13.10-2
$$MS_{po} = \frac{K_{po} P_{po-a}}{P_{po}} - 1$$
$$MS_{po} = \frac{0.91 \times 659}{421} - 1$$
$$MS_{po} = 0.42$$

Joint Shear Margin
First the joint shear factor is calculated. The joint shear factor is given by **Equation 13.10-17**:
$K_{js} = K_{js\text{-}overwrap} \times K_{js\text{-}EOD} \times K_{js\text{-}splice} \times K_{js\text{-}secbond}$

Joint Shear Overwrap Factor ($K_{js\text{-}overwrap}$)
From **Table 13.10-20**, $K_{js\text{-}overwrap}$ = 1.0

Joint Shear Effects of Defect ($K_{js\text{-}EOD}$)
From **Table 13.10-21**, $K_{js\text{-}EOD}$ = 0.86 for Eddie Bolt

Joint Shear Splice Factor ($K_{js\text{-}splice}$)
From **Table 13.10-22**, $K_{js\text{-}splice}$ = 1.0

Copyright 2015 Lockheed Martin Corporation.
Note: The current version is always the version on the Lockheed Martin network.

Joint Shear Secondary Bond ($K_{js\text{-}secbond}$)
From **Table 13.10-23**, $K_{js\text{-}secbond} = 1.0$

$K_{js} = K_{js\text{-}overwrap} \times K_{js\text{-}EOD} \times K_{js\text{-}splice} \times K_{js\text{-}secbond}$

$K_{js} = 1.0 \times 0.86 \times 1.0 \times 1.0$
$K_{js} = 0.86$
From **Table 13.10-18** for 75ºF
$P_{js\text{-}a} = 1574$ lb/in
$P_{js} = 560$ lb/in
Using Equation 13.10-16,

$$MS_{js} = \frac{K_{js} P_{js-a}}{P_{js}} - 1$$
$$MS_{js} = \frac{0.86 \times 1574}{560} - 1$$

$MS_{js} = 1.42$

Lateral Bend Margin

First the lateral bend factor is calculated. The lateral bend factor is given by **Table 13.10-25**:
$K_{lb} = K_{lb\text{-}overwrap} \times K_{lb\text{-}EOD} \times K_{lb\text{-}splice} \times K_{lb\text{-}secbond}$

Lateral Bend Overwrap Factor ($K_{lb\text{-}overwrap}$)
From **Table 13.10-26**, since there are no overwraps, From $K_{lb\text{-}overwrap} = 1.0$

Lateral Bend Effects of Defects Factor ($K_{lb\text{-}EOD}$)
From **Table 13.10-27**, for all fasteners $K_{lb\text{-}EOD} = 0.97$

Lateral Bend Splice Factor ($K_{lb\text{-}splice}$)
From **Table 13.10-28**, $K_{lb\text{-}splice} = 1.0$, since there are no splices

Lateral Bend Secondary Bond Factor ($K_{lb\text{-}secbond}$)
From **Table 13.10-29**, $K_{lb\text{-}secbond} = 1.0$, since there are no secondary bond

$K_{lb} = K_{lb\text{-}overwrap} \times K_{lb\text{-}EOD} \times K_{lb\text{-}splice} \times K_{lb\text{-}secbond}$

$K_{lb} = 1.0 \times 0.97 \times 1.0 \times 1.0$
$K_{lb} = 0.97$
From Equation 13.10-18,
$$MS_{lb} = \frac{K_{lb} M_{lb-a}}{M_{lb}} - 1$$
where
$M_{lb-a} = 240$ in-lb/in From **Table 13.10-24** for 75ºF
$M_{lb} = 60\ in - lb/in$
$$MS_{lb} = \frac{0.97 \times 240}{60} - 1$$
$MS_{lb} = 2.88$

Copyright 2015 Lockheed Martin Corporation.
Note: The current version is always the version on the Lockheed Martin network.

Combined pull-off and shear

From Equation 13.10-22

$$R_{po-js} = \sqrt{\left(\frac{P_{po}}{K_{po}P_{po-a}}\right)^2 + \left(\frac{P_{js}}{K_{js}P_{js-a}}\right)^2}$$

$$R_{po-js} = \sqrt{\left(\frac{421}{0.91 \times 659}\right)^2 + \left(\frac{560}{0.86 \times 1574}\right)^2}$$

$$R_{po-js} = 0.8149$$

From Equation 13.10-21

$$MS_{po-js} = \frac{1}{R_{po-js}} - 1$$

$$MS_{po-js} = \frac{1}{0.8149} - 1$$

$$MS_{po-js} = 0.23$$

Combined pull-off and lateral bend

From Equation 13.10-25

$$R_{po-lb} = \left(\frac{P_{po}}{K_{po}P_{po-a}}\right) + \left(\frac{M_{lb}}{K_{lb}M_{lb-a}}\right)$$

$$R_{po-lb} = \left(\frac{421}{0.91 \times 659}\right) + \left(\frac{60}{0.97 \times 240}\right)$$

$$R_{po-lb} = 0.9598$$

From Equation 13.10-27

$$MS_{po-lb} = \frac{1}{R_{po-lb}} - 1$$

$$MS_{po-lb} = \frac{1}{0.9598} - 1$$

$$MS_{po-lb} = 0.04$$

Combined joint shear and lateral bend

From Equation 13.10-28

$$R_{js-lb} = \sqrt{\left(\frac{P_{js}}{K_{js}P_{js-a}}\right)^2 + \left(\frac{M_{lb}}{K_{lb}M_{lb-a}}\right)^2}$$

Copyright 2015 Lockheed Martin Corporation.
Note: The current version is always the version on the Lockheed Martin network.

$$R_{js-lb} = \sqrt{\left(\frac{560}{0.86 \times 1574}\right)^2 + \left(\frac{60}{0.97 \times 240}\right)^2}$$

$$R_{js-lb} = 0.4874$$

From Equation 13.10-27

$$MS_{js-lb} = \frac{1}{R_{js-lb}} - 1$$

$$MS_{js-lb} = \frac{1}{0.4874} - 1$$

$$MS_{js-lb} = 1.05$$

<u>Combined pull-off, joint shear, and lateral bend</u>

From Equation 13.10-30

$$R_{po-js-lb} = \sqrt{\left(\frac{P_{po}}{K_{po}P_{po-a}} + \frac{M_{lb}}{K_{lb}M_{lb-a}}\right)^2 + \left(\frac{P_{js}}{K_{js}P_{js-a}}\right)^2}$$

$$R_{po-js-lb} = \sqrt{\left(\frac{421}{0.91 \times 659} + \frac{60}{0.97 \times 240}\right)^2 + \left(\frac{560}{0.86 \times 1574}\right)^2}$$

$$R_{po-js-lb} = 1.0451$$

From Equation 13.10-29

$$MS_{po-js-lb} = \frac{1}{1.0451} - 1$$

$$MS_{po-js-lb} = -0.04$$

The minimum margin of safety is determined using Equation 13.10-31

$$MS_{crit} = Minimum\{MS_{po}, MS_{lb}, MS_{js}, MS_{po-js}, MS_{po-lb}, MS_{js-lb}, MS_{po-js-lb}\}$$

$$MS_{crit} = Minimum\{0.42, 2.88, 1.42, 0.23, 0.04, 1.05, -0.04\}$$

$$MS_{crit} = -0.04;\ Pull-off, shear, and\ Lateral\ Bend$$

An overwrap can be used to mitigate the negative margin.

13.10.11 IM7/977-3 & AF191 Adhesive, 350ºF Autoclave Cure Material System

The IM7/977-3, AF191 adhesive material system is described in **Table 13.10-33**. The specification for this preform is the same as that given in Section 13.10.9. The testing that was performed for this material is limited and there are

Copyright 2015 Lockheed Martin Corporation.
Note: The current version is always the version on the Lockheed Martin network.

a number of geometries and combined load scenarios that have not been investigated. Prior to use of this material system for design these need to be explored further.

Table 13.10-33 IM7/977-3 & AF191 Adhesive 350ºF Cure Material System

Skin	Web	Web Thickness (in)	Adhesive
IM7/977-3 Tape Prepreg	IM7/977-3 2D Weave Fabric Prepreg	0.166	AF191 -10G, (0.1 lb/ft^2), glass scrim carrier, AF-191 -08K, (0.08 lb/ft^2) –nylon fabric scrim carrier -65ºF to 250ºF service temperature

13.10.11.1 Stress Method and Pull-off Allowables

The pull-off B-Basis allowables in lb/in for the IM7/977-3 pi-joint bonded assembly is given **Table 13.10-24**. Two material batches were used for developing B-basis allowables. The values are obtained for a 4 inch span specimen which is simply supported.

Table 13.10-34 Pull-off Allowables $P_{po\text{-}a}$ (lb/in) for a Simply Supported 4 inch Span Quasi Layup [25/50/25] with a Web Angle = 90º (Reference 13-33).

Plies	Thickness (in)	Temperature		
		-65ºF	75ºF	220ºF
48	0.266	902	1006	708

The 48 plies consists of 46 tape and two outer fabric plies. The values in the table can be interpolated between temperatures to estimate allowable when operating temperature is different than the test temperature. The pull-off margins can be calculated using Equation 13.10-2, where K_{po} is defined in **Table 13.10-35**.

Table 13.10-35 Pull-off Factors Defined (K_{po})

$K_{po} = K_{span} \times K_{po\text{-}overwrap} \times K_{po\text{-}EOD}$		Equation 13.10-32
Factors	Symbol	Table Reference
Span length factor	K_{span}	**Table 13.10-10**
Pull-off overwrap factor	$K_{po\text{-}ovewrap}$	**Table 13.10-14**
Pull-off effects of defects	$K_{po\text{-}EOD}$	**Table 13.10-15**

Test data to determine the web angle factor, 0º ply percent factor, pull-off splice factor, and pull-off secondary bond factor is not available for this material system and would require additional testing.

13.10.11.2 Stress Method and Joint Shear Allowables

The joint shear allowable is dependent only on temperature and is independent of web angle, span length, skin lay-up, and skin thickness. The shear allowable is given in **Table 13.10-36**.

Table 13.10-36 Joint Shear Allowable at Room Temperature

	-65ºF	75ºF	220ºF	250ºF
Joint Shear (lb/in)	no data	2190	no data	no data

The joint shear margin of safety can be determined using Equation 13.10-16. The joint shear factors are defined in **Table 13.10-37**.

Copyright 2015 Lockheed Martin Corporation.
Note: The current version is always the version on the Lockheed Martin network.

Table 13.10-37 Joint Shear Factors Defined (K_{js})

$K_{js} = K_{js\text{-}overwrap} \times K_{js\text{-}EOD}$		Equation 13.10-33
Factors	**Symbol**	**Table Reference**
Joint shear overwrap factor	$K_{js\text{-}ovewrap}$	**Table 13.10-20**
Joint shear Effect of Defect factor	$K_{js\text{-}EOD}$	**Table 13.10-21**

Test data to determine joint shear splice factor and secondary bond factor is not available for this material system and would require additional testing

13.10.11.3 Stress Method and Lateral Bend Allowables

Lateral bend data is not available for this material system.

13.10.11.4 Combined Pull-off and Joint Shear Interaction

The combined pull-off and joint shear interaction margin can be determined using Equation 13.10-21.

13.10.11.5 Combined Pull-off and Lateral Bend Interaction

Since the lateral bend test data does not exist this interaction cannot be determined for this material system.

13.10.11.6 Combined Joint Shear and Lateral Bend Interaction

Since the lateral bend test data does not exist this interaction cannot be determined for this material system.

13.10.11.7 Combined Pull-off, Lateral Bend, and Joint Shear Interaction

Since the lateral bend test data does not exist this interaction cannot be determined for this material system.

13.10.12 IM7/MTM45-1 & FM309-1M Adhesive, Out of Autoclave (OoA) Cure Material System

This section reserved for future use. The draft of the material properties and allowables for this material system is available in Reference 13-30. The stress methods based on this allowable will be developed later.

13.10.13 Durability and Damage Tolerance

This is a topic of ongoing discussion with the customers and therefore reflects past trends specific to pi-joints. A general discussion of the durability and damage tolerance requirement is provided in Section 15 and customer specific requirements are given in Reference 13-35.

The non-impact durability requirements for bonded pi-joint ensures that the joint adequately resists (i) detrimental effects of loading (static and cyclic), delamination, wear, and environment, over its lifetime. The joint is subjected to a low-cycle spectrum and constant amplitude load of at least two service life times at a reference load usually 2/3 of typical ultimate strength. Subsequent to the cyclic loading the joint pull-off, joint shear, or lateral bend strength are verified to be at least 150% DLL. If the residual strength requirement cannot be satisfied then the reference load is

Copyright 2015 Lockheed Martin Corporation.
Note: The current version is always the version on the Lockheed Martin network.

reduced until the requirement is met. The static allowables are reduced by the ratio of the reduced reference load to the 2/3 ultimate load. Refer to Section 15 for further discussion.

The impact durability requirements, which are probabilistic based, account for "nuisance" damage that occurs during handling and manufacturing, *e.g.*, tool drop. A 4 or 6 ft-lb energy level is usually employed to impact the joint. Subsequent to impact loading the joint is subjected to a spectrum fatigue for at least two life times after which the joint has to withstand a residual static load specified by the program. This load usually varies between 105% and 115% of design limit load for visible damage and 150% of design limit load if the damage is not visible. It is also required that the damage does not cause fluid ingression or leaks over the life span of the structure. For regions of low probability of occurrence this requirement is imposed after repair.

Damage tolerance requirements are specified for fracture critical zones. This requires that the joint withstand a residual static load specified by the program, after it is impacted at a specified energy level up to 100 ft-lb and subjected to a spectrum fatigue of at least two life times.

In addition to the durability and damage requirements for the joint, the skin and web also needs to be verified for durability and damage tolerance (fracture critical zones only).

Testing

The pi-joint is impacted at critical locations using a ½ inch (for 4 and 6 ft-lb) or 1 inch impactor (for higher energy level associated with damage tolerance) as specified by the program. Typical impact locations for a pi-joint is shown in **Figure 13.10-20**.

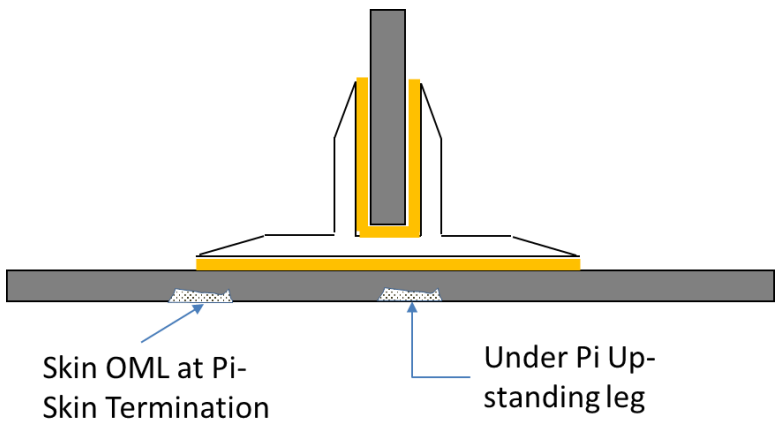

Figure 13.10-20 Critical Impact Locations for Pi-joint

.

A large test panel is impacted at several locations from which elements for fatigue and subsequent static tests are cut (**Figure 13.10-21**).

Copyright 2015 Lockheed Martin Corporation.
Note: The current version is always the version on the Lockheed Martin network.

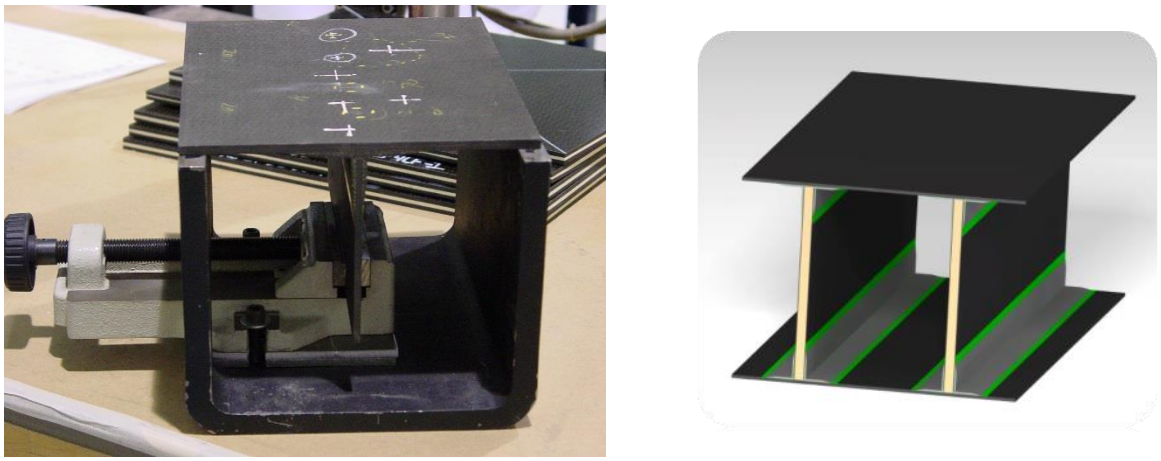

Figure 13.10-21 Impact Fixture along with the Specimen is Shown on Left and a Box Specimen Prepared for Impact is Shown on Right

A one inch impactor and the impact machine is shown in **Table 13.10-22**.

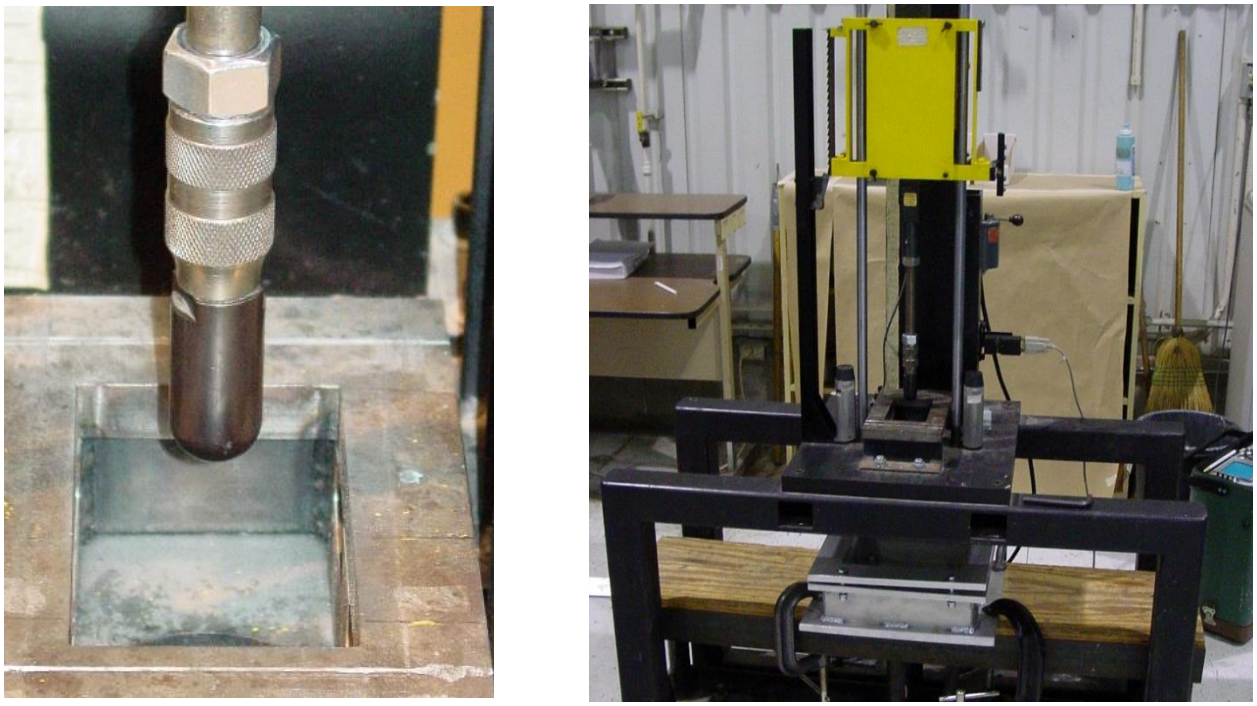

Figure 13.10-22 One inch Impactor and Impact Machine

The impacted area is inspected using a suitable NDE method and extent of damage is ascertained. The impacted specimen and a UT scan of the impacted region is shown in **Figure 13.10-23**

Copyright 2015 Lockheed Martin Corporation.
Note: The current version is always the version on the Lockheed Martin network.

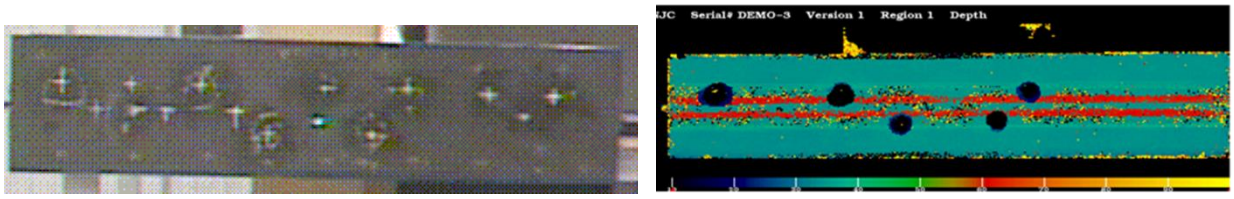

Figure 13.10-23 Impacted Pi-Joint and it's LASER UT Scan

13.10.14 Pi-preform Splicing/Darting Methods

Figure 13.10-19 depicts one method of splicing a pi-preform, where it has to carry a significant axial load. In situations where the axial load is not significant, the pi-preform can be butt-joined with overwraps. Additional testing needs to be performed to determine knockdowns, if any, to the allowables.

The pi-preform legs may need to be darted (cut) if they are used in a curved region with significant curvature. Plunge cuts are made at 45° angle to the length and staggered to reduce the effect of discontinuity. The cut legs overlap till the base. The pitch of the darts depends on the radius of the curved region and the length of the preform. **Figure 13.10-24** shows the pi darts for the case where the pi legs are situated on the concave side.

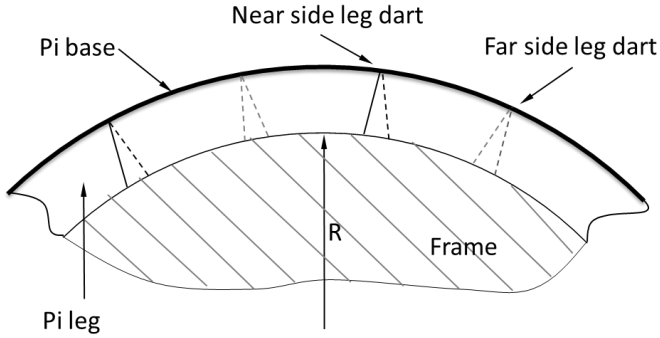

Figure 13.10-24 Pi-preform Leg Darts for Concave Case

When the legs are situated on the convex side as shown in **Figure 13.10-25** the gaps between the darts are filled with "v" shaped preform remnants.

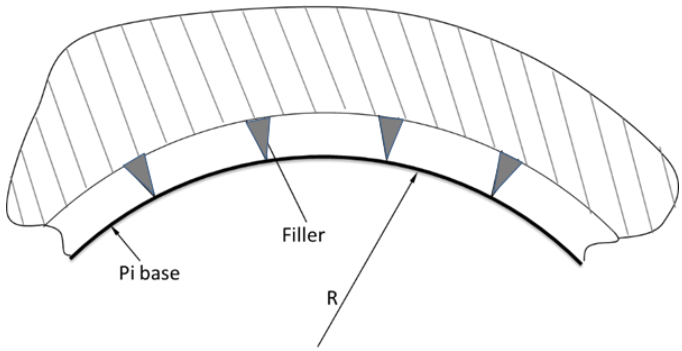

Figure 13.10-25 Pi-preform Leg Darts for Convex Case

Darting is usually not required when the curvature is shallow, for short runs, and when the curvature reverses.

Copyright 2015 Lockheed Martin Corporation.
Note: The current version is always the version on the Lockheed Martin network.

These splices/darts should be carefully considered during analysis. If the pi-preform carries high axial loads or if the joint is located near regions of high stress concentration then additional testing may be needed to determine knockdowns to the allowables if any.

13.10.15 IBOND Analysis Method

IBOND is a detail analysis tool correlated to experimental data that is currently under development. This section is reserved for future use.

13.10.16 Other Analysis Methods

This section reserved for future use.

13.10.17 Additional Checks

Axial strains in the preform and skin should be checked against the critical FHT or FHC allowable for the service environment using a fastener prescribed by the program. This is done to ensure repairability. The repair fastener chosen should be commensurate with the size of the preform base flange and the pull-off loads. If none is specified 3/16 in. Eddie bolt for the skin and a 3/16 in. protruding head fastener for the web can be used. Skin should have enough thickness for countersink fastener head if that is the repair process (see Section 11). Also the skin and web area should be checked for bearing strength. If the skin is fracture critical then the skin has to be checked for damage tolerance.
For the top wing skin countersunk blind fasteners are typically used. The effect of using blind fasteners on the allowables should be determined using element tests as described in Section 13.10.18. Furthermore blind fastener installation should always have tail side inspected for proper formation of the bulb. This can be performed using boroscope.

13.10.18 Effects of Defects

There are a number of manufacturing related defects that can impact the strength of bonded pi-joints. These are simulated in test coupons so that reduction factors can be determined. . These defects are inserted into the test elements and subsequently tested for different loading conditions (pull-off, joint shear, lateral bend) and environment (ETW, CTD, RTA) under static load and fatigue cycling. Table 13.10-38 represents a recommended comprehensive list of defects which should be considered for any pi joint effects of defect test program.

Table 13.10-38 Effects of Defect Tests (Reference 13-17)

Specimen Type	Defect	Figure	Comments
1	Embedded 2x Detectable Flaw Directly Under Web Between Preform Base and Adhesive	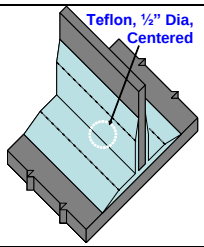	The minimum detectable flaw size as defined by quality assurance is ¼ inch diameter (Reference 13-34). Therefore ½ inch flaw size is embedded.

Copyright 2015 Lockheed Martin Corporation.
Note: The current version is always the version on the Lockheed Martin network.

Specimen Type	Defect	Figure	Comments
2	Embedded 2x Detectable Flaw Directly Under Web Between Preform Base and FM300 Adhesive	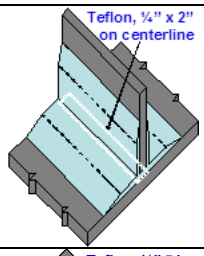	This is representative of a backing material left in the bondline.
3	Embedded Flaw under Base Flange	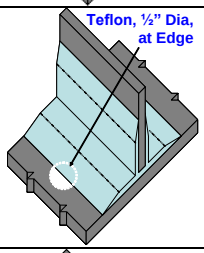	Represents a semi-circular flaw between the edge of the preform and base
4	Embedded Flaw under Base Flange	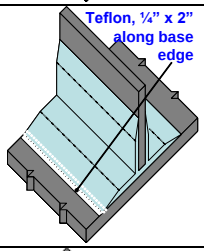	Represents a line flaw between the edge of the preform and base
5	Embedded Flaw Centered in Upstanding Leg	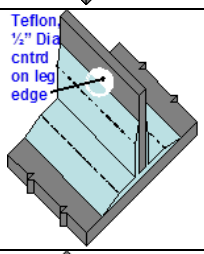	Represents a semi-circular flaw between the edge of the preform and web
6	Embedded Flaw Centered in Upstanding Leg	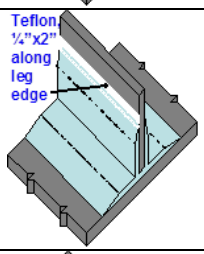	Represents flaw that runs full length of preform upstanding legs.
7	Embedded Flaw at Edge of Upstanding Leg	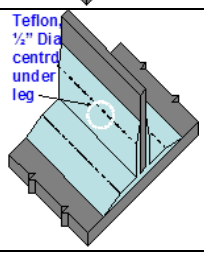	Represents defect between adhesive and web.

Copyright 2015 Lockheed Martin Corporation.
Note: The current version is always the version on the Lockheed Martin network.

Specimen Type	Defect	Figure	Comments
8	Embedded Flaw at Edge of Upstanding Leg	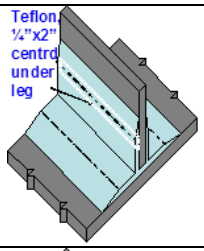	Represents continuous defect between adhesive and web.
9	Teflon Film under Preform Base with Fasteners	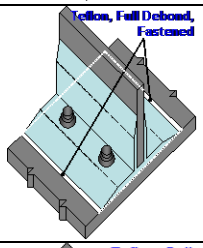	Represents low quality bond between preform and laminate that is repaired with a fastener. Diameter of the fastener depends on the width of the preform base and varies between 3/16 inch to ¼ inch.
10	Teflon Film in Upstanding Leg with Fasteners	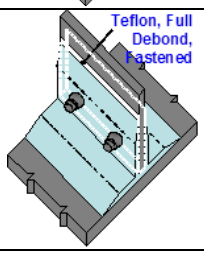	Represents large area defect between the upstanding leg and the preform repaired by fasteners.
11	Teflon in Radius	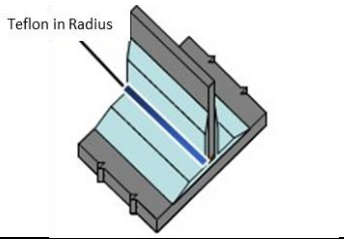	Represents defect at the pi corner that cannot be detected using NDI
12	Teflon under Web	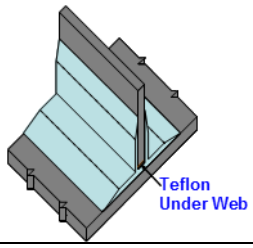	Represents defect between the web and pi clevis that cannot be detected using NDI
13	Pristine Fastened in Preform Base	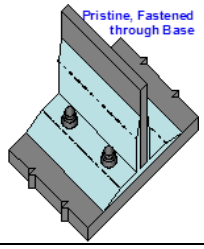	Effect of using fasteners in a the base of a pristine coupon

Copyright 2015 Lockheed Martin Corporation.
Note: The current version is always the version on the Lockheed Martin network.

Specimen Type	Defect	Figure	Comments
14	Pristine Fastened in Upstanding Leg	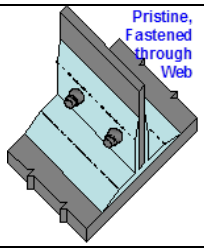	Effect of using fasteners in the upstanding leg of a pristine specimen
15	Peel Ply Left on Base Laminate	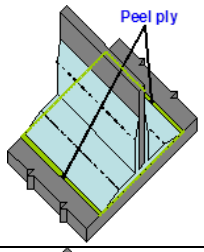	This flaw is representative of forgetting to remove the peel ply from the base laminate and fabricating a co-bonded assembly with the peel ply
16	Peel Ply Left on Base with Fasteners	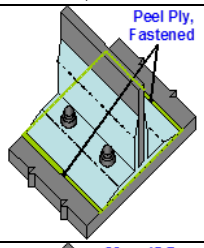	This is representative of not removing peel ply from the base laminate and repairing with fasteners
17	30 & 45 Day Adhesive Out-time Under Base	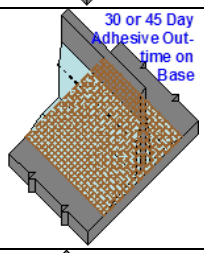	This represent adhesive with 30 & 45 days out-time applied between the preform and base laminate.
18	30 & 45 Day Adhesive Out-time in Upstanding Leg	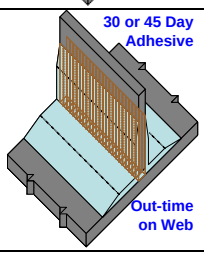	This represent adhesive with 30 & 45 days out-time applied between the preform and upstanding leg
19	45 Day Adhesive Out-time in Upstanding Leg with Fasteners	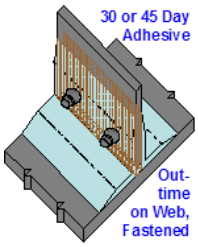	This represents adhesive with 45 days out time, which is used between the upstanding leg and

Copyright 2015 Lockheed Martin Corporation.
Note: The current version is always the version on the Lockheed Martin network.

Specimen Type	Defect	Figure	Comments
20	Web Below Preform Nominal Thickness	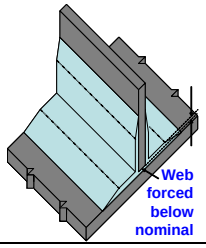	This is representative of the web being below the nominal thickness of the preform base.
21	Web 0.060 Above Preform Nominal Thickness	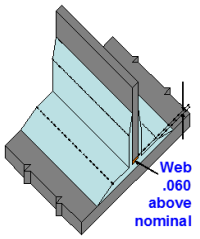	This represents the web being above the nominal thickness of the preform base under the upstanding leg. The figure on the left shows the web being 0.06 inch above nominal which implies it is 0.17 inch above preform base if the preform thickness is 0.11 inch.

The effect of defects is determined for both static and fatigue loading. For fatigue loading, a maximum spectrum load (MSL), as a certain percent of the DLL is determined. Employing the MSL, the joint element is subjected to a critical spectrum load for at least two life times and the residual strength is determined. If the residual strength is lower than the MSL, it is reduced until this condition is satisfied and the static strength is reduced accordingly. This process is explained in Section 15. It is conservative to use the bolt and Teflon repair allowable for all bolted repairs shown in the above table.

13.10.19 Repairs

Repairs for pi-joints will be discussed in detail in Section 19.

13.10.20 FEA Modeling Conventions and Considerations

In general finite element analysis is employed to obtain internal loads which are used in proprietary in-house analysis software tools to obtain the final margins. The finite element model could be a coarse grid model such as the models used in complete Air Vehicle Finite Element Model suitable for linear analysis or a fine grid breakout model suitable for non-linear analysis. The breakout model should have sufficient fidelity to capture the non-linear effects, which requires that there be at least four to six elements along the narrow width of the plate and sufficient number of elements along the longer side such that an aspect ratio between 1 – 1.25 is maintained.

Furthermore the edge restraints should be modeled accurately. If the adjacent panels have the same aspect ratios and have the same pressure applied to them then the edge supports of the panel can be assumed to be clamped since the slope and displacement along the centerline of the substructure must be zero. If the adjacent panels are different such as in the case of edge panels then simply supported boundary conditions can be assumed. Clamped conditions can also be assumed for the panel when double row of fasteners are used to attach the panel to the substructure or if the substructure has sufficient torsional rigidity to prevent rotation.

When working with the breakout model it is recommended that the model should include at least an additional bay length on all sides. Also, free body boundary loads should be applied instead of displacements to the breakout model.

Copyright 2015 Lockheed Martin Corporation.
Note: The current version is always the version on the Lockheed Martin network.

In a finite element model, modeling the composite material property is significantly different and complex than modeling isotropic properties. The different techniques for modeling the material properties are further discussed in Reference 13-18.

In a coarse grid finite element model the skin and the web are modelled using shell elements and the pi-preform is modelled using bar elements. If the model has sufficient granularity such that the skin element size is smaller than the base of the pi-preform then the pi-preform can be modelled as a shell either by using duplicate shell elements or adding the preform as a ply in the PCOMP card. However this results in a complex finite element model due to the fine mesh. When modelling the skin, preform, and the web using shell and bar elements proper care should be taken to correctly offset the web and preform from the skin

The free-body loads should be calculated at the intersection of the web and the skin. If the pi-preform is modelled as a bar element, the free-body loads at the intersection should be calculated with and without the bar element and the highest values selected to calculate the margins. The same strategy can be adopted when modeling the preform as a duplicate shell element in which case the free-body is calculated with and without the duplicate shell and the highest values used to calculate the margins.

When performing detailed analysis, geometrically non-linear analysis should be used to correctly account for the membrane forces. See Section 8 for details.

Copyright 2015 Lockheed Martin Corporation.
Note: The current version is always the version on the Lockheed Martin network.